# A PRELIMINARY STUDY ON THE USE OF RESERVOIR SIMULATION AND COAL MINE VENTILATION METHANE MEASUREMENTS IN DETERMINING COAL RESERVOIR PROPERTIES

A THESIS SUBMITTED TO
THE GRADUATE SCHOOL OF NATURAL AND APPLIED SCIENCES
OF
MIDDLE EAST TECHNICAL UNIVERSITY

BY

SİNEM SETENAY ERDOĞAN

IN PARTIAL FULFILLMENT OF THE REQUIREMENTS
FOR
THE DEGREE OF MASTER OF SCIENCE
IN
PETROLEUM AND NATURAL GAS ENGINEERING

FEBRUARY 2011

Approval of the thesis:

**"A PRELIMINARY STUDY ON THE USE OF RESERVOIR SIMULATION AND COAL MINE VENTILATION METHANE MEASUREMENTS IN DETERMINING COAL RESERVOIR PROPERTIES"**

submitted by **SİNEM SETENAY ERDOĞAN** in partial fulfillment of the requirements for the degree of **Master of Science in Petroleum and Natural Gas Engineering Department, Middle East Technical University** by,

Prof. Dr. Canan Özgen
Dean, Graduate School of **Natural and Applied Sciences** _____

Prof. Dr. Mahmut Parlaktuna
Head of Department, **Petroleum and Natural Gas Eng.** _____

Prof. Dr. Ender Okandan
Supervisor, **Petroleum and Natural Gas Engineering Dept.** _____

Assoc. Prof. Cevat Özgen Karacan
Co-Supervisor, **Office of Mine Safety and Health Research, NOISH, U.S.A.** _____

**Examining Committee Members:**

Prof. Dr. Mahmut Parlaktuna
Petroleum and Natural Gas Engineering Dept., METU _____

Prof. Dr. Ender Okandan
Petroleum and Natural Gas Engineering Dept., METU _____

Assoc. Prof. Cevat Özgen Karacan
Office of Mine Safety and Health Research, NOISH, U.S.A. _____

Prof. Dr. Tanju Mehmetoğlu
Petroleum and Natural Gas Engineering Department, METU _____

Prof. Dr. Nurkan Karahanoğlu
Geological Engineering Department, METU _____

**Date:** 07.02.2011

**I hereby declare that all information in this document has been obtained and presented in accordance with academic rules and ethical conduct. I also declare that, as required by these rules and conduct, I have fully cited and referenced all material and results that are not original to this work**.

Name, Lastname: Sinem Setenay ERDOĞAN

Signature:

# ABSTRACT

## A PRELIMINARY STUDY ON THE USE OF RESERVOIR SIMULATION AND COAL MINE VENTILATION METHANE MEASUREMENTS IN DETERMINING COAL RESERVOIR PROPERTIES

Erdoğan, Sinem Setenay

M.Sc., Petroleum and Natural Gas Engineering Department

Supervisor : Prof. Dr. Ender Okandan

Co-Supervisor : Assoc. Prof. Cevat Özgen Karacan

February 2011, 169 Pages

This thesis investigates methane emissions and methane production potentials from abandoned longwall panels produced or emitted due to mining activities either from coal seam or any underlying or overlying formations. These emissions can increase greenhouse gas concentrations and also pose a danger to the underground working environment and to miners.

In addition to the safety issues, recovery and utilization of this gas is an additional source of energy.

In this study, methane concentrations measured from ventilation air ways in Yeni Çeltek Coal Mine, which is located in Suluova basin, Amasya, and contains thick, laterally extensive Lower Eocene coal seams, were integrated within a numerical

reservoir model. Key reservoir parameters for history matching are cleat permeabilities, cleat porosity, diffusion time and Langmuir volume and Langmuir pressure. Thirteen cases were studied. According to the results, Case-10 determined as the best fitted case for both of the production wells. Cleat permeabilities and Langmuir pressure were the most effective parameters. Reservoir parameters matched are cleat permeabilities of 5, 4 and 1 md and fracture dimensions of 0.8, 0.4, and 0.1 m in x, y and z direction respectively, 2 % cleat porosity, 0.3 % water saturation. Diffusion time was determined as 400 days and 2000 kPa Langmuir volume and 6.24279 $m^3$ /tone gas content estimated. According to these results it can be said that methane production will not be economically feasible, however; to remedy underground working conditions and safety of workers methane management should be taken into consideration.

# ÖZ

## KÖMÜR REZERVUAR ÖZELLİKLERİNİN BELİRLENMESİNDE KÖMÜR MADENİ HAVALANDIRMA SİSTEMİ METAN GAZI ÖLÇÜMLERİ VE REZERVUAR SİMÜLASYON TEKNİĞİNİN KULLANILMASI ÜZERİNE BİR ÖN ÇALIŞMA

Erdoğan, Sinem Setenay

Yüksek Lisans, Petrol ve Doğal Gaz Mühendisliği Bölümü

Tez Yöneticisi : Prof. Dr. Ender Okandan

Ortak Tez Yöneticisi: Assoc. Prof. Cevat Özgen Karacan

Şubat 2011, 169 Sayfa

Bu çalışmada, terk edilen uzun ayak panolarındaki madencilik aktivitelerine bağlı olarak, kömür tabakasından, kömür tabakasının altında ya da üstünde yatan başka tabakalardan kaynaklanabilen metan emisyonları ve bu gazın üretim potansiyeli araştırılmıştır. Bu emisyonlar atmosferdeki sera gazı konsantrasyonlarını arttırırken, ayrıca yer altı çalışma koşulları ve madenciler için tehlike arz edebilir. Güvenlik sorunlarının dışında, bu gazın üretilip kullanılması yeni bir enerji kaynağı oluşturur.

Bu çalışmada Alt Eosene yaşlı, kalın ve yatay uzanan kömür tabakasının bulunduğu Amasya-Suluova baseninde yer alan Yeni Çeltek kömür madeninin, üretime kapatılan panellerinin olduğu havalandırma sisteminin ölçtüğü metan emisyonları nümerik rezervuar modeli ile birleştirilerek kullanılmıştır. Tarihsel çakıştırma için kullanılan parametreler kırık geçirgenliği, difüzyon zamanı, Langmuir basıncı ve Langmuir hacmidir. On üç farklı durum denenmiş ve alınan sonuçlara göre onuncu deneme her iki

üretim kuyusuna da en iyi uyan deneme olarak belirlenmiştir. Kırık geçirgenliği ve Langmuir basıncı en etkili parametreler olarak ortaya çıkmıştır. Alınan sonuçların ışığında x, y ve z yönünde sırasıyla kırık geçirgenliği 5, 4 ve 1 md, kırık uzanımı 0,8, 0,4 ve 0,1 m, kırık gözenekliliği % 2 ve su doygunluğu % 0,3 olarak bulunmuştur. Difüzyon zamanı 400 gün olarak ortaya çıkarken Langmuir basıncı 2000 kPa ve Langmuir hacmi 6,24279 $m^3$/ton olarak ortaya çıkmıştır. Bu sonuçlar ışığında, ekonomik bir gaz üretiminden bahsetmek çok mümkün olamasa da, maden çalışma şartlarının arttırılması ve maden ve işçi güvenliği açısından metan yönetimi ve bertaraftı mutlaka değerlendirilmelidir.

To My Family

# ACKNOWLEDGMENTS

I wish to express my deepest gratitude to her supervisor Prof. Dr. Ender OKANDAN for her guidance, advice, criticism, encouragements, insight and tolerance and support throughout the research.

I also would like to express my deepest gratitude to my co-supervisor Assoc. Prof. C. Özgen KARACAN not only for his guidance, criticism, invaluable support encouragements and insight throughout this study but also for his continuous confidence in me, for his sincere friendship and his unforgettable and invaluable contributions to my life.

My thesis committee members Prof. Dr. Mahmut Parlaktuna, Prof. Dr. Ender Okandan, Assoc. Prof. C. Özgen Karacan, Prof. Dr. Nurkan Karahanoğlu, and Prof. Dr. Tanju Mehmetoğlu are very appreciated for their comments and suggestions.

I wish to appreciate to my mother, Nevzin Erdoğan, my father, Ali Cevat Erdoğan, and my sister, İlkay Sıdal, for their continual encouragement, understanding and support in every stage of my life and the entire study.

My special thanks also go to Petroleum and Natural Gas Engineering Department co-workers for their continual friendship and encouragement throughout the study.

I am deeply thankful to my dear friend Irmak Sargın for her friendship, never-ending support, understanding and inspiration.

This study was supported by the General Directorate of Turkish Coal Enterprises,TKI, and Yeni Çeltek Coal and Mining Corporation.

# TABLE OF CONTENT

## LIST OF TABLES

### TABLES

## LIST OF FIGURES

**FIGURES**

# CHAPTER-1

# INTRODUCTION

Coal is the most abundant fossil fuel in the world. It was the number one energy source in the second half of the 18$^{th}$ century and has been the driving force behind the industrial revolution as the feedstock for iron and steel industry. Although coal is still important as an energy source in most parts of the world as is crucial as the primary source of coke making and steel industry, its widespread use is blamed as one of the reasons of increase in carbon dioxide levels in the atmosphere. In addition, coal beds are known to contain gas, mainly methane, from coalification process. Methane is found either free gas or in adsorbed state in coal seams is known as coal bed methane (CBM).

Methane in coal seams is hazard to coal mining if not diluted by air provided by ventilation system of the mine. Thus, one of the most important duties of ventilation in underground coal mines is to keep methane levels well below the explosive limit by diluting methane emissions that occur during mining, which is called coal mine methane (CMM). Methane entering a mine can create a localized zone of high concentration in an area of low air velocities and quantities. The concentration of methane in these zones may pass through a range between 5% and 15%, known as the explosive range. In this range, methane can be ignited easily with the presence of an ignition source to create a violent methane explosion that may propagate throughout the coal mine in the presence of combustible coal dust. In recent years, there have been many fatalities in underground coal mine explosions in which methane was contributing factor. Table 1 shows some of the major mine explosions (United Nations, 2010) after 2000.

**Table 1: Some of the major coal mine explosions that occurred after 2000 (Modified from United Nations, 2010)**

| Country | Date | Coal Mine | Fatality |
|---|---|---|---|
| China | 14 Feb., 2005 | Sunjlawan, Haizhou shaft, Fuxin | 214 |
| USA | 2 Jan., 2006 | Sago, West Virginia | 12 |
| Kazakhstan | 20 Sept., 2006 | Lenina, Karaganda | 43 |
| Russia | 19 March, 2007 | Ulyanovskaya, Kemerovo | 108 |
| Ukraine | 19 Nov., 2007 | Zasyadko, Donetzk | 80 |
| USA | 5 April, 2010 | Upper Big Branch, West Virginia | 29 |
| Turkey | 17 May, 2010 | Karadon, Zonguldak | 30 |

In addition to safety concerns, methane that is emitted from coal mines represents approximately 8% of the world's anthropogenic methane emissions contributing 17% to the total anthropogenic greenhouse gas emissions (US Enviromental Protecting Agency, 2003). By 2020, CMM emissions are projected to increase, with estimates as high as 793 Mt $CO_2$e (x1000 tons $CO_2$ equivalent).

Underground coal mining is the most important source of fugitive methane emissions; nearly 70% of this methane is emitted through mine ventilation air (VAM) at low concentrations.

Following coal mining activities, coal mines typically sealed and abandoned either temporarily or permanently. As work stops within the mines, the methane liberation decreases but it does not stop completely. Following an initial decline, abandoned mines can liberate methane at near steady state rate over an extended period of time. The following factors influence abandoned mine emissions:

- Time since abandonment;
- Gas content and adsorption characteristics of coal;
- Methane flow capacity of the mine;
- Mine flooding;
- Presence of vent holes; and

- Mine seals.

The methane emissions in the abandoned mines are called abandoned mine methane (AMM) (International Coal Bed Methane Conference, 2005). Methane emission potential of a longwall mine, when abandoned, can be larger than room-and-pillar mines since mining of a large block of coal causes caving of immediate formations, strata disturbances and fracturing in the overlying and underlying rock horizons. This volume of disturbed rock, called gob, can be the source of long-term methane emissions into the abandoned workings and loose rock formations.

The rate and amount of methane build up in abandoned longwall workings is usually proportional to how much coal is left gob, the amount of mine void that is not flooded as well as the existence of other gas sources within the gas emission zone (gob) of the abandoned area and the gas content and reservoir properties of the mined coal seam as unmined coal bed can still interact with the sealed area. Furthermore, gas accumulation and pressure build-up within abandoned mines can be dangerous for the active mines, if they are nearby. Therefore, some abandoned mines can be left venting to prevent gas accumulation.

As demonstrated in the previous paragraphs, CMM and AMM is not only a hazard to mining, it is also an important issue from an environmental point of view. Capturing and utilizing this gas will not only improve mining safety and will also decrease greenhouse gas emissions and will provide an additional energy source that otherwise will be lost. Therefore, instead of releasing methane emissions of abandoned mines to the atmosphere, recovery and utilization should be considered. Depending on the quality of CMM gas produced, it can be directly injected into a pipeline to be utilized as town gas, or can be improved by stripping the contaminants, such as oxygen and nitrogen. There are available and demonstrated technologies for improving the quality of CMM and AMM. These technologies have been demonstrated and are being successfully used in the U.S. and in Australia.

For instance, in the U.S., the majority of the methane from active and abandoned mines is vented to the atmosphere and only 38 abandoned underground mines recover methane (EPA, 2009). According to the U.S. EPA AMM inventory in 2009, there were 469 abandoned gassy underground mines, 38 of which recovered and utilized AMM. The total 2009 CMM emissions in the U.S. are estimated to be 187 Bscf of methane. Of this amount, underground mines accounted for 73 percent, surface mines accounted for 17 percent, and post-mining emissions accounted for 10 percent. Figure 1 depicts U.S. CMM emissions by source category.

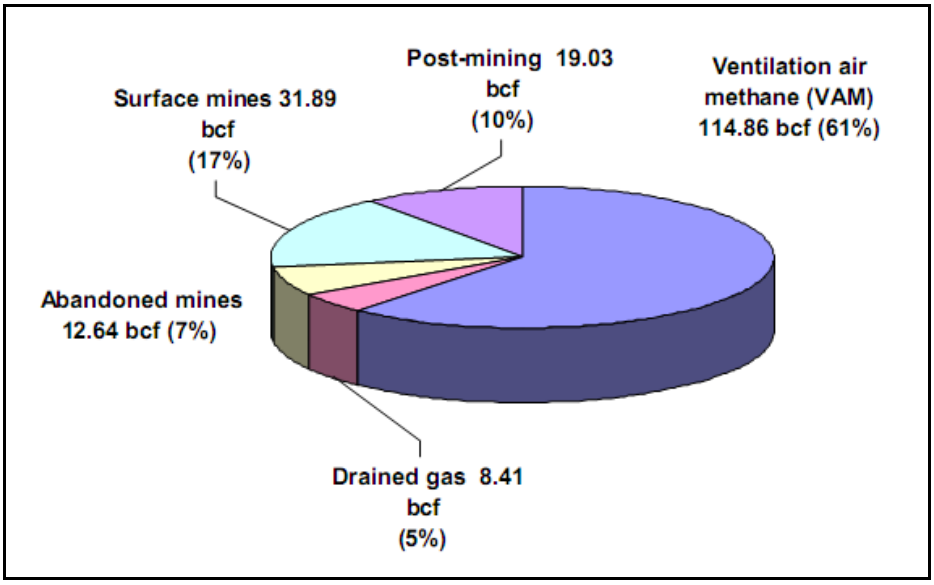


**Figure 1: 2009 U.S. CMM emissions by source category (Courtesy of Ruby Canyon Engineering, 2010)**

Recognizing the importance of capturing and using CMM for mine safety, energy production and greenhouse gas reduction, different countries are implementing various CMM projects. However, depending on the economic, social and regulatory conditions in each country, the implementations of different CMM projects are faced with multiple challenges that may slow down or curtail their progress. These challenges must be

addressed and resolved with the collaboration of both government agencies and the private sector in each country, and also through cooperation on an international level. Along these lines, the Global Methane Initiative, currently comprised of 38 partner countries, engages both governments and private sector entities; bringing together the technical and market expertise, financing, and technology necessary for methane capture and utilization at an international level.

In 2010, Turkey officially has become a member of the Global Methane Initiative (GMI) (former Methane-to-Markets) and will be joining the group in Coal Mines, Landfills, and Oil and Gas Subcommittees. Turkey is primarily interested in capturing methane from both coal beds and coal mines to reduce emissions and use the gas as a domestic energy source, as well as looking to reduce emissions from the landfill and oil and gas sectors.

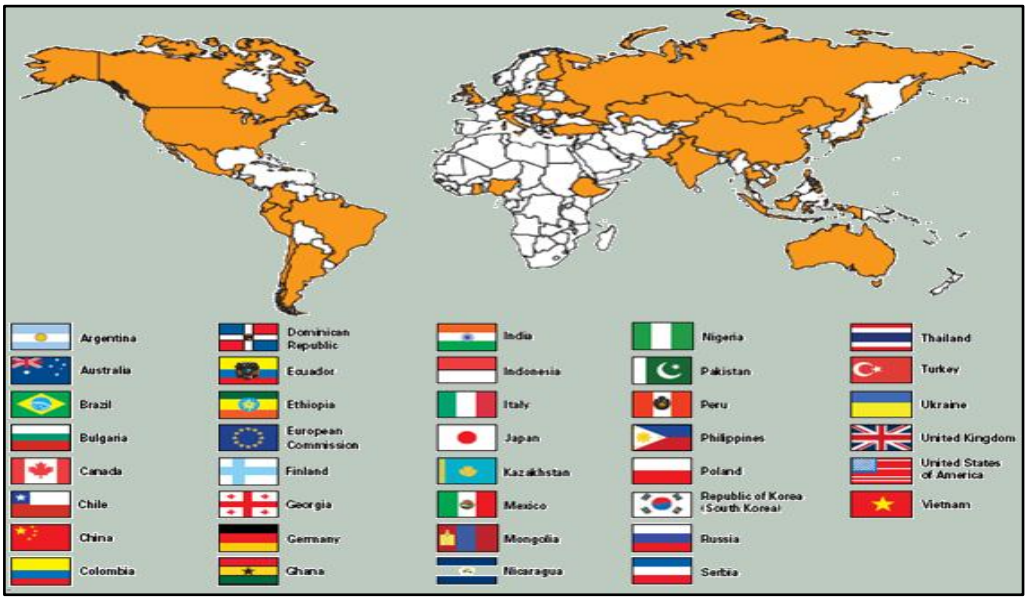


**Figure 2: Members of the Initiative (Global Methane Initiatives, 2010)**

Based on EPA's Global Anthropogenetic emissions of non-$CO_2$ Greenhouse Gases Report, 2010; Turkey's estimated anthropogenetic methane emissions ranked $12^{th}$ in the world. Oil and natural gas systems represents half of Turkey's anthropogenic methane emissions, 57.2 MM tones $CO_2$ equivalent, and an additional 26 %( 28 MM tones $CO_2$ equivalent) come from agriculture (manure management), coal mining and wastewater.

Turkey expressed interest in developing clean energy opportunities for use of methane captured from both coal beds and coal mines to reduce emissions and use the gas.

Turkey's involvement in GMI is important since it is expected to start and flourish collaborative projects in capturing CMM and AMM in the years to come. However, it is equally important to already start some of the background work that large-scale collaborative projects under GMI can be built on.

In that regard, this study can be considered one of the few studies that investigate methane emissions and methane production potentials from abandoned longwall panels in Turkey. More specifically, this study focuses on emissions of Yeni Çeltek Coal operation in Amasya.

As mentioned in the previous paragraphs, predicting emission potential from abandoned mine workings requires knowledge about a number of influential factors, including characterization of overlying strata and the reservoir properties of the coal seam. Thus, this study focuses on characterization of the overlying strata over the abandoned panels and proposes a pilot study to predict coal seam reservoir properties by integration of ventilation data measured in air ways with the numerical reservoir simulation. To our knowledge, this approach and history matching of ventilation air data have not been tried and demonstrated in the literature before to estimate coal seam reservoir properties.

# CHAPTER-2

# LITERATURE REVIEW

In order to make an evaluation of coal mine methane emission and production potential from abandoned mines, both the properties of coal as gas reservoir and the geomechanical changes caused by underground mining should be understood well. This chapter reviews the general characteristics of coal as a reservoir and underground mining operations, more specifically longwall mining, that impact gas flow and accumulation.

## 2.1 ORIGIN OF COAL

Coal is a solid brittle, combustible, carbonaceous rock formed by decomposition and alteration of vegetation by compaction, temperature, and pressure (Speight, 2005). The term coal refers sedimentary rocks; contain organic material more than 50 percent by weight and more than 70 percent by volume (Ahmed, Centilmen, & Roux, 2006)

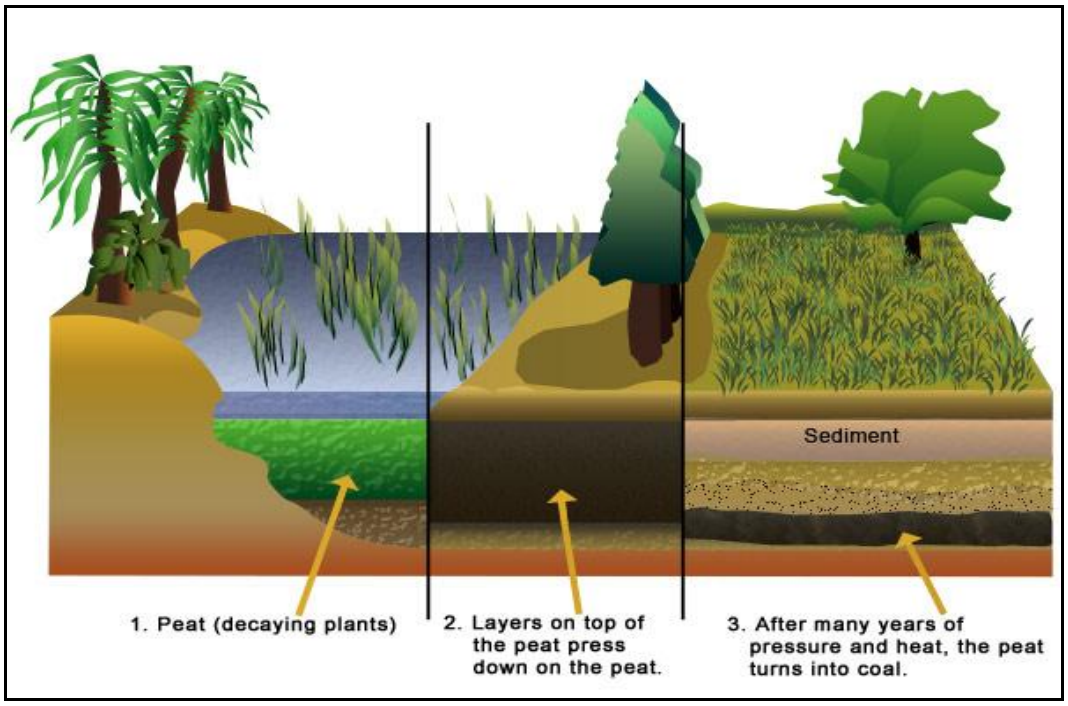


**Figure 3: Diagram of how vegetation became coal (Library and Archives Canada, 2010)**

The process of coal formation begins in a swamp. When plants died, their biomass (dead bodies, mosses, leaves, twigs, and other parts of trees) was deposited in anaerobic, aquatic environment where low oxygen levels interrupt the decaying process and $CO_2$ release to preserve as much carbon as possible. Successive generations of this type of plant growth and death formed deep deposits of un-oxidized organic matter. At various intervals, the deposits are covered by sand and mud when a river floods or when ocean levels rise. Under the weight of these sediments, the peat may lose some of its water and gases, eventually turning into a soft brown coal called lignite. With increasing pressures or temperatures, more water and gases are driven off, forming the common bituminous family of coals. Finally, high temperatures and pressures may cause bituminous coal to turn into a hard black coal called anthracite.

The product from the initial decomposition is called peat. During the formation of peat, vegetal material altered both chemically and physically.


**Figure 4: Peat (Geology.com, 2010)**

Change from peat to coal is associated with a progressed decrease in moisture, oxygen and volatile material and increase in the percentage of fixed carbon, sulphur and ash content.

The progress reduction in moisture and volatile content leads increase in rank of coal on which several geologic factors play role. These factors can be listed as follows (Stefanko, 1983):

- Pressure and heat accompanied with depth of burial
- Time

- Structural deformation
- Heat of nearby intrusive igneous rocks
- Plant decomposition and environment of coal accumulation

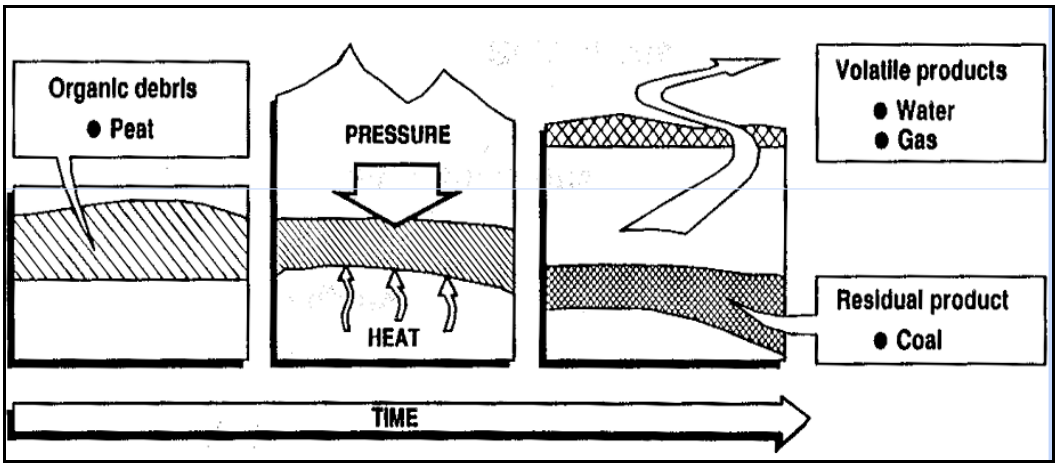


**Figure 5: Coalification Process (Mohaghegh & Aminian, 2007)**

## 2.2 COAL TYPES

Coal type reflects the nature of the plant debris from which the original peat was derived, including the mixture of plant components (wood, leaves, algae, etc.) involved and the degree of degradation to which they were exposed before burial. It is about the amount of different organic materials and the kinds and amount of minerals that coal contained.

Coal exists as various types, and each type has distinctly different properties from the other types.

American Society for Testing and Materials' (ASTM) classification system distinguishes

among four coal classes, each of can be subdivided into several groups:

1. ANTHRACITE

Anthracite, the highest rank of coal, is used primarily for residential and commercial space heating. This class is composed of three subdivisions as: meta-anthracite, anthracite, semi-anthracite.

Meta-anthracite is super anthracite that has a fixed carbon content as 98% or more and volatile matter content of 2% or less. It is very rarely found and not used for fuel.

Anthracite has a fixed carbon content that ranges from 92 to 98% and volatile matter content of 2 to 8%. It has an iron black color and dull to brilliant luster. It burns with a short pale blue flame, emits little odor and does not coke. Its fuel value is not as much as the semi-anthracite or high-bituminous coal.

Semi-anthracite has a fixed carbon content ranges from 86 to 92% and volatile content ranges from 8 to 14%. It has almost same properties with anthracite coals however semi-anthracite coals has more cleats which making it a very friable coal. Since it has more volatile material its combustion is more rapidly and efficiently than anthracite coals.

This class contains hard, brittle, and black lustrous coals and generally referred to as hard coal. The moisture content of fresh-mined anthracite generally is less than 15 %. The heat content of anthracite ranges from 22 to 28 million Btu / ton on a moist, mineral-matter-free basis.


**Figure 6: Antracite (Geology.com, 2010)**

2. BITUMINOUS

Bituminous coal is a dense coal, usually black, sometimes dark brown, often with well defined bands of bright and dull material, used primarily as fuel in steam-electric power generation, with substantial quantities also used for heat and power applications in manufacturing and to make coke.

This class can be divided into medium volatile bituminous and low volatile bituminous coals. Low volatile bituminous coal has fixed carbon content in the range between 78 - 86% while medium volatile bituminous coal has fixed carbon content in the range of 69 – 78%. These coals are nearly smokeless in burning. The moisture content of bituminous coal is usually less than 20 % by weight. The heat content of bituminous coal ranges from 21 to 30 million Btu/ton on a moist, mineral-matter-free basis.

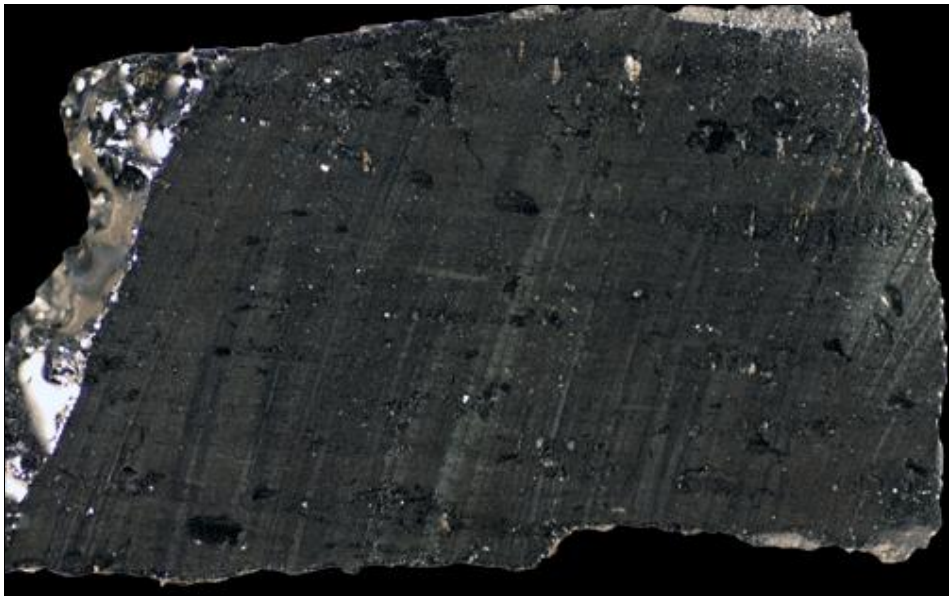

**Figure 7: Bituminous coal (Geohistory.valdosta.edu, 2010)**

3. SUB-BITUMINOUS

Coals whose properties are in the range from those of lignite to those of bituminous coal are called sub-bituminous coals, used primarily as fuel for steam-electric power generation. It may be dull, dark brown to black, and soft and crumbly at the lower end of the range, to bright, black, hard, and relatively strong at the upper end. Sub-bituminous coal contains 20 to 30 % inherent moisture by weight. The heat content of sub-bituminous coal ranges from 17 to 24 million Btu / ton on a moist, mineral-matter-free basis.

4. LIGNITE

Lignite is the lowest rank of coal which used almost exclusively as fuel for steam-electric power generation. This class can be divided into two groups as lignite and brown coal. Lignite is consolidated and the brown coals are un-consolidated. (Stefanko, 1983) These two sub-class, lignite and brown coal are often used as interchangeably because they are both in brown color and have similar properties. Lignite has a high inherent moisture content, sometimes as high as 45% and the heat content of ranges from 9 to 17 million Btu/ton on a moist, mineral-matter-free basis (Speight, 2005).


**Figure 8: Lignite (Geology.com, 2010)**

Coal used for this study is in the lignite class and Yeni Çeltek Coal Enterprise provided properties of the coal.

**Table 2: Coal types and their properties (Suarez-Ruiz & Crelling, Applied Coal Petrology, 2008)**

| | | | | | % Vitrinite Reflectance | | % Vitrinite Reflectance | |
|---|---|---|---|---|---|---|---|---|
| | | | | | (oil, 546 nm) | (Diessel, 1992a) | (oil, 546 nm) | (Teichmüller, 1982)* |
| Rank Stage | % Carbon (daf) | % Volatile Matter (daf) | Gross Specific Energy (MJ/kg) | % in situ Moisture | $R_{random}$ | $R_{max}$ | Rank Subclass | $R_{random}$ |
| Wood | 50 | >65 | | | | | | |
| Peat | 60 | >60 | 14.7 | 75 | 0.2 | 0.2 | | 0.26 |
| Lignite | 71 | 52 | 23 | 30 | 0.4 | 0.42 | | 0.38 |
| Subbituminous | 80 | 40 | 33.5 | 5 | 0.6 | 0.63 | C | 0.42 |
| | | | | | | | B | 0.49 |
| | | | | | | | A | 0.65 |
| High volatile Bituminous | 86 | 31 | 35.6 | 3 | 0.97 | 1.03 | C | 0.65 |
| | | | | | | | B | 0.79 |
| | | | | | | | A | 1.11 |
| Medium volatile Bituminous | 90 | 22 | 36 | <1 | 1.47 | 1.58 | | 1.5 |
| Low volatile Bituminous | 91 | 14 | 36.4 | 1 | 1.85 | 1.97 | | 1.92 |
| Semianthracite | 92 | 8 | 36 | 1 | 2.65 | 2.83 | | 2.58 |
| Anthracite | 95 | 2 | 35.2 | 2 | 6.55 | 7 | | 5 |

## 2.3 CLASSIFICATION OF COALS

Generally, two types of classification system defined which are scientific and commercial. The scientific systems of classification are concerned with origin, composition and fundamental properties of coals, while the commercial systems addresses trade and market issues, utilization, technological properties and sustainability for certain end uses.

Mostly used classification system classifies the coals as follows:

High rank coals, which are medium volatile bituminous coals or higher ranked coals, are classified based on their fixed carbon and volatile material content. On the other hand, low-rank coals are classified in terms of their heating values.

The rank classification system used in the United States derives from the needs for classifying coal for its principal commercial uses: combustion for electric power generation and product of coke for the metallurgical industry however it has certainly

satisfactory for scientific uses as well (Miller, 2005).

This classification system, developed by the American Society for Testing and Materials (ASTM), is based on dry, mineral-matter-free volatile matter free heating value.

The ASTM classification establishes four classes of coal, each of which is subdivided into two or more groups. In common usage the names of the ranks are taken from the class names-anthracite, bituminous, sub-bituminous, and lignite.

**Table 3: ASTM Coal Classification by Rank (Schobert, The Geochemistry of Coal, 1989)**

**ASTM Coal Classification by Rank**

| Class and group | Fixed carbon, % | Volatile matter, % | Heating value, Btu/lb |
|---|---|---|---|
| I. Anthracitic | | | |
| 1. Metaanthracite | >98 | <2 | |
| 2. Anthracite | 92–98 | 2–8 | |
| 3. Semianthracite | 86–92 | 8–14 | |
| II. Bituminous | | | |
| 1. Low volatile | 78–86 | 14–22 | |
| 2. Medium volatile | 69–78 | 22–31 | |
| 3. High volatile A | <69 | <31 | >14,000 |
| 4. High volatile B | | | 13,000–14,000 |
| 5. High volatile C | | | 10,500–13,000 |
| III. Subbituminous | | | |
| 1. Subbituminous A | | | 10,500–11,500 |
| 2. Subbituminous B | | | 9,500–10,500 |
| 3. Subbituminous C | | | 8,300–9,500 |
| IV. Lignitic | | | |
| 1. Lignite A | | | 6,300–8,300 |
| 2. Lignite B | | | <6,300 |

Two additional terms are used in the classification process, coal type and coal grade.

Coal grade is refers to the behavior of the coal during use. It has implications of the coal quality and therefore the economic value of the coal. Actually, grade is not used for classification because grade of the coal is determined by the type and rank (Schobert, The Geochemistry of Coal, 1989).

## 2.4 RANK OF COAL

Rank is defined as the degree of maturation of coal and it is indication of the extend metamorphism (or coalification) the coal undergoes. There is a continuous gradation of composition and properties from the original unaltered plant material through coals of increasing carbon content to nearly pure graphitic carbon. The composition of a particular coal along this sequence from plant material to graphite represents the extent of its geochemical maturation. The extent of maturation of a coal determines its rank (Schobert, The Geochemistry of Coal, 1989). Since there is a continuous increase in carbon content with increasing maturation and also greater degrees of maturation usually require longer times, the rank of a coal provides a qualitative indication of its age and carbon content which is calculated on a dry, mineral-matter-free basis. The heating value increases with rank but begins to decrease with semi-anthracitic and higher rank coals. This decrease in heating value is due to the significant decrease in volatile matter (Miller, 2005). American Society for Testing Materials (ASTM) consortium devised a classification system that is based on the chemical properties of the whole coal and the optical properties of the vitrinite maceral group. The properties most commonly used for rank classification in the U.S. include fixed carbon content, volatile matter content, sulfur content, gross calorific value and vitrinite reflectance (Mavor, Close, & McBane, 1994).

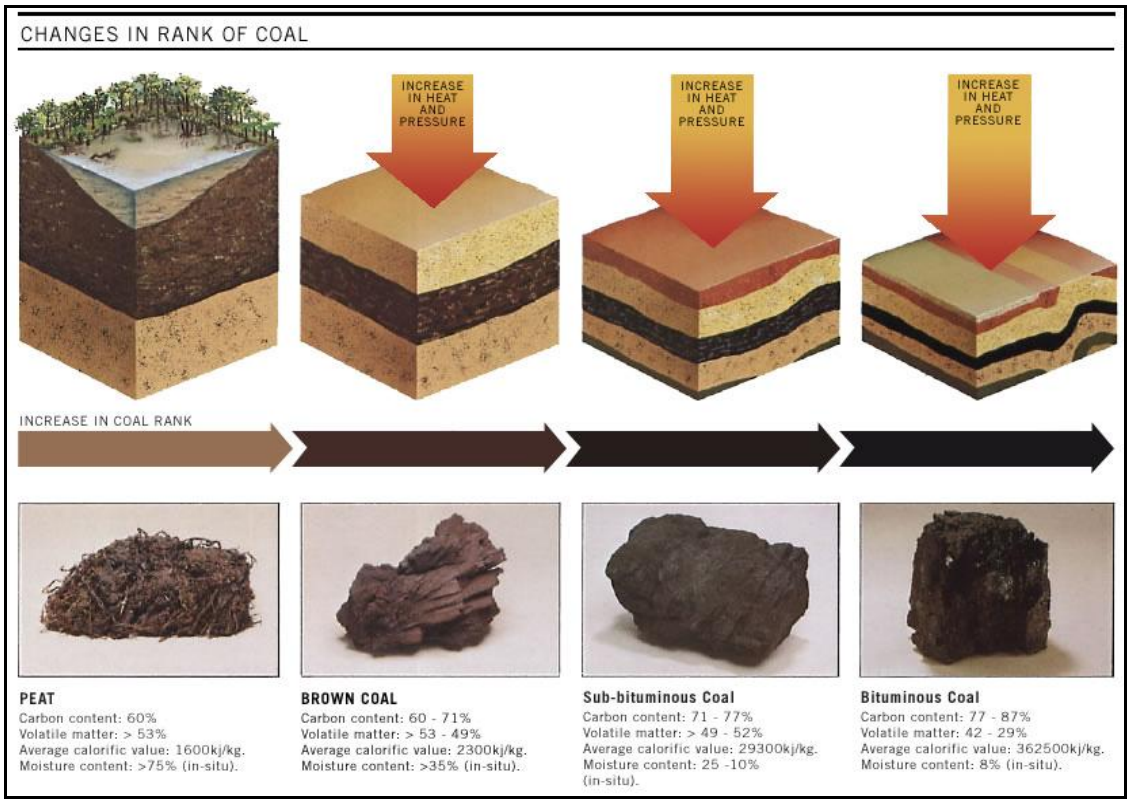


**Figure 9: Change in properties of coal with temperature and pressure (Rank of Coal, 2010)**

## 2.5 RESERVOIR CHARACTERISTICS OF COAL BEDS

Methane bearing coals are considered to be the significant gas resource. Although coal is a porous medium, it has a more complex structure than conventional clastic reservoirs. Therefore, the coal seam needs more attention as a gas reservoir.

Coal is classified as a continuous-type, unconventional gas reservoir, as coal bed methane plays typically covers large areas of sedimentary basins and because gas is stored dominantly in an adsorbed rather than a free state unlike conventional gas reservoirs. Although coal reservoirs tend to be continuous, they are extremely

heterogeneous and have complex reservoir properties.

In most conventional reservoir rocks, gas sourced from elsewhere and migrated from its original source, however in coal bed methane reservoirs most of the gas evolved in situ (Riese, Pellzmann, & Snyder, 2005).

Trapping mechanism in coal differ from conventional mechanisms as in coal the major fraction of methane is adsorbed on internal rock surfaces. Adsorbed molecules cling to the surface by the van der Waals forces and storage capacity is increased with confining pressure (Suarez-Ruiz & Crelling, Applied Coal Petrology, 2008). Since the dominant mechanism for gas storage is adsorption, dynamics of the reservoir system is highly complex.

### 2.5.1 POROSITY

Compared to many sedimentary rocks, coal beds have the capacity of storing huge amount of methane. Properties like adsorption depend largely on coals' degree of porosity. However, porosity as conventional meaning implies that the pore volume percentage occupied by pores. On the other hand, porosity in coals are mostly implies the internal surface area of the pores.

Coal has a nano-porous aromatic fabric with an extremely large internal surface area where gases can absorb. Therefore, coal can hold an extensive amount of gas in pores with an adsorbed state in which the trapping mechanism of gas is provided by hydrostatic pressure.

Coal is a heterogeneous and anisotropic porous media, which characterized by two distinct porosity (dual-porosity) systems: macropores and micropores. The macropores, also known as cleats, constitute the natural fractures common to all coal seams. Micropores, are the primary porosity matrix system of coal seams and makes the

majority of coal's total porous structure or the matrix, contain the vast majority of the gas.

Pore diameter in a coal matrix is extremely small so that micropores are in accessible to water.

## 2.5.2 PERMEABILITY

Coal deposits are naturally fractured gas reservoirs. The principal fracture network in coal, as names cleat, is comprised of closely spaces almost vertical fractures. Cleats consist of two types as face cleats and butt cleats. These fractures divide the coal into discrete matrix blocks, bounded on the sides by fractures and on the top and bottom by bedding surfaces (Levine, 1996) . Face cleats are continuous and can extend for long distances. Butt cleats are short and discontinuous, generally vertical to the face cleats. Since face cleats are more permeable than the butt cleats, they constitute main pathways for gas production and the butt cleats behave as feeder network.

Due to the nature of two fracture sets, coal seam permeability in vertical direction is usually significantly lower than horizontal permeability, concluded as permeability anisotropy.

Transport of methane within coal seam is considered to flow along cracks and fissures rather than diffuse through them. Gas flow rate depends on the permeability of the coal and neighboring strata. The term permeability refers the gateway for methane through mass of coal. The flow rates can be measured by utilizing Darcy's equation in terms of milidarcies.

Laboratory experiments had been showed that coal, free from cracks, is substantially impermeable therefore flow through coal is occurred in the fracture system.

The transport mechanism has simply three stages. The first stage involves a very slow diffusion from and through the micropores to microfractures. Secondly, the flow of gas proceeds through microfractures to cleats or fractures, and the last stage is gas movement through cleats and fractures to the open surface.

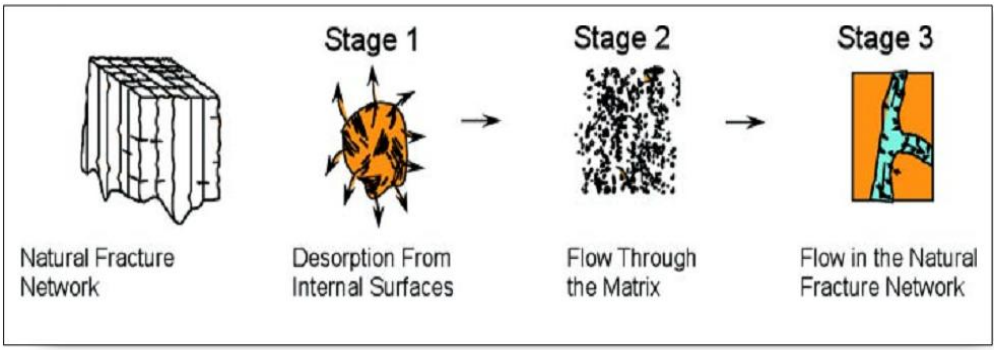


**Figure 10: Gas storage and transport mechanisms for coal reservoirs (Zuber & Boyer, 2010)**

Cleat permeability is one of the most important physical parameters governing gas emission from coal (Jones, Ahmed, Abou-Sayed, Mahyera, & Sakashita, 1982). In order to plan the gas drainage system properly in the mine, information about gas pressure, gas composition, and location of the gas reservoirs and permeability of the seam is required.

The following factors influence the coal permeability (Enever & Hennig, 1997)

- Effective stress
- Coal petrography
- Mineralization
- Degree of fracturing

- Gas type and pressure
- Water

## 2.5.3 METHANE ADSORPTION-DESORPTION BEHAVIOR IN COAL

Compared to conventional reservoir rocks, coal beds have the capacity of storing huge amount of methane. The quantity of gas that can be stored in the pore space of most sedimentary rocks is a function of temperature and pressure. However, coal can hold a significant amount in the pores, since it has an extensive internal surface, with an adsorbed state (Cote, Collings, Pilcher, & Talkington, 2004, April).

The difference in storage capacity is due to primarily coal's internal pore structure. Coal has a nano-porous aromatic fabric with an extremely large internal surface area where gases can absorb. The adsorption capacity of coal varies greatly depending on the composition of the gas being adsorbed and the composition of the coal (Suarez-Ruiz & Crelling, Applied Coal Petrology The Role of Petrolgy in Coal Utilization, 2008).

Methane is stored mainly in the matrix of the coal and partly in fracture spaces. In the coal, methane molecules are packed tightly as a monolayer on the large internal surface area which defined as adsorption and held there by hydrostatic pressure (US EPA, 2009)

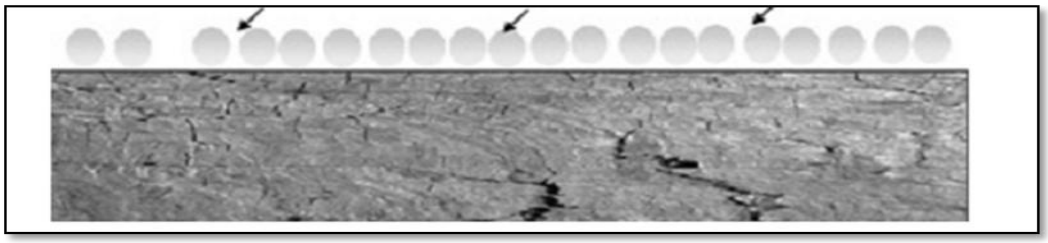

**Figure 11: The adsorbed gas to the coal matrix (Oraee & Goodarzi, 2010)**

In "CBM Principle and Practice Guide" prepared by Halliburton, according to Brunauer's definition the isotherm refers the volume of gas adsorbed on a solid surface as a function of pressure for a specific temperature, gas, and solid material (Halliburton, 2007). Adsorption isotherms are mathematical functions that characterize the theoretical adsorption mechanism and used for calculate the theoretical gas content of the coal seam. According to Brunauer's study, sorption isotherms classifies as five different types. Type I isotherms defines the mechanism at the adsorption of gases in microporous solids. At higher pressures the absorbed gas amount becomes asymptotic with pressure and at higher temperatures absorbed gas amount is decreased. At low pressures, large volumes of gas desorbed with small changes in pressure. (Halliburton, 2007)

Type I isotherms closely describe the adsorption/desorption behavior of methane on coals. For the most excepted model for methane sorption behavior is the Langmuir Isotherm. As pressure in the coal seam increased with depth or the hydrostatic pressure of water in the capillaries, the capacity of coal for adsorbing more methane improves.

The major assumptions in deriving the Langmuir's equation are as follows:

- One gas molecule is adsorbed at a single adsorption site. (monolayer string of the molecules)
- An adsorbed molecule does not affect the molecule on the neighboring site.
- Sites are indistinguishable by the gas molecules.
- Adsorption is on an open surface, and there is no resistance to gas access to adsorption sites.

At equilibrium for a given temperature, rate of molecules attached to the surface is equal to rate of molecules of detached from the surface. This can be described as follows:

r =rate of adsorption and desorption from complete monolayer coverage at constant temperature

θ =fraction of sites covered or fraction of monolayer coverage

P =pressure

rθ =rate of gas molecules leaving those occupied adsorption sites

k (1-θ) P = rate of gas molecules attaching to adsorption sites

where

k =adsorption equilibrium constant

Equating the adsorption and desorption rates:

rθ = k (1-θ) P

Rearranging the equation:

$$\theta = \frac{\left(\frac{k}{r}\right)P}{1+\left(\frac{k}{r}\right)P}$$ **Equation 1**

Since θ can be defined as the fraction of monolayer coverage

$$\theta = \frac{V}{V_{max}}$$ **Equation 2**

Where

V= gas volume adsorbed per unit weight of solid at pressure P

$V_{max}$= maximum monolayer volumetric capacity per unit weight of solid

Since k/r would be constant at a given temperature, it is denoted as "b" as a constant, then the equation is become:

$$V = V_{\max} \frac{bP}{1 + bP_L} \qquad \textbf{Equation 3}$$

This equation is Langmuir equation and b is the Langmuir constant or reciprocal of the Langmuir pressure, $P_L$, defined as the pressure that a gas content equal to half of the maximum monolayer capacity (Halliburton, 2007).

The Langmuir equation can be used for construction of the isotherm for methane adsorption characteristics on coal seam in different pressures with the constant temperature, which is similar to the coalbed methane production conditions. (Halliburton, 2007)

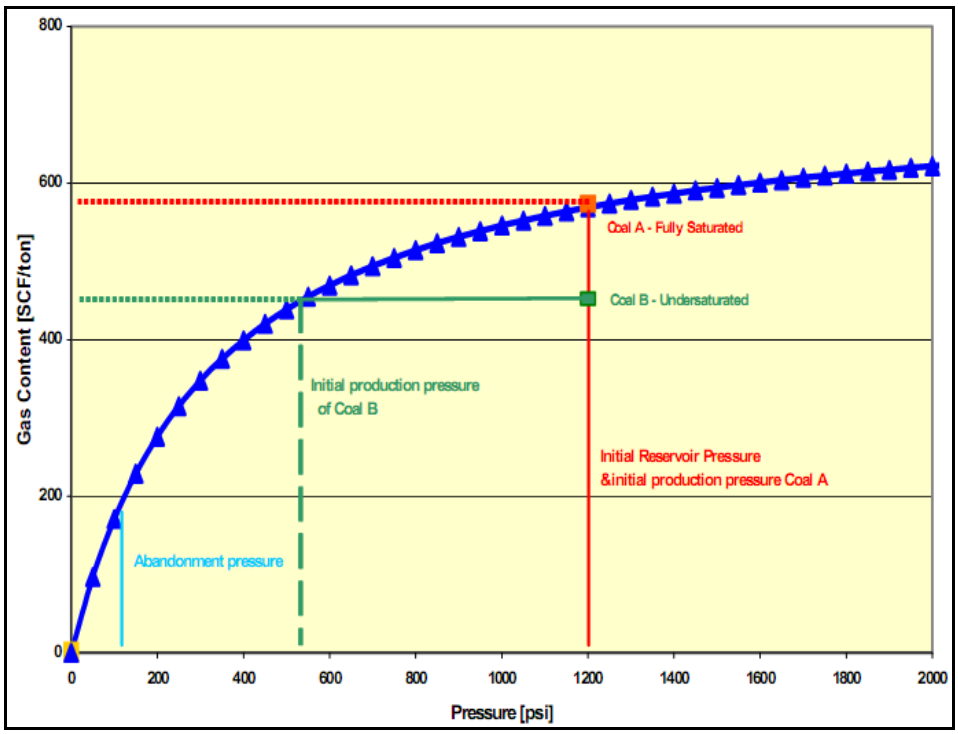


**Figure 12: Langmuir isotherm (Saulsberry & Schraufnagel, 1996)**

An isotherm can be used to estimate the maximum amount of methane that might be adsorbed in the coal, the pressure at which desorption will start, and the amount of methane remaining in the coal at an assumed abandonment pressure.

Langmuir pressure constant ($P_L$) represents the pressure at which gas storage capacity equals one half of the maximum storage capacity ($V_L$) or a characteristic measure of residence time for a gas molecule on the surface (Karacan Ö. C., Evaluation of the relative importance coalbed reservoir parameters for prediction of methane inflow ratesduring mining of longwall development entries, 2008) and to show the effects, different $P_L$ values are plotted on the following chart Figure 13.

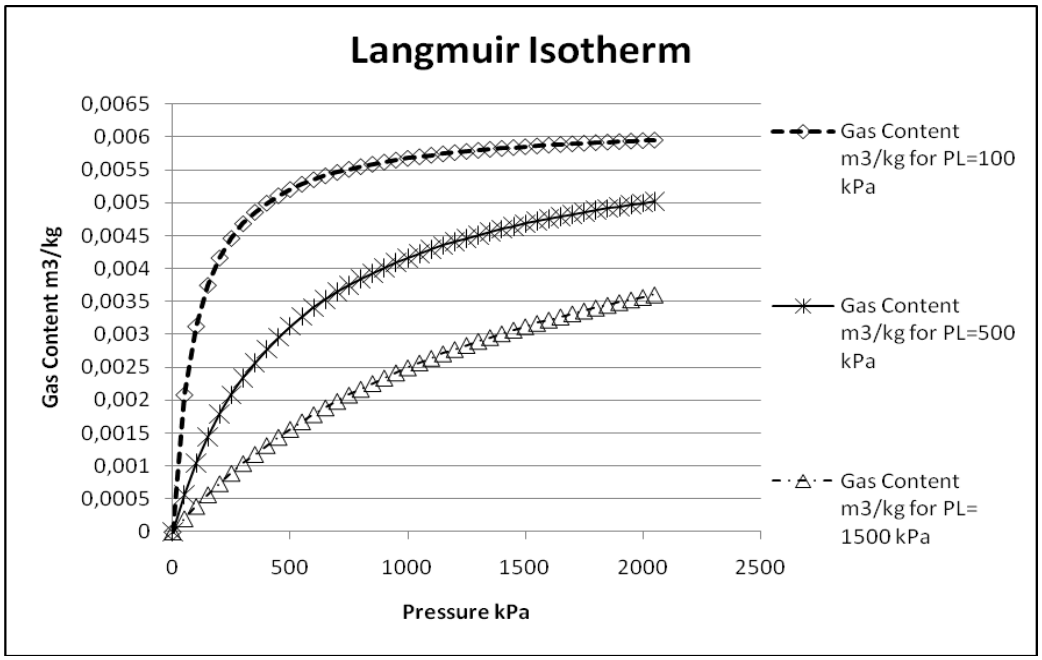


**Figure 13: Langmuir Isotherm for different $P_L$ values**

There are other parameters also effect the shape of the isotherm. Construction of the isotherm based on the assumption of the constant temperature however, it is a known fact that the adsorption capacity of coal decreases with increasing temperature. The composition of the adsorbed gas also affects the isotherm's shape and therefore adsorption capacity of the coal. Different gasses have different affinities to coal therefore composition of the gas is important for the methane storage capacity. Moisture competes with methane for adsorption on the coal surface. On the other hand moisture may block the gas access to micropores therefore gas adsorption measurements shows higher results on dry coal samples than the wet ones. Ash content should be also taken into account since ash is the part of coal which does not adsorb gas.

## 2.5.4 GAS CONTENT

The idea of all coal seams can be accepted as gassy is not wrong in order to be in the safe zone for design and process of a mine.

In coalbed methane is predominantly stored within micropores as a molecularly adsorbed state. Gas content is the standard volume of gas per unit weight of coal or rock and usually is reported in units of standard cubic feet per ton (scf/ton). The in situ gas content of coal seam can be determined by using two methods: pressure coring and direct method.

In the pressure coring gas content method contains trapping a core sample from the seam downhole within a sealed barrier to prevent any loss during retrieval of the core to surface. Total in-situ gas content can be measured by collecting the gas volume desorbs from the core. This method is the only method that directly measures the gas content of a cored rock sample. However this method requires specialized equipment which may not be functional to use in the field circumstances (Nelson, 1999).

The most commonly used method to measure the methane content of coal is the U.S. Bureau of Mines, Direct Method.

Standard cores usually provide the most reliable gas content estimates. Other types of samples, such as side-wall cores, drill cuttings, and chips from slotting procedures, are not as reliable as standard cores. If there is no active drilling on a prospect, other methods including estimation from depth and rank relationships or methane emission from coal mines in the area are sometimes used to estimate gas content (Mohaghegh & Aminian, 2007).

Direct method was originally developed to determine the severity of natural emissions during underground mining operations. In this method sealing freshly cut core or drill cuttings coal samples in airtight desorption canister and then measuring the volume of gas desorbs from the sample as a function of time at ambient temperature and

pressure conditions (Nelson, 1999).This method is widely used and referred as " canister desorption experiments". The volume of gas is measured by displacing the gas by water from a graduated cylinder. In this method the basic inaccuracy arise from the lost gas volume while retrieving the sample to the surface (Zuber, Sawyer, Schraufnagel, & Kuuskraa, 1987).

## 2.6 MINING COAL

### 2.6.1 MINING OF COAL USING LONGWALL METHOD AND CREATION OF "GOB"

Mining of coal deposits are performed by either surface extraction methods or using underground mining methods depending on the depth of coal deposits. In underground mining, longwall mining is the preferred method as it can maximize coal production. However, the coal seams that are to be mined with longwall technique should be continuous with few geological discontinuities, like splits and extensive faulting.

In longwall mining operations, a mechanical shearer progressively mines a large block of coal, called a panel, which is outlined with development entries or gate roads. This is a continuous process in an extensive area, where the roof is supported only temporarily during mining with hydraulic supports that protect the workers and the equipment on the face. As the coal is extracted, the supports automatically advance with the rate of mining, and the roof strata are allowed to cave behind the supports. This process creates a highly fragmented and fractured rock body behind, called a "gob" (Figure 14).

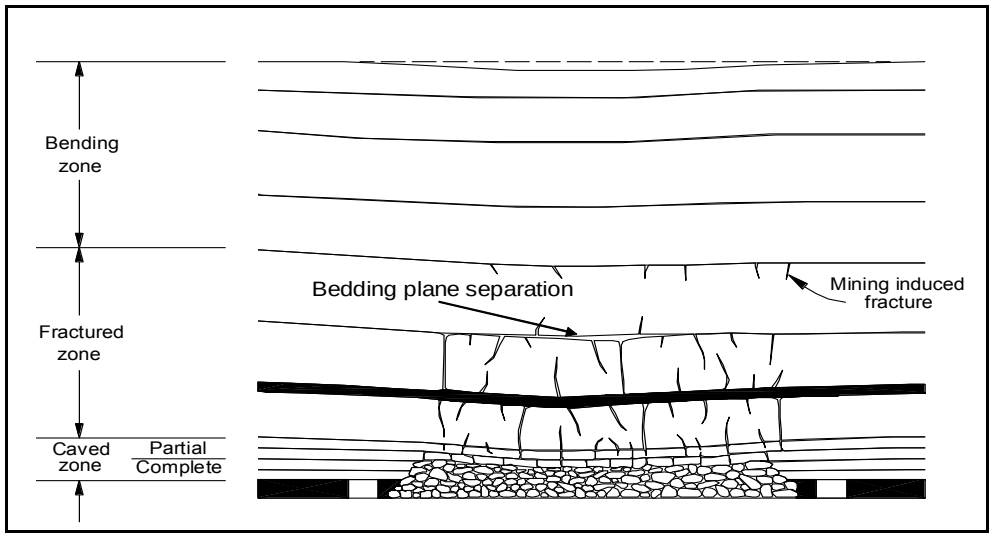


**Figure 14: Schematic cross-section showing strata movements above a longwall panel (Esterhuizen & Karacan, 2005)**

It has been suggested by (Palchik, 2003) that the "gob" is comprised of three district zones, as shown in Figure 14: a) a caved zone which is highly fragmented, and generally extends upwards three to six times the thickness of the mined coalbed. In this zone, the overlying rock layers fall into the mine void and are broken into irregular shapes of various sizes. It has been found that the height of the caved zone could reach four to eleven times the thickness of the mining height where overburden rocks are weak and porous, b) a fractured zone (Figure 14) which is characterized by mining-induced vertical fractures, and horizontal fractures caused by separations along bedding planes. The caving of the mine roof causes an area of relieved stress in this zone. The blocks in each of the broken rock layers are contacted either fully or partially across the vertical fractures, with the number and extent of the fractures diminishing with increasing height above the caved zone. The thickness of the fractured zone can vary up to 100 times the height of the mined coalbed, depending on the characteristics of the associated rock strata, thickness of the overburden, and the size of the longwall panel, c) and a bending zone where the strata may subside but do not fracture.

For gas migration and methane accumulation point of view, the occurrence of such an extensive area of mining-induced stress relief and resultant rock damage is important as it changes the gas flow-related properties in the overlying formations. Any gas that is contained within the coal beds in this area of relieved stress will be released slowly over time, while free gas in other porous formations, such as sandstones, will be released more quickly, as the permeability of these zones is dramatically increased and new permeability pathways are created. Relaxation of the roof and floor rocks and the associated fracture connectivity allows gas to flow from all surrounding gas sources toward the low-pressure sink of the underground workings, including the caved zone. Gas-bearing strata, particularly overlying gas-bearing coalbeds and sandstones, can be directly exposed to the caved zone or connected to it by fractures. In the absence of methane drainage boreholes such as gob gas ventholes, this released gas, commonly referred to as "gob gas" may enter the mine atmosphere from above during active mining and create a safety hazard (Karacan Ö. C., Reconciling longwall gob gas reservoirs and venthole production performances using multiple-rate drawdown well test analysis, 2009).

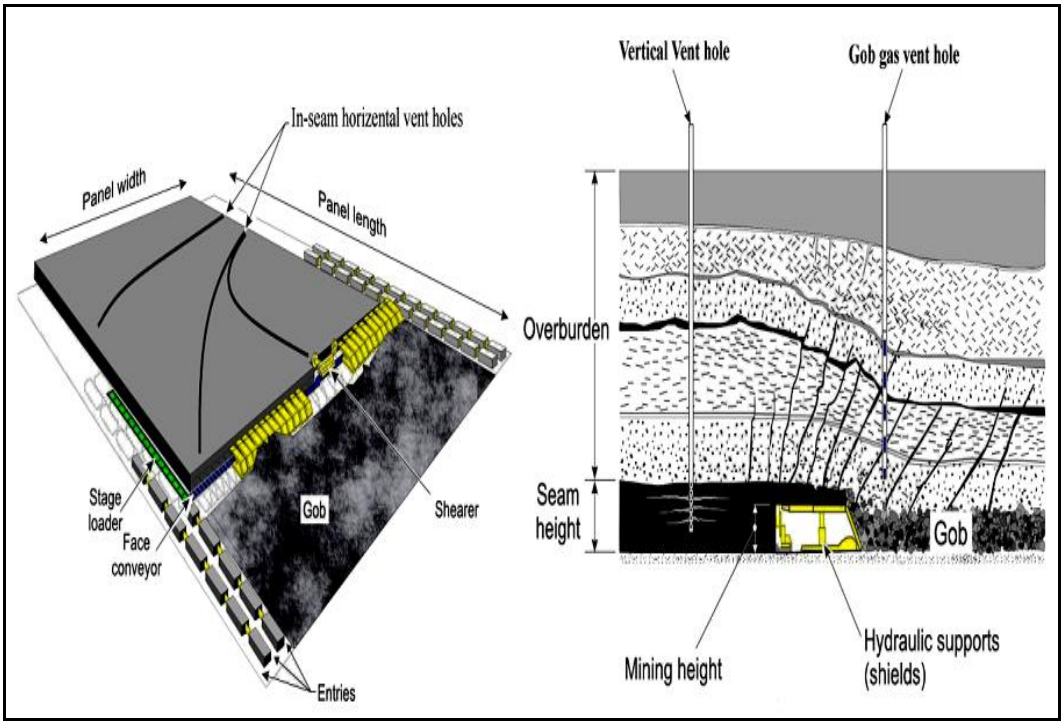


**Figure 15: Underground mining and ventilation system (Karacan, Modeling and prediction of ventilation methane emissions of U.S. longwall mines using supervised artificial neural networks, 2008)**

However, if the panels are sealed and the mined abandoned, the gas released within the gob starts to accumulate in the abandoned gob area, in case it does not leak into the atmosphere, to create a gas reservoir from which methane can be produced economically as energy source and to reduce green house gas emissions.

### 2.6.2 METHANE EMISSION SOURCES DURING AND POST LONGWALL MINING FOR BUILDING OF AN ABANDONED MINE METHANE RESERVOIR

During longwall mining and afterwards, methane emissions can originate from three major sources. These sources can be summarized in the following manner: 1) gas emissions from the coal ribs surrounding the ventilation system, 2) gas emissions from the active longwall face and mined coal on the conveyor belts (this source applies only when the mine is active and producing coal), and 3) gas emissions from subsided strata (Mucho, Diamond, Garcia, Byars, & Cario, 2000).

The first gas source originates from the unmined coal bed adjacent to the development entries of the bleeder system and from the solid coal ribs. Although this emission tends to decrease over time, it may become a significant contributor to the ventilation system during mining, and methane accumulation in abandoned mines. The second source is the combination of the gas content from the mined coal itself and the methane being emitted from the fresh face on the longwall, and is only a consideration when the mine is active. The third source is the fractured and caved rock in the subsided strata (gob) overlying the extracted panel as the longwall face advances, as described in the previous section. The third source applies for gas accumulation in both active mines and for abandoned mines.

### 2.6.3 TYPICAL METHANE CONTROL PRACTICES IN ACTIVE AND ABANDONED LONGWALL MINES

Gob gas ventholes are commonly used to control the methane emissions from the fractured zone and are drilled from the surface to a depth that places them above the caved zone so they do not directly interact with the ventilation system (Figure 16).

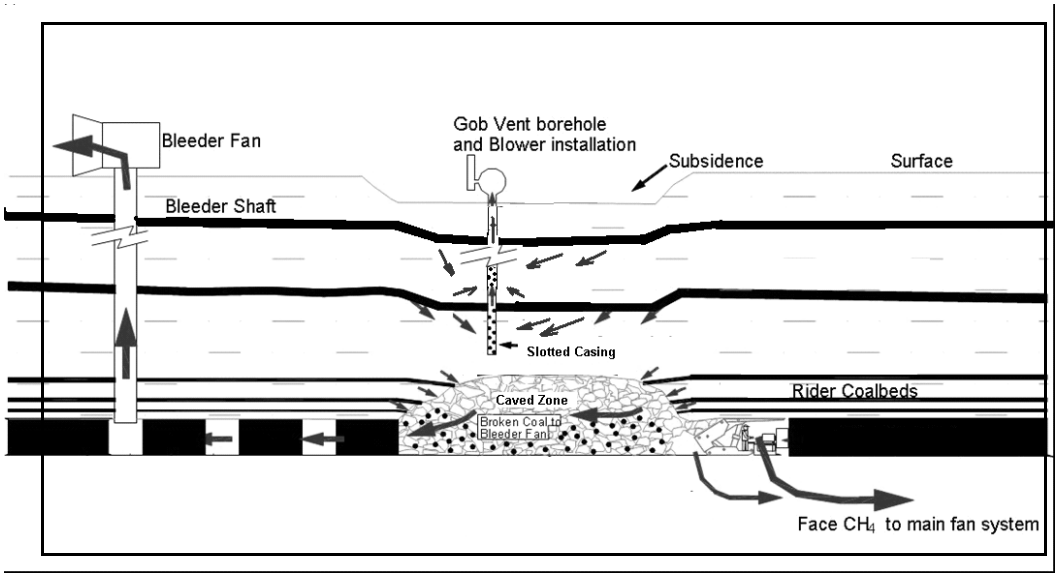


**Figure 16: Schematic of strata response to longwall mining (modified from Singh and Kendorski, 1981)**

The bottom section of the casing is slotted and placed adjacent to the expected gas production zone to improve gas drainage. These ventholes generally become productive after the mining-induced fractures propagate under the well (Diamond, 1994) during active mining. Thus, the recovery of methane from gob areas requires a consideration of both rock mechanics and fluid dynamics principles, since gas flow through fractured strata is mainly controlled by the associated permeability.

Exhausters are placed on gob gas ventholes to maintain a vacuum on the wellbore, so that they operate at the minimum possible flowing pressure and create a pressure sink in the overburden strata to induce gas flow towards the venthole. Gas production may exhibit variable gas quality. In the early stages of production, the gas quality is generally high (> 80%), and there is very little contamination by mine ventilation air. Relatively high production rates are usually sustained for only a few weeks or in some cases for a few months (Diamond et al., 1994). Later in time, gob gas production may exhibit decreased methane levels as ventilation air is drawn from the active mine

workings. The quality of the gas from gob wells can be controlled to some extent by varying the vacuum on the well to correspond with the profile of expected methane release. However, for mine safety in active mines, maintaining the methane concentration in the mine within statutory limits is always the overriding factor for controlling the vacuum on the gob gas ventholes. Therefore, commonly when the methane concentration in the produced gas reaches 25% (close to the upper limit of explosive methane + air mixture), the exhausters are de-energized as a safety measure, and the holes may be allowed to free flow.

The location of the ventholes on the panel is also important. They are usually drilled close to the sides of the panels since mining-induced fractures on the sides are open due to tensional forces. These boreholes may perform 77% better in terms of production amount than the holes drilled on the centerline of the panel where the compressional forces are greater and close the fractures. Improvements in venthole gas drainage evaluation and prediction capabilities for site-specific mining conditions and circumstances can address longwall gas control issues in active mining, and gas production as an energy source after abandonment of the panels by sealing. A theoretical reservoir modeling approach is the best, if not the only means to predict methane emissions in advance of mining and after abandoning the panels.

### 2.6.4 MODELING APPROACH FOR OPTIMIZING GOB GAS VENTHOLE PERFORMANCES

In general, experience suggests that it is difficult to make accurate gas production estimates for gob wells and that these predictions are underestimated relative to actual gob gas venthole production by a factor of two or more. The key factors to this underestimation of gas production capability are the difficulty in predicting the degree of stress relief in gas-bearing strata associated with longwall mining and, consequently, the drainage radius for each well (Zuber, 1998).

A detailed model to realistically represent the multiple variables associated with underground coal mining operations and their interaction and influence on the performance of gob gas ventholes does not currently exist. Previously, (Ren & Edwards, 2002) used a computational fluid dynamics (CFD) modeling approach to investigate gas capture from surface gob gas ventholes. That paper introduced how this approach could be used to improve the design of surface gob wells for methane recovery while minimizing the leakage of air into the gob. The results indicated that the position of the wells plays an important role in determining gas production rate. Wells drilled into the areas where fractures extend towards the methane source bed were likely to achieve higher capture efficiency. Lunarzewski (Lunarzewski L. , 1998) used boundary element and sequential bed separation methods for floor and roof strata relaxation and immediate roof bending separation, as well as gas emission rate calculations to develop "Floorgas" and "Roofgas" simulation programs to characterize the strata relaxation zones, gas emission boundaries, and parameters for gas emission prediction. Tomita et al. (Tomita, Deguchi, Matsuyama, Li, & Kawahara, 2003) developed a three-dimensional (3-D) finite element model (FEM) to predict the volume of methane gas emitted from surrounding coal and rock layers based on stress distribution and permeability change.

Reservoir-modeling methods and simulators have been developed over the years that can realistically represent the complex physics of reservoir flow mechanisms in unconventional reservoirs, such as coalbeds, and gas production operations with diverse well completions (King and Ertekin, 1991). These simulators have been successfully applied in various coal basins for gas recovery from coalbeds using both vertical and horizontal boreholes (Ertekin,1988; Zuber, 1998; Young et al., 1993; Young et al., 1991). However, modeling of the reservoir behavior and prediction of gob gas venthole performances during active longwall mining requires that additional variables be considered that are not encountered in a static reservoir environment. These considerations are due to the moving boundary conditions and geomechanical response of rock units to the stresses and strains imposed by an advancing longwall face, and by

the changing reservoir properties above a panel as a response to mining. In one study, (Zuber M. , 1997) coupled the moving boundary condition due to mining and modeled the face and rib emissions during development mining. However, this study was mainly conducted on a single grid layer to analyze the gas emissions from ribs and newly exposed coal face during development mining, and thus did not consider the longwall mining environment and methane control issues associated with gobs. In a more recent study, (Karacan, Diamond, Esterhuizen, & Schatzel, May 18-19, 2005) developed a 3-D model of a new longwall mining district to simulate the effects longwall panel width would have on methane emissions and the performance of gob gas ventholes. The focus of that effort was the prediction of the incremental amount of methane emissions to be expected due to increasing panel widths and optimizing gob gas venthole completion and placement practices to capture more of this gas to prevent it from entering the underground workplace. As mine matures and coal seams are mined out, mines are closed and eventually abandoned and generally during reclamation process they can be sealed by filling the shafts or portals with gravel and shielding them with a concrete seal. Vent pipes and boreholes can be cemented to plug. When mining operations are abandoned, the methane gas production declined but the methane liberation does not stop completely. After the initial decline period, methane liberation continues at near-steady rate over an extended period of time. Even if the mine is ceased, emissions can emit to the atmosphere through the conduits particularly (Franklin, Scheehle, Collings, & Pilcher, October 2004). The rate of emissions is depending on the natural sealing character of the surrounding strata and sealing degree of artificial conduits. Diffuse emissions can occur if the overlying strata include fractures and fissures which provide flow paths through the surface.

## 2.7 YENI ÇELTEK COAL MINE

Coal is the main commodity for providing energy in Turkey. It represents for almost the half of the Turkey's total energy production (% 43 of that comes from lignite) (Uner, Kose, Gokten, & Okan, 2008). The lignite reserve is reported about 8.05 Gt in 1994 (Karayigit, Eris, & Cicioglu, 1996). However, since lignite is a low-rank coal, it is mainly used in electricity generation coal-powered thermal plants and in domestic use.

For instance, in 2009 74.9 Mt of lignite was used for electricity generation, 14.2 Mt for household heating and 15.1 Mt for industrial use, which consists of steam and coking coal generation. (General Directorate of Turkish Coal Enterprises TKI , Turkish Statistical Institute, 2010)

Extensive geological and geochemical studies have been conducted for the coal reserves in Turkey by the General Directorate of Mineral Resources (MTA) and Turkish Coal Enterprises (TKI). However studies on petrographical properties of coal and coalbed methane exploration are still limited in Turkey (Karayigit, Eris, & Cicioglu, 1996). Therefore, this study was dedicated to the latter and Yeni Çeltek coal mine was selected as the study area.

Yeni Çeltek lignite mine is located about 15 km east of Merzifon, 35 km north-west of Amasya and 90 km of Samsun. In the Yeni Çeltek Lignite Mine, longwall mining method is used. The length of the longwall panels are about 8 meters in width and have varying lengths. The faces are supported by two or sometimes three rows of 40 ton-capacity individual hydraulic supports, installed under steel caps with 1.25 meters long. The excavated coal is transported by double chain conveyors in the face, and by band conveyors in the gate roads, and by loco-trains in the mine roadways. Finally, after travelling a long distance, the coal is transported to the surface with the help of a skip. (Taşel, Ozan, Unver, & Bildik, 2001)

According to the study conducted at METU Mining Engineering Department (Taşel, Ozan, Unver, & Bildik, 2001) thickness of the coal seam ranges from 8 to 12 meters. However, the quality of the coal in various layers of the seam are varying and the coal is interbedded by various carbonaceous and shale units. Therefore, only the upper portion of this seam is mined due to its higher calorific value, determined as 4100 kcal/kg.

### 2.7.1 GEOLOGICAL SEQUENCE

The Yeni Çeltek coal mine is located in the Suluova (Amasya) basin which contains thick and laterally extensive Lower Eocene coal seams. Distribution of Eocene formations is shown in Figure 17 .

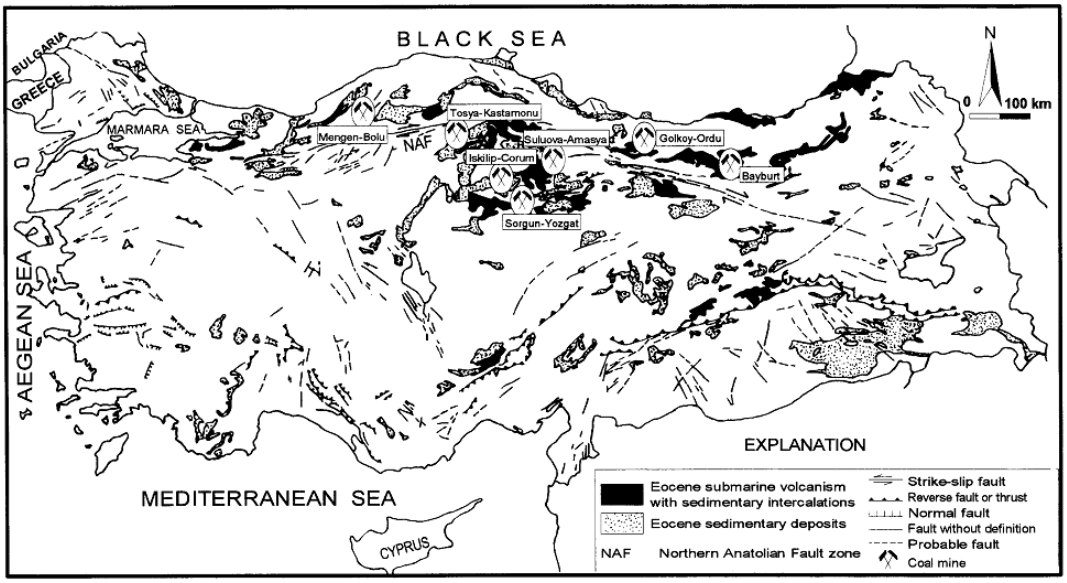


**Figure 17: Distribution of Eocene rock and location of the Sorgun and Suluova modified (Karayigit, Eris, & Cicioglu, 1996)**

Geological map, sequential stratigraphy log and cross-section according to the Suluova basin are presented Figure 18 and Figure 19.

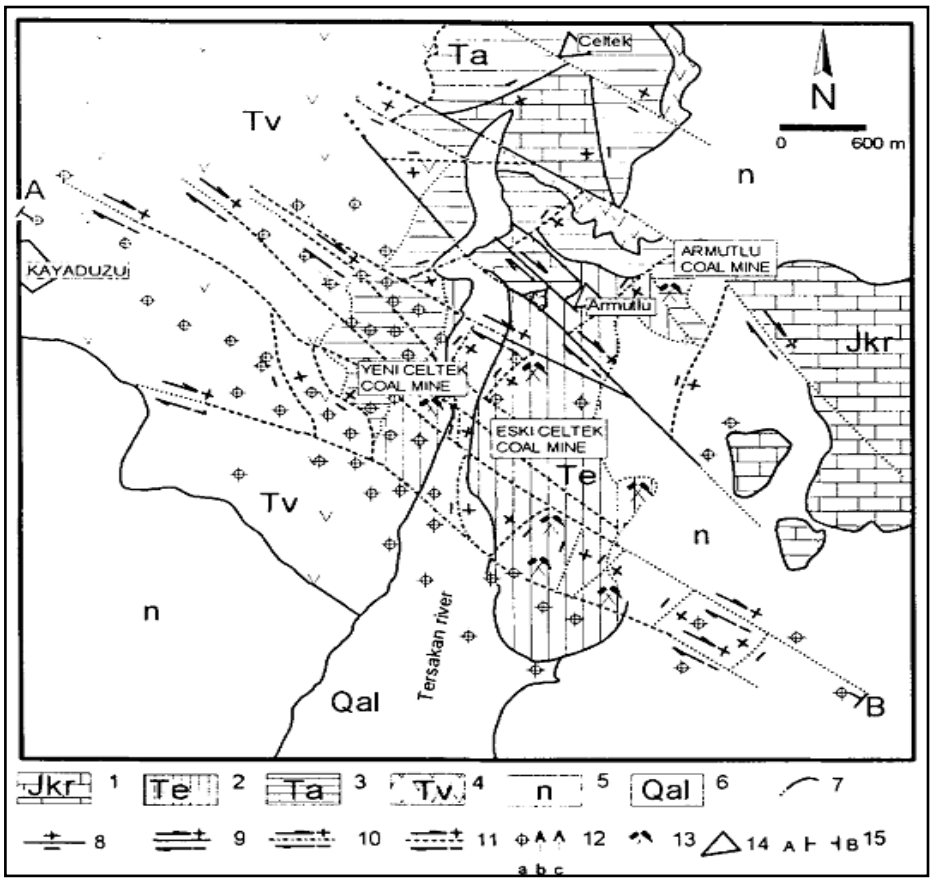


**Figure 18: Geological map of Suluova basin.**

Where : (1) Yozgat Granitoid; (2)Celtek Formation; (3) Undifferentiated Eocene rocks; (4) Cekerek Formation-marl; (5) Cekerek Formation-tuff;(6) Cekerek Formation-basalt and agglomerate; (7) Artova Ophiolitic Complex; (8) Neogene deposits; (9) alluvium; (10) bedding; (11) boundary; (12) normal fault; (13) thrust fault; (l 4) borehole; (15) coal mine; (16)village; and (17) line of cross-section. (Karayigit, Eris, & Cicioglu, 1996)

The basement of the Suluova basin consists of Jurrasic-Crateceous limestones which are grey and thin bedded and include brown to light brown claystones within the coal seam. These formations are folded formations with observed karstification. The coal seam and the bituminous shales are thought to be accumulated in lacustrine environment as evidenced by sub-bituminous shales of the Celtek formation that include abundant amorphous kerogens with characteristics of those formed in fresh water environment. (Karayigit, Eris, & Cicioglu, 1996).

Çeltek formation in Suluova basin is formed of, from bottom to top, alterations of conglomerate, sandstone, marl, coal seam, bituminous shales, alterations of sandstone and marl, and bituminous shales.

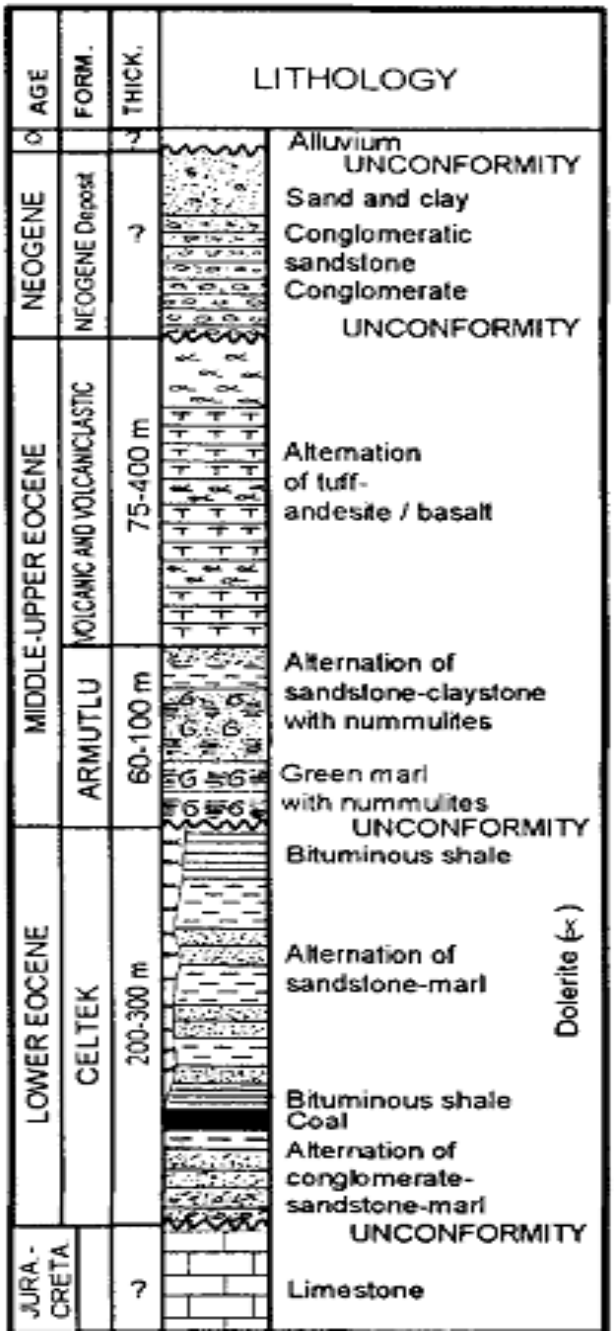


**Figure 19: Generalized stratigraphic sequence (Karayigit, Eris, & Cicioglu, 1996)**

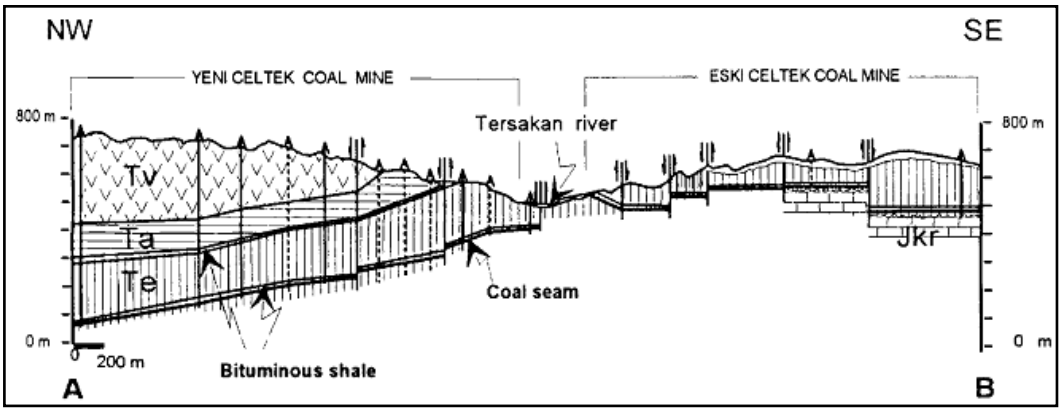


**Figure 20: Geological cross-section through the Yeni Çeltek to Eski Celtek coal mines (Karayigit, Eris, & Cicioglu, 1996)**

According to (Karayigit, Eris, & Cicioglu, 1996), the vitrinite reflectance values vary between 0.46 and 0.60 with an average of, 0.53%, and the calorific values vary between 11500 and 14000 BTU/lb on moisture and mineral matter free basis. Furthermore, the H/C and O/C atomic ratios, show that Yeni Çeltek coals can be classified as either sub-bituminous A to high-volatile C bituminous coal. This transitional character in maturation combined with the structural characteristics of the basin may be one of the reasons of experiencing intermittent and sometimes continuous gas emissions during mining.

# CHAPTER-3

## 3.1 STATEMENT OF PROBLEM

Recognizing the importance of capturing methane and using CMM for mine safety, greenhouse gas emission reduction and energy production, it should be stated that determining emissions potential from abandoned mine panels requires knowledge of influential factors including characterization of overlying strata and the reservoir properties of the coal seam.

This study focuses on characterization of the coal seam over the abandoned panels. The pilot area selected from the Yeni Çeltek Coal Mine where ventilation data were available was utilized to estimate the fluid flow related reservoir properties of the coal seams with CMG' s GEM reservoir simulator.

The findings of this study can further be used to investigate the methane emissions and possibility of productions from the gobs of abandoned mine panels in Yeni Çeltek Coal Mine. The ventilation data obtained from the measurement stations in this region were used to match the calculations of the reservoir simulation model discussed next by varying the coal properties.

## 3.2 PILOT AREA VENTILATION DATA

The objective of this study is to conduct a pilot study to explore the fluid flow related reservoir properties of the coal seams by using ventilation data and reservoir simulation for Yeni Çeltek Coal Mine. The findings of this study can further be used to investigate

the methane emissions and possibility of productions from the gobs of abandoned mine panels in Yeni Çeltek Coal Mine. In order to characterize the coal, numerical reservoir simulations of gas emissions into ventilation systems were evaluated by using ventilation flow data in fresh air stations and return airway stations in the selected region shown in Figure 21 and as an extended view in Figure 22. The ventilation data obtained from the measurement stations in this region was used to match the calculations of the reservoir simulation model discussed next by varying the coal properties.

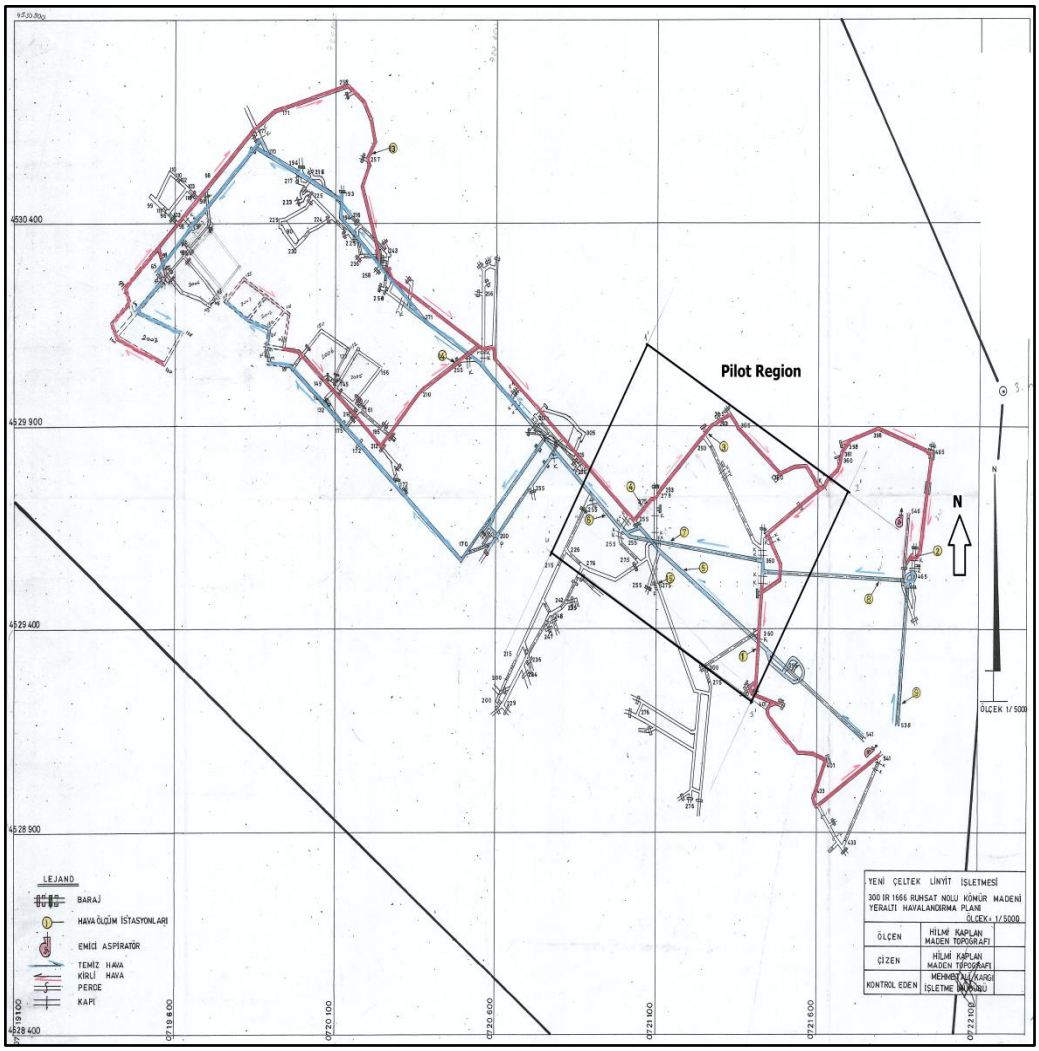


**Figure 21: Yeni Çeltek Coal Mine plan. The marked area is the pilot region used for the model.**

Ventilation data were measured for fresh air roadways (intake) at stations 5, 6, 7, 8, 9, 15 and 16, and for return airways carrying methane percentages were measured at stations 1, 2, 3, 4, 13 and 14. In addition to ventilation data according to intake and return airways, recorded ventilation airline pressures and the cross sectional areas of measurement locations were measured. From these data flow velocities across the air ways calculated.

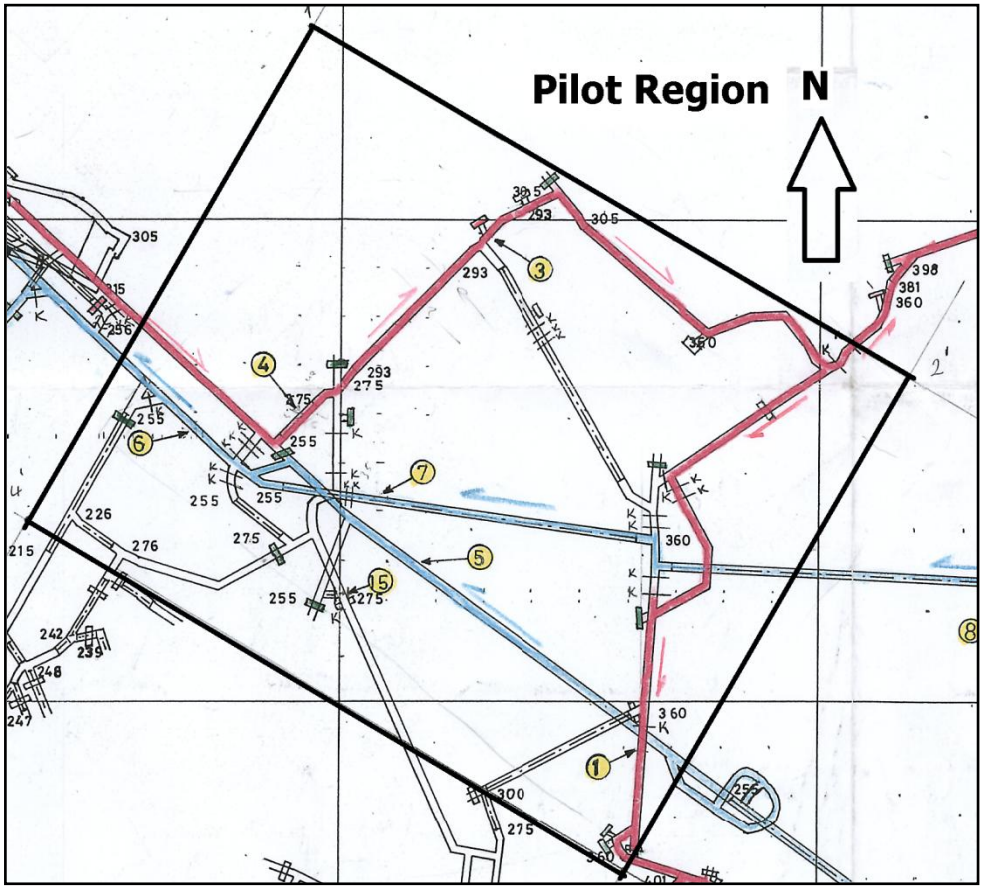


**Figure 22: Extended figure of pilot region.**

In selected region blue lines represents fresh air ways and red lines are return air ways of the ventilation system. The stations in this area for intake track are 5, 7, and 6 while for return track stations are 1, 3 and 4.

Figure 23 shows ventilation pressures measured at different dates in the mine. The data shows that the pressures changed between 970 and 990 millibar. The pressure data can be considered relatively steady and possibly fluctuates with changing cross sectional area in various locations in intake and return ways. The cross sectional areas of measurement locations are given in Figure 24 and in Figure 25 for intake and return,

respectively. Nevertheless, although the fluctuation in ventilation air pressure is not too much, this much variation in pressure may have significant effects on methane release from coals and from sealed gob areas into the working locations and to the return airway. This type of methane emission fluctuations have been observed in coal mines due to fluctuations in atmospheric pressure.

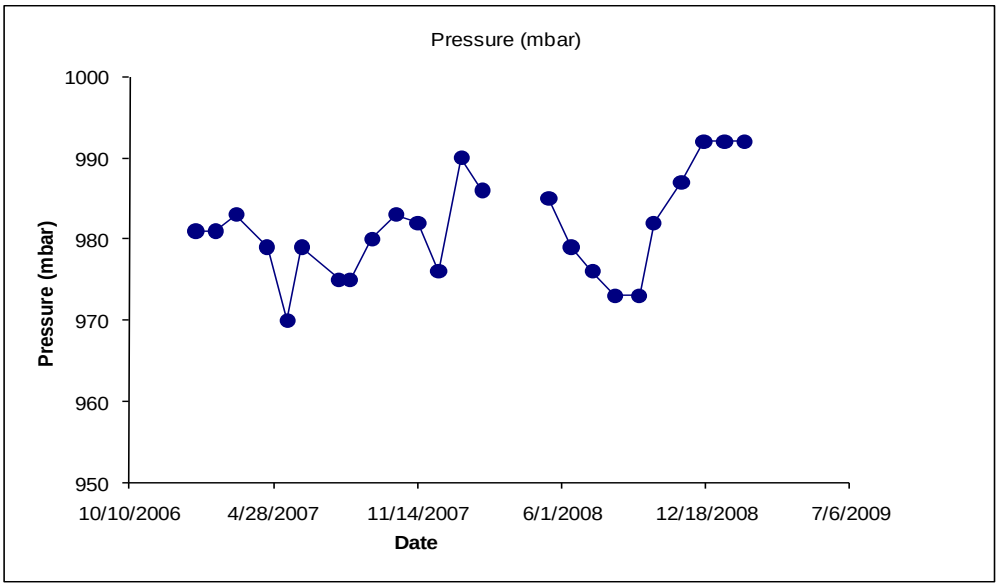


**Figure 23: Measured ventilation pressures in the mine at various dates.**

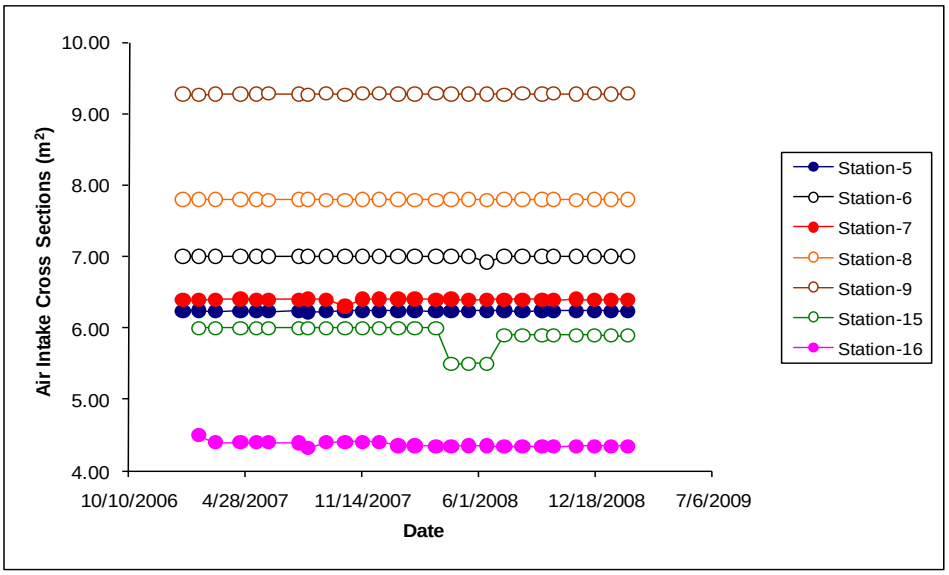


**Figure 24: Cross sectional area of air intakes at measurement stations at different dates.**

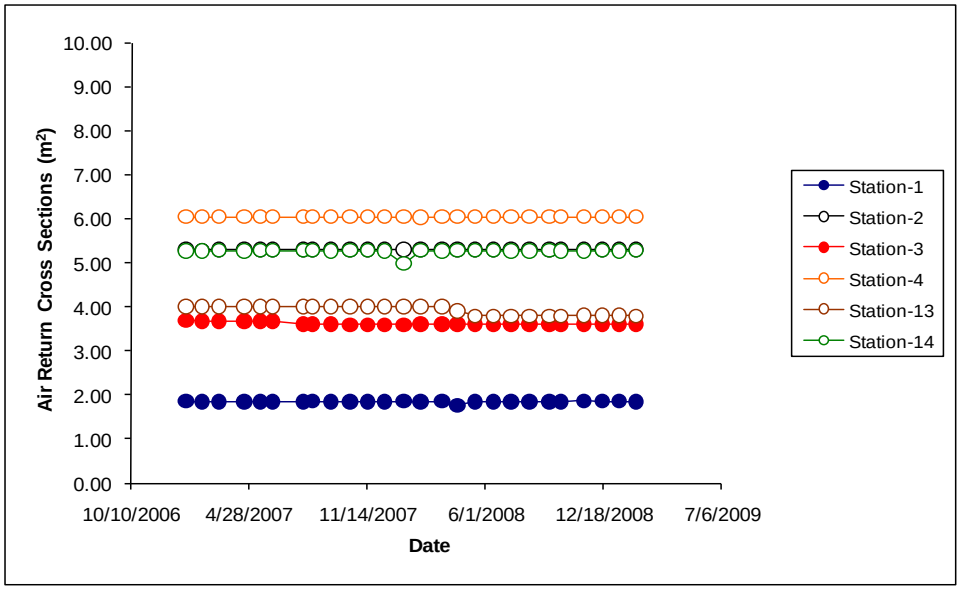


**Figure 25: Cross sectional area of air return at measurement stations at different dates.**

The most important field data, in addition to mine maps, were the measured air flow quantities in return and intakes as well as methane percentages from which actual amounts of methane in the return air stream could be calculated. These data together with the pressure data were used in the numerical simulation for matching purposes to estimate the properties of Yeni Çeltek coal seam.

Figure 26 and Figure 27 show intake air volume rates and velocities, respectively, at different stations. These data show that the highest air quantity was measured at station 6 (about 1000 $m^3$/min) with others are almost having the same amounts in the order of 300-500 $m^3$/min. The calculated velocities on the other hand changed between 50-150 m/min, depending on the measurement location and the date of measurement.

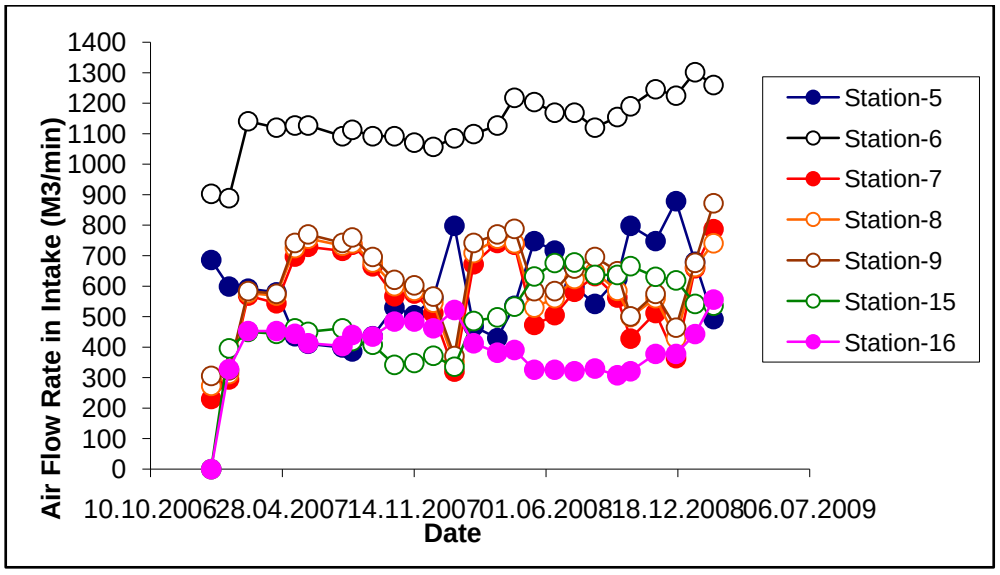


**Figure 26: Air volume flow rates measured at intake stations.**

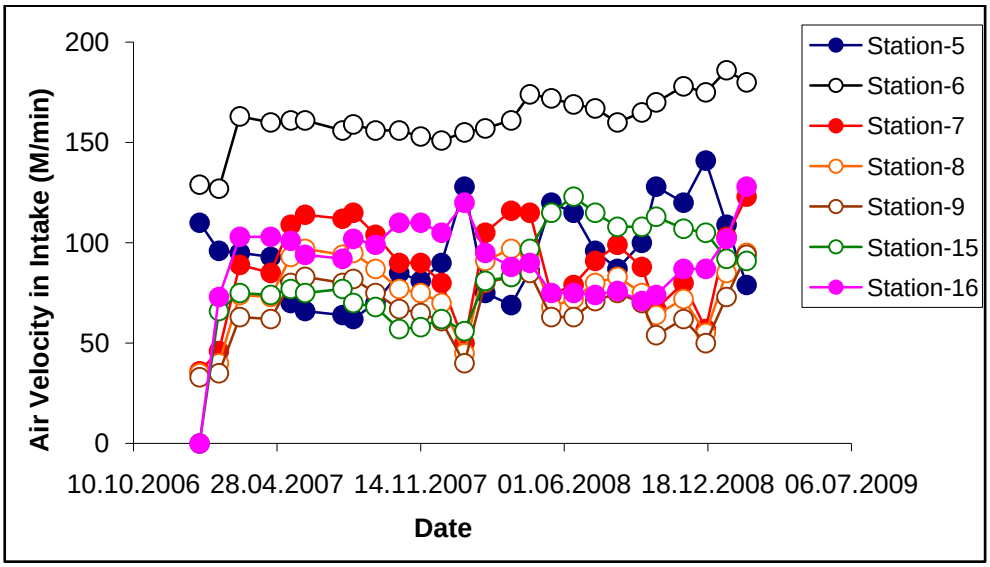


**Figure 27: Air velocities calculated for intake stations at different dates.**

In underground coal mines, methane percentages in ventilation air above 1% are usually out of allowable limits. In some countries the legal limit can be as high as 2%. However, in most developed nations and coal producing countries the limit is maximum 1% anywhere in the mine to maintain safety and operators are liable to provide adequate ventilation and production practices to keep methane under these levels. Methane percentage measurements at return stations in the Yeni Çeltek mine showed that (Figure 28) methane levels are generally under 1% at all locations and at all times, except station 14 especially before February of 2008. The observed peak in the methane percentage around January 10$^{th}$ of 2008 may be due to the change in the cross sectional area of this station, as shown in return airway cross sections figure.

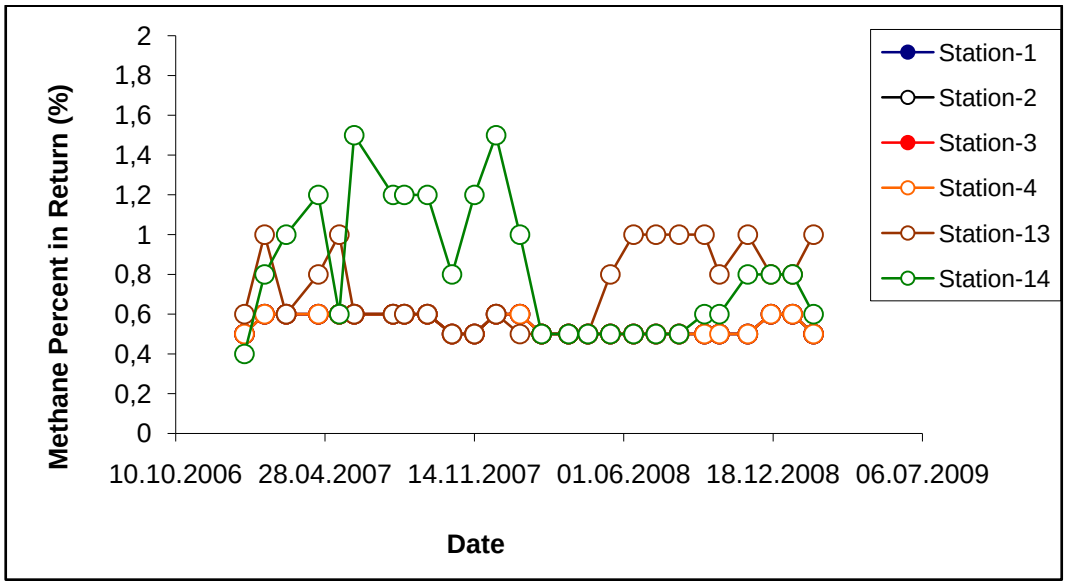


**Figure 28: Methane percentage measured in return air stations.**

Using measured methane percentages in Figure 28 and air flow rates, methane emission rates (or methane rates) could be calculated. These data are shown below in Figure 29. Methane flow rate data presented in this figure shows that stations 3 and 4 are where the methane rates are highest consistently at around 7 $m^3$/min. Higher methane rates are also observed at station 13 after August 14$^{th}$, 2008. An examination of methane flow rate together with pressure shows that the emission in methane correlates with changes in the ventilation pressure, as expected (Figure 30). These figures show the importance of evaluating pressures with methane rates to maintain a safe mining operation from methane emissions point of view and also to produce maximum amount of high quality methane if production from abandoned areas are sought.

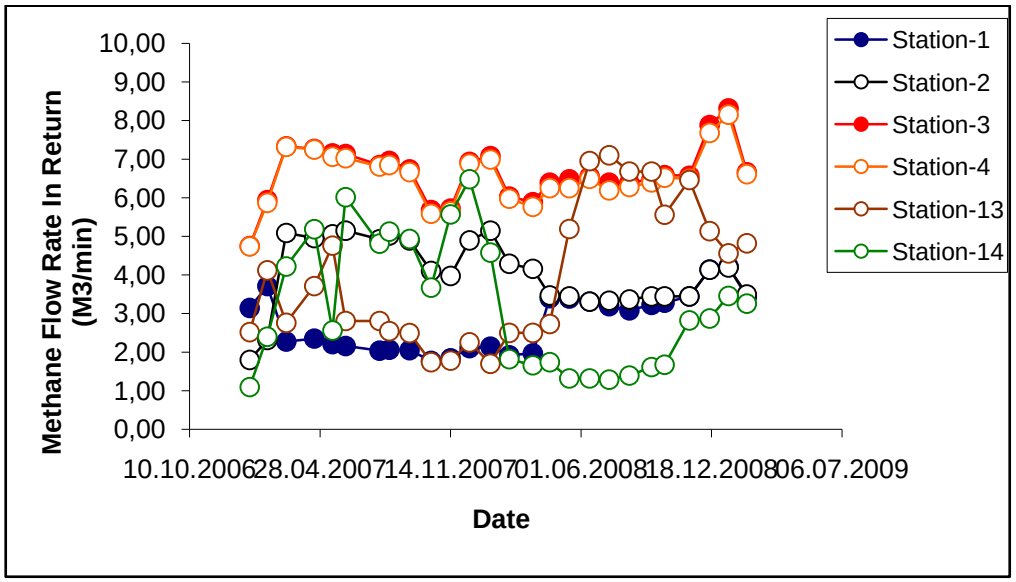


**Figure 29: Methane flow rates calculated at measurement stations in return**

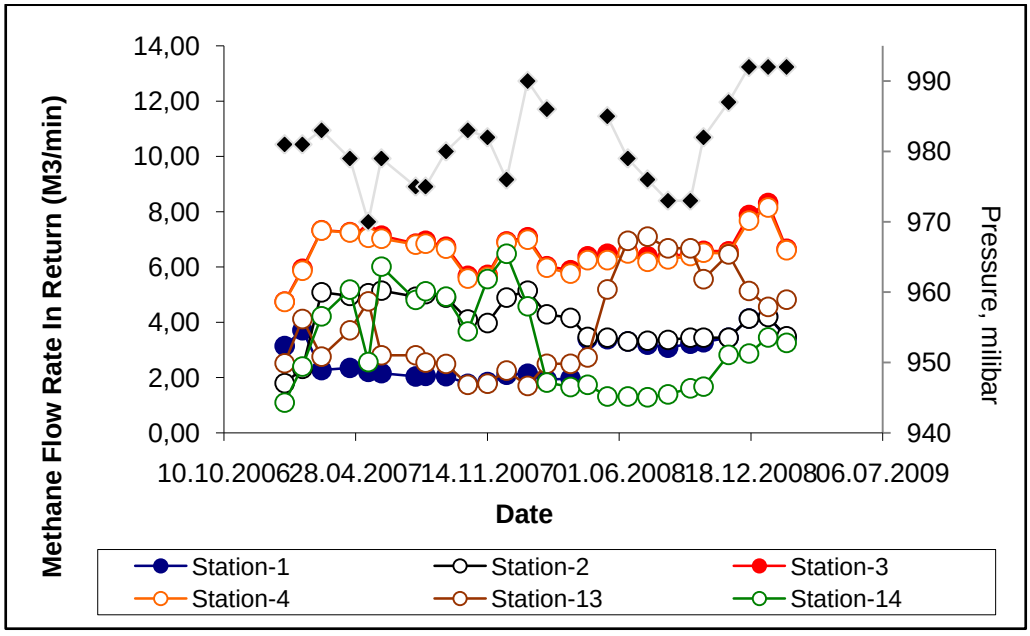


**Figure 30: Relations between changing in-mine pressures and methane flow rates in return stations.**

In the following sections, presented measurements will be used in reservoir simulator and will try to be matched by changing coal properties. In the reservoir model, measurement stations were represented by either injection (intake) or production (return) wells to monitor the flow rates and methane concentrations. Pressures were also given as operating constraints to these wells.

# CHAPTER-4

# METHODOLOGY

A base coalbed reservoir model was constructed for selected region to determine the coal reservoir properties numerically by simulate fluid flow in unmined sections of the coalbed and evaluating calculated gas rates from simulation with the field's ventilation measurements. The base model was designed as a uniform continuous coalbed reservoir using Computer Modeling Group's simulator GEM in the dual porosity formulation to model cleat and matrix interactions during gas flow and Gilman and Kazemi type of shape factor are preferred for dual-porosity unsteady state gas transportation.

Following assumptions were made in generating base model:

- The coalbed reservoir model contains two phases as gas and water; however, water defined as immobile within relative permeability curves.
- Porosity in micropore and macropore system is unchanged with pressure
- The temperature remains constant.
- Fractures were uniformly distributed.
- Gas volume desorbed from the coal surface is estimated from available sorption isotherm.
- Gas transport through coal matrix system is a diffusion process, while gas and water flow to the wellbore via cleat network obeys Darcy's law in general however, in our model we do not have water flow within cleat system.
- Gas is not soluble in water.

The model was constructed as two layers both composed of coal in a 3-D structure to accordingly reflect spatial descriptions of the geometries and properties of the discontinuities of the coalbed.

In this manner square grids were used with dimension 3mx3m grid blocks in I and J direction respectively. In vertical direction two coal layers are constructed as 2m thick for roof coal and 3m thick for mining layer. The selected region was represented with 204 x 206 x 2 grids as illustrated in Figure 31.

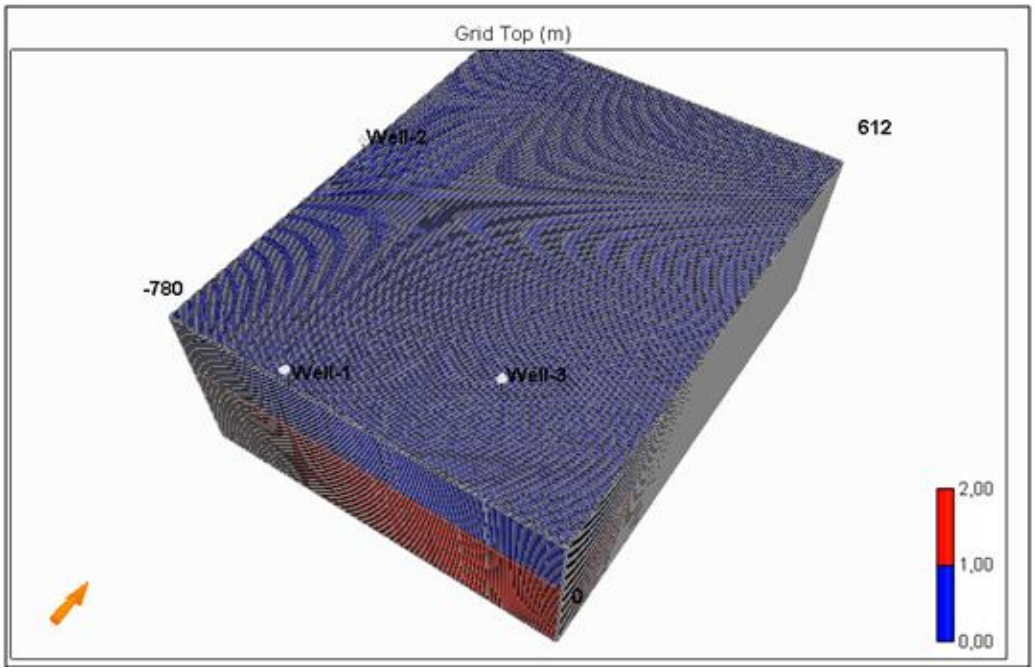


**Figure 31: Base model mesh with two coal layers.**

Gas production was model from two vertical, unstimulated, 0.5 m radius wells which are perforated at the mining layer as open hole. Air provided by ventilation system in mine is modeled by $N_2$ injection from Well-1. Station-4 (intake air measurement station), station-1 and station-3 (air measurement stations at return track), seen in Figure 22, are used for the wells as the injector and producer wells respectively. The boundary condition for injection well is handled with assigning injected gas composition as 0.5% $CH_4$ and 99.5% $N_2$.

Permeability is assigned as 0.0001 md in I, J and K direction for the coal matrix while fracture permeabilities, cleat system permeabilities, are defined as 4 md for I and J direction and for K direction fracture permeability is defined as 1 md.

For the ventilation road definition, the return line is only defined in the production zone because of the elevation difference with the intake and return lines in mine. Return line was modeled as shown in Figure 32, as void spaces by defining infinite permeability by giving maximum value allowed in simulator, in second layer with the aim of allowing gas molecules to flow without any resistance. The fresh air current was provided with the injection well (Well-1) defined at the intake measurement station (Station 4).

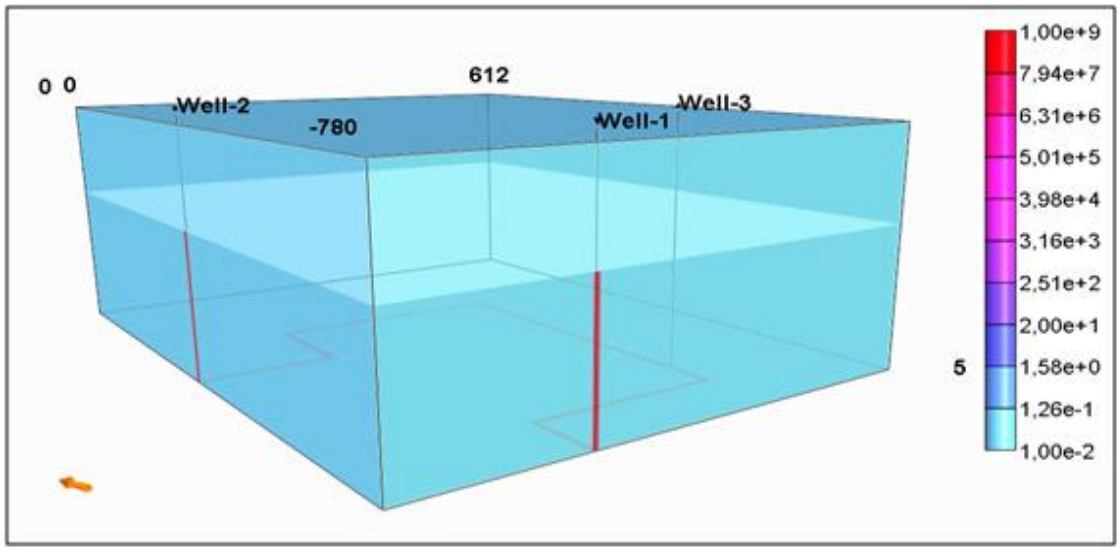


**Figure 32: Permeability for return track**

The shape of the return line was simplified in order to define the roads with the simulator square grids however length of the ventilation line is kept constant as in the mine to ensure that emission road length will be the same with the mine.

The porosities were defined as 0.05% for coal matrix, 0.1 for cleats and to reflect void

space of the ventilation line the maximum allowed porosity is defined as 99%.

Total time simulated was 766 days. Methane flow rate and pressure data from ventilation measurements were input as well operation constraints as in Figure 33, Figure 34 and Figure 35.

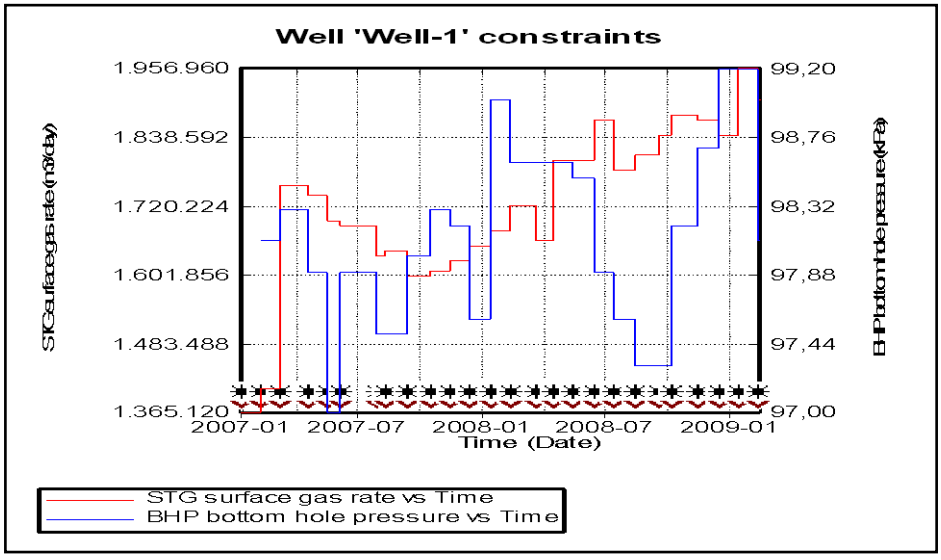


**Figure 33: Well-1 operation constraints: Maximum surface gas rate and Minimum bottomhole pressure in time.**

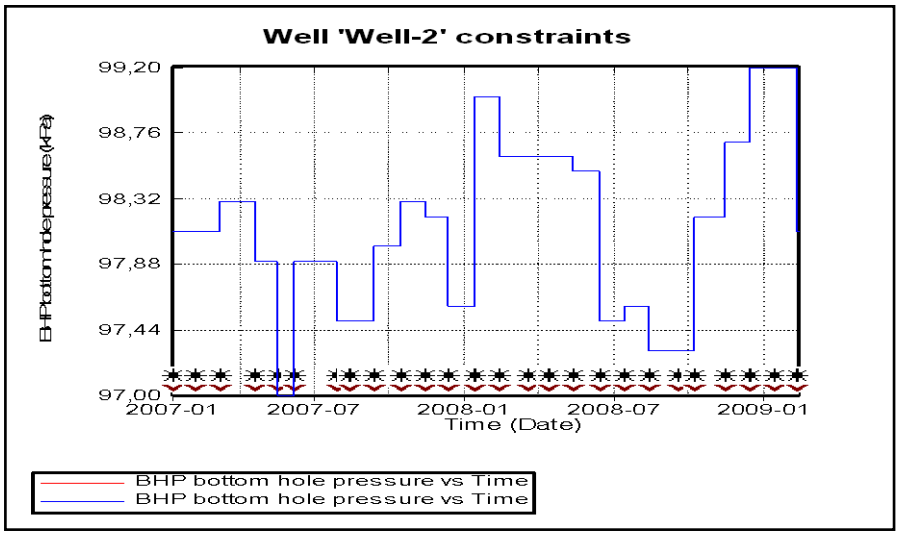


**Figure 34: Well-2 operation constraint: Minimum bottomhole pressure in time.**

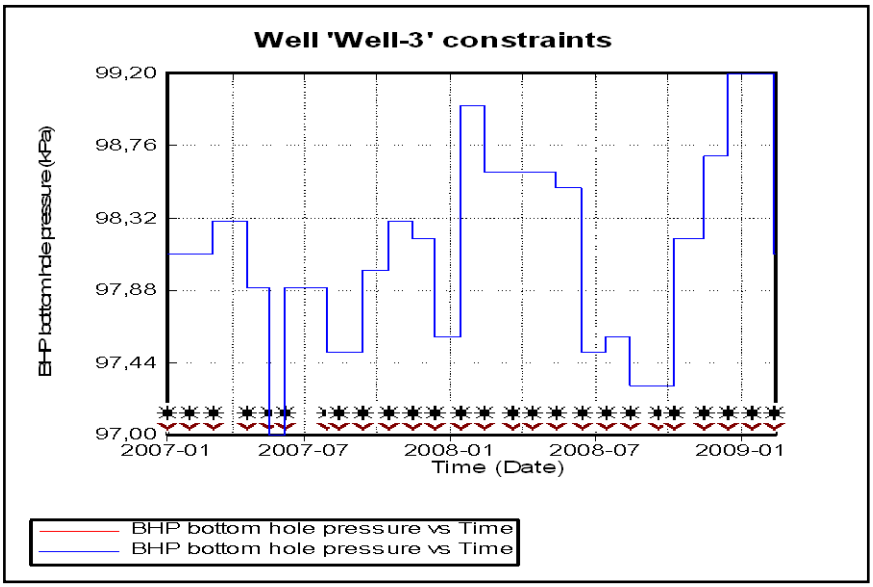


**Figure 35: Well-3 operation constraint: Minimum bottomhole pressure in time.**

The model was constructed as diphase which are gas and water. Since water

production data were not available, therefore in was assumed that there was minimum mobile water in the area and assigned in relative permeability curves for fracture accordingly, Figure 36.

In simulator, four types of rocks were defined so that model can reflect the fluid flow in coal matrix and cleat system as well as in the defined void space for return line. For coal matrix Table 4 was defined and relative permeability curves can be seen in Figure 37 and Figure 38, and in return line relative permeability values seen in Table 5 and Figure 38and Figure 39 accordingly.

**Table 4: Relative permeability curves defined for undisturbed coal matrix**

| **Rock Type 1** | **Matrix For Undisturbed Coal** | | | | **Rock Type 2** | **Fracture System In Undisturbed Coal** | | |
|---|---|---|---|---|---|---|---|---|
| SWT | drainage | | | | SWT | drainage | | |
| Sw | Krw | Kro | Pcow | | Sw | Krw | Kro | Pcow |
| 0.2 | 0 | 0.000006 | 0 | | 0.2 | 0 | 0.000006 | 0 |
| 0.45 | 0.024065 | 0 | 0 | | 0.45 | 0.004065 | 0 | 0 |
| 0.6 | 0.049308 | 0 | 0 | | 0.6 | 0.009671 | 0 | 0 |
| 0.75 | 0.088292 | 0 | 0 | | 0.75 | 0.019506 | 0 | 0 |
| 0.9 | 0.12765 | 0 | 0 | | 0.9 | 0.041798 | 0 | 0 |
| 0.95 | 0.154878 | 0 | 0 | | 0.95 | 0.054878 | 0 | 0 |
| 0.9999 | 0.2 | 0 | 0 | | 0.9999 | 0.071138 | 0 | 0 |
| | | | | | | | | |
| SGT | | | | | SGT | | | |
| Sg | Krg | Krog | Pcog | | Sg | Krg | Krog | Pcog |
| 0.005 | 0 | 0.000006 | 0 | | 0.005 | 0 | 0.000006 | 0 |
| 0.01 | 0.0460829 | 0 | 0 | | 0.01 | 0.05626 | 0 | 0 |
| 0.05 | 0.103687 | 0 | 0 | | 0.05 | 0.172811 | 0 | 0 |
| 0.25 | 0.236175 | 0 | 0 | | 0.25 | 0.470046 | 0 | 0 |
| 0.3 | 0.259217 | 0 | 0 | | 0.3 | 0.532258 | 0 | 0 |
| 0.4 | 0.309908 | 0 | 0 | | 0.4 | 0.619816 | 0 | 0 |
| 0.52 | 0.366359 | 0 | 0 | | 0.52 | 0.735023 | 0 | 0 |
| 0.6 | 0.403226 | 0 | 0 | | 0.6 | 0.817972 | 0 | 0 |
| 0.8 | 0.5 | 0 | 0 | | 0.8 | 1 | 0 | 0 |

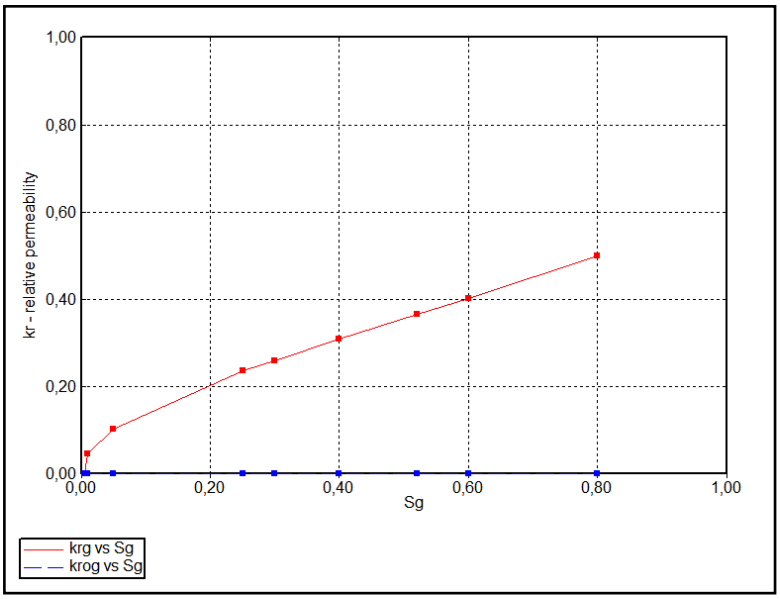


**Figure 36: Water relative permeability curve for undisturbed coal**

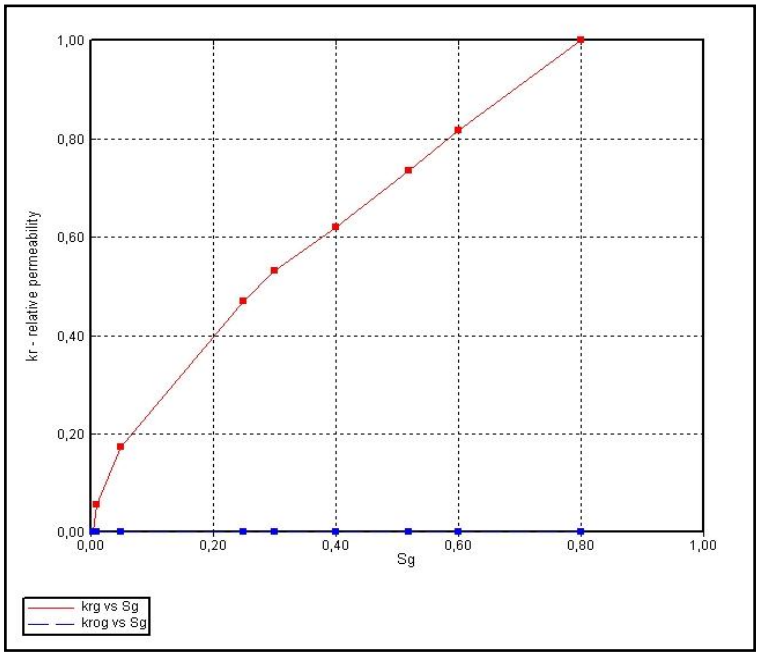


**Figure 37: Gas relative permeability for undisturbed coal**

**Table 5: Relative permeability table defined for return line.**

| **Rock type-3** | **Matrix Ventilation Roads** | | | | **Rock type-4** | **Fracture Ventilation Roads** | | |
|---|---|---|---|---|---|---|---|---|
| SWT | Drainage | | | | SWT | Drainage | | |
| Sw | Krw | Kro | Pcow | | Sw | Krw | Kro | Pcow |
| 0.2 | 0 | 0.000006 | 0 | | 0.2 | 0 | 0.000006 | 0 |
| 0.45 | 0.024065 | 0 | 0 | | 0.45 | 0.00459 | 0 | 0 |
| 0.6 | 0.049309 | 0 | 0 | | 0.6 | 0.01131 | 0 | 0 |
| 0.75 | 0.088293 | 0 | 0 | | 0.75 | 0.021309 | 0 | 0 |
| 0.9 | 0.12765 | 0 | 0 | | 0.9 | 0.04147 | 0 | 0 |
| 0.95 | 0.154878 | 0 | 0 | | 0.95 | 0.054878 | 0 | 0 |
| 0.9999 | 0.2 | 0 | 0 | | 0.9999 | 0.071138 | 0 | 0 |
| | | | | | | | | |
| Sg | Krg | Krog | Pcog | | Sg | Krg | Krog | Pcog |
| 0.005 | 0 | 0.000006 | 0 | | 0.005 | 0 | 0.000006 | 0 |
| 0.01 | 0.046083 | 0 | 0 | | 0.01 | 0.9 | 0 | 0 |
| 0.05 | 0.103687 | 0 | 0 | | 0.05 | 1 | 0 | 0 |
| 0.25 | 0.236175 | 0 | 0 | | 0.25 | 1 | 0 | 0 |
| 0.3 | 0.259217 | 0 | 0 | | 0.3 | 1 | 0 | 0 |
| 0.4 | 0.309908 | 0 | 0 | | 0.4 | 1 | 0 | 0 |
| 0.52 | 0.366359 | 0 | 0 | | 0.52 | 1 | 0 | 0 |
| 0.6 | 0.403226 | 0 | 0 | | 0.6 | 1 | 0 | 0 |
| 0.8 | 0.5 | 0 | 0 | | 0.8 | 1 | 0 | 0 |

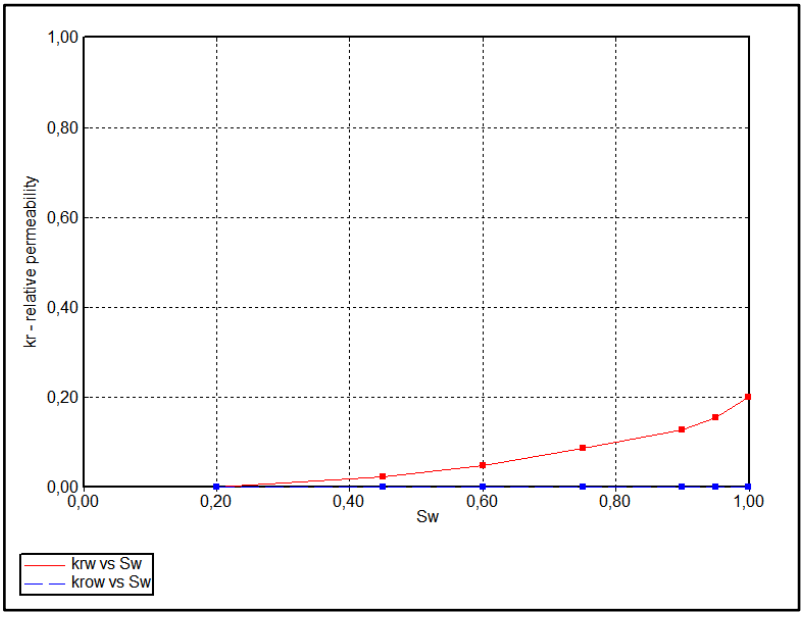


**Figure 38: Water relative permeability curve defined in return line.**

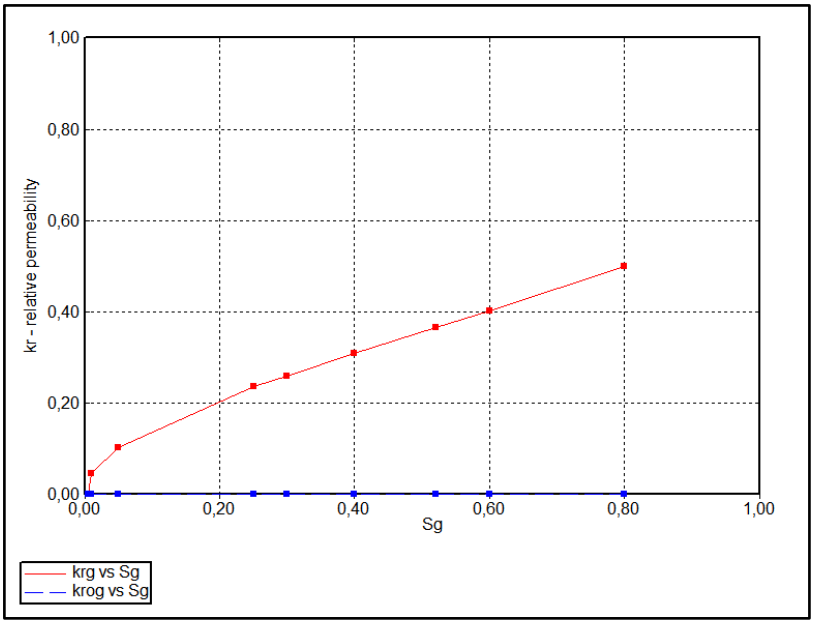


**Figure 39: Gas relative permeability curve defined for return line.**

Table 6 shows reservoir parameters used in construction of base model.

**Table 6: Values of some of reservoir parameters of used in modeling the coalbed**

| Coal | Matrix | | Cleat | |
|---|---|---|---|---|
| Parameter | Matrix | Void | Fracture | Void |
| Permeability I, md | 0.0001 | 10 | 4 | 1E+09 |
| Permeability J, md | 0.0001 | 10 | 4 | 1E+09 |
| Permeability K, md | 0.0001 | 10 | 1 | 1E+09 |
| Porosity | 0.0005 | 0.1 | 0.02 | 0.999 |
| Fracture Spacing I, m | | | 0.5 | 0.1 |
| Fracture Spacing J, m | | | 0.25 | 0.1 |
| Fracture Spacing K, m | | | 0.1 | 0.1 |
| Water Saturation | 0.05 | | 0.2 | 0.01 |
| Rock Compressibility, 1/kPa | 5.00E-06 | | 0.0005 | |
| Reference Pressure ( for rock compressibility) | 100 | | 100 | |
| Overall Coal Thickness, m | 5 | | | |
| Net Pay Thickness, m | 3 | | | |
| Pressure | 517 | 98 | 517 | 98 |
| Coal Density (kg/m3) | 1435 | | | |
| Langmuir Volume m3/ton | 6.24279 | | | |
| Langmuir Pressure, kPa | 1034 | | | |
| Coal Desorption time, day | 100 | | | |
| Standard Pressure, kPa | 101.325 | | | |
| Standard Temperature, °C | 15.56 | | | |

Langmuir isotherm, which defines the relationship of coalbed pressure to the capacity of holding gas at a constant temperature for a give coal, constructed for base case is given Figure 40.

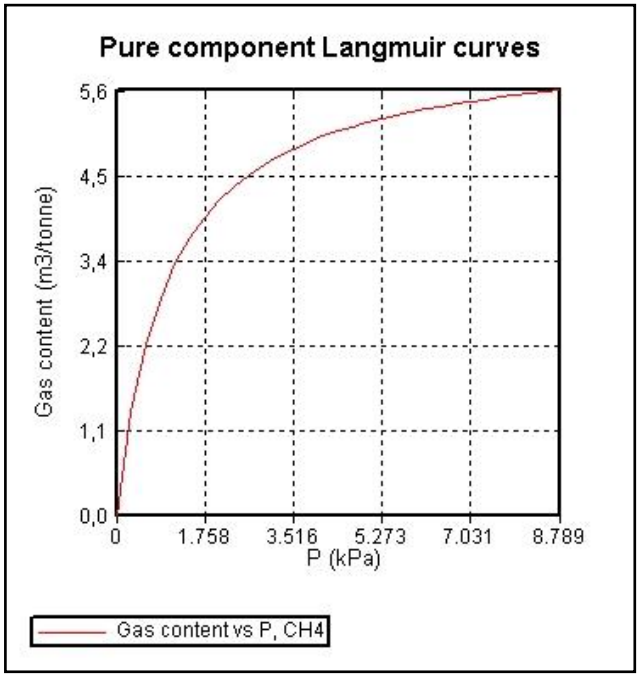


**Figure 40: Langmuir isotherm for base model.**

# CHAPTER-5

# RESULTS AND DISCUSSION

In this study, ventilation data measured in air ways of a longwall mine was integrated with the numerical reservoir simulation. The aim was characterizing the gas storage and flow properties of the coal seam. A 3-D coalbed reservoir model was constructed and several cases were run in the simulator to match the computed methane rates, air rates and bottom-hole pressures with the measured ventilation data by changing key reservoir parameters.

## 5.1 BASE CASE

The construction of the base model and parameters were explained in previous section and reservoir parameters used in base model was given in Table 7.

**Table 7: Values of some of reservoir parameters of used in modeling the coalbed**

| Coal | Matrix | | Cleat | |
|---|---|---|---|---|
| Parameter | Matrix | Void | Fracture | Void |
| Permeability I, md | 0.0001 | 10 | 4 | 1E+09 |
| Permeability J, md | 0.0001 | 10 | 4 | 1E+09 |
| Permeability K, md | 0.0001 | 10 | 1 | 1E+09 |
| Porosity | 0.0005 | 0.1 | 0.02 | 0.999 |
| Fracture Spacing I, m | | | 0.5 | 0.1 |
| Fracture Spacing J, m | | | 0.25 | 0.1 |
| Fracture Spacing K, m | | | 0.1 | 0.1 |
| Water Saturation | 0.05 | | 0.2 | 0.01 |
| Rock Compressibility, 1/kPa | 5.00E-06 | | 0.0005 | |
| Reference Pressure ( for rock compressibility) | 100 | | 100 | |
| Overall Coal Thickness, m | 5 | | | |
| Net Pay Thickness, m | 3 | | | |
| Pressure | 517 | 98 | 517 | 98 |
| Coal Density (kg/m3) | 1435 | | | |
| Langmuir Volume m3/ton | 6.24279 | | | |
| Langmuir Pressure, kPa | 1034 | | | |
| Coal Desorption time, day | 100 | | | |
| Standard Pressure, kPa | 101.325 | | | |
| Standard Temperature, ˚C | 15.56 | | | |

Base case was used to determine the general behavior of the constructed model and key reservoir parameters that should alter.

Methane rates calculated from air rate and methane concentrations at the measurement stations in air ways and according pressure values are presented in rates Figure 41 and Figure 42 respectively.

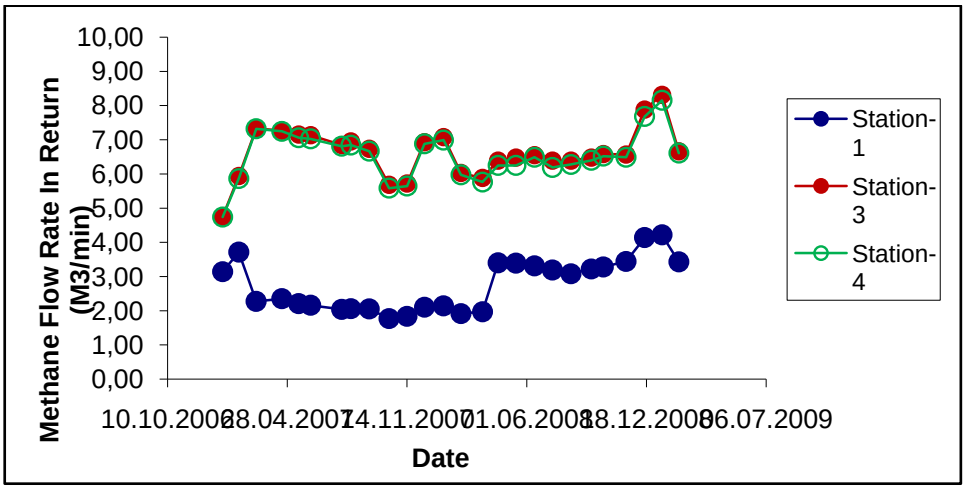


**Figure 41: Measured methane flow rate in return line.**

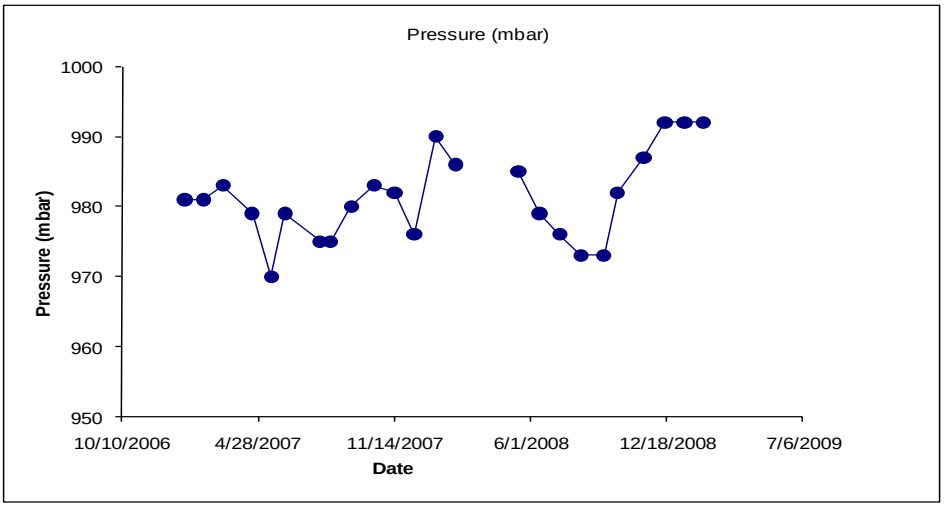


**Figure 42: Pressure measurements at various dates.**

Results of base case run were compared with the field measurements in Figure 43, Figure 44 and Figure 45.

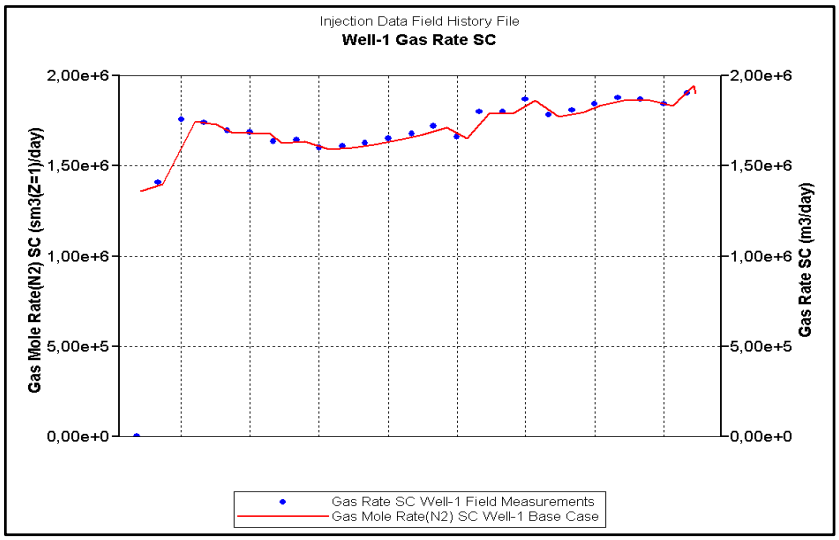


**Figure 43: Base case run results and field measurements for Well-1 $N_2$ injection rates**

In model, maximum surface gas rate was assigned as operational constraint therefore reservoir model behaves operated accordingly as seen in Figure 43.

By defining injection well (Well-1), we have an assumption of same air volume passed through the pilot area ventilation air ways was injected in the simulation.

Expected result is while gas flows through defined void grid blocks with infinite permeability and maximum porosity as air roads methane gas desorption according to the pressure difference between the coal seam and air road. Consequently, concentration difference between the injected gas and coal seam methane gas is decreased and from production wells according to the material balance calculations within simulator, methane rates were tracked.

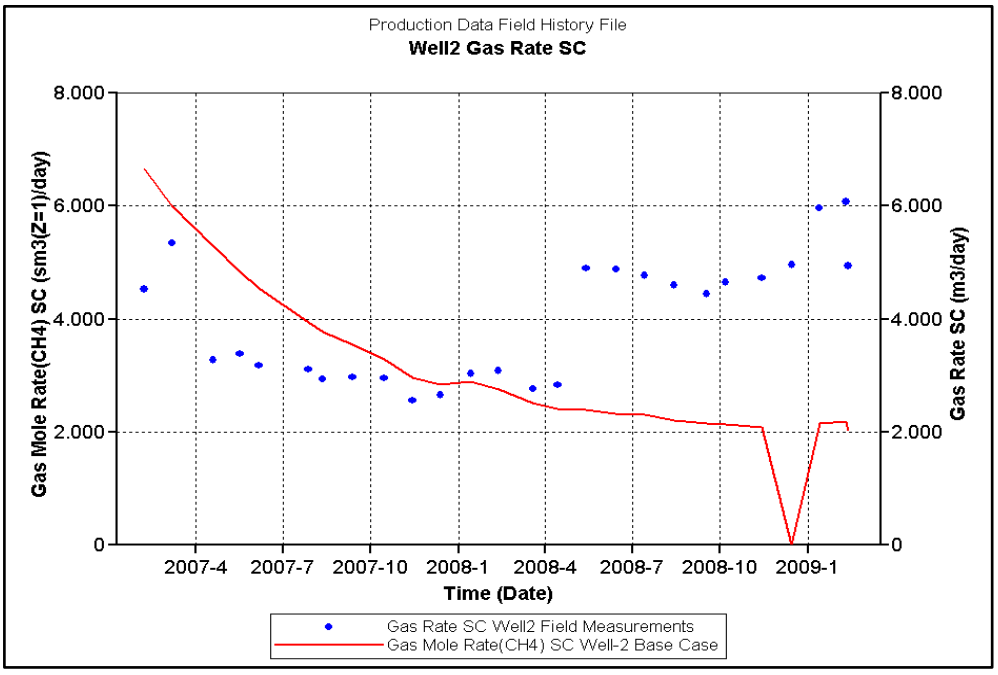


**Figure 44: Base case run results and field measurements for Well-2 $CH_4$ production rates**

In Figure 44, computed methane rates from base case and field measurements are seen. Although base case computed injection rates were in harmony with the field measurements, computed methane rates from Well-2 and field measurements of Station-3 differs both in rates and general behavior. The general behavior of the rates was changed after 14.04.2008. Although in Figure 43 from 14.04.2008 injection rates were increased, base case computed rates were not follow the injection trend. Rates were uniformly decreased. Lowest methane rate was detected at 15.12.2008 as zero m3/day.

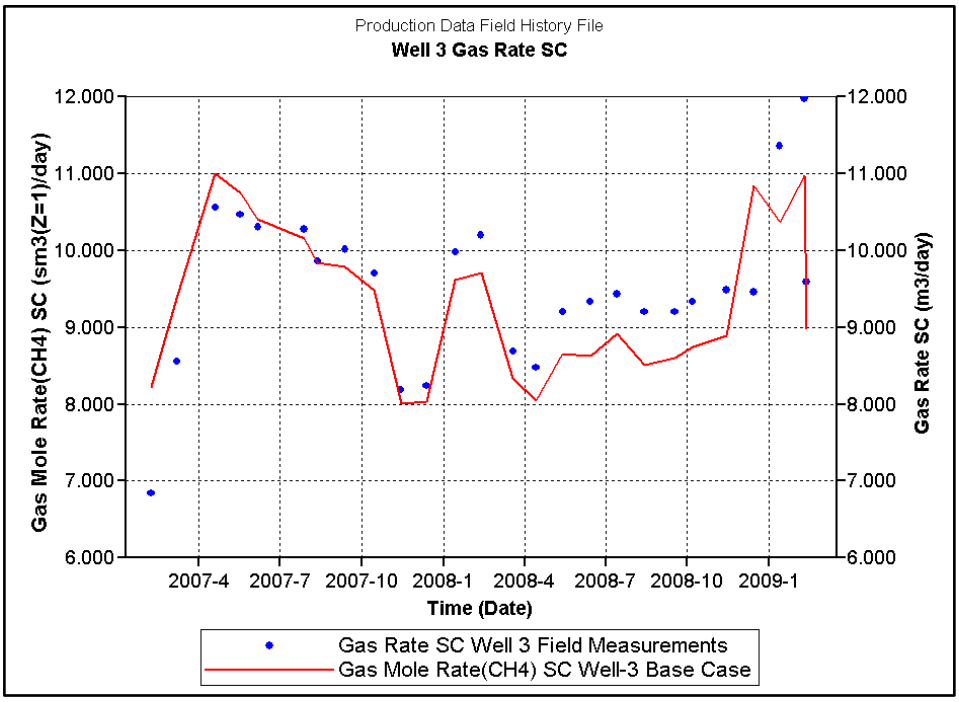


**Figure 45: Base case run results and field measurements for Well-3 $CH_4$ production rates**

In this figure base case methane rate for Well-3 and field measurements according to Station-3 were present. For Well-3, base case computed rates were almost matched with the actual field rates and general behavior of rates is similar to field measurement data.

Bottomhole pressures according to injector and producer wells are present in Figure 46 and Figure 47.

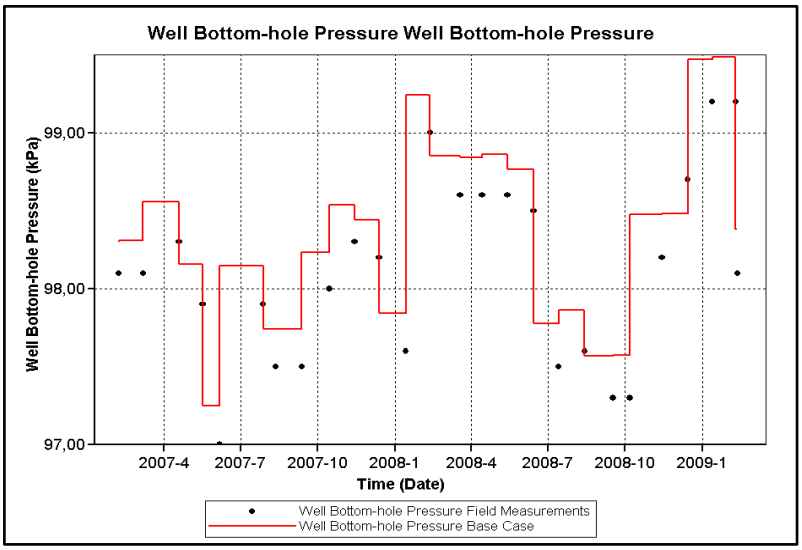


**Figure 46: Bottom-hole pressure according to injector well, Well-1.**

For Well-1 since operational constraint defined was surface gas rate, model match parameter for injector well is bottomhole pressure. As seen in Figure 46 bottomhole pressures were slightly higher than field measured pressures. In this point, it should be pointed that the field measurements were not actual bottom-hole pressures since the measured at the ventilation measurement stations.

In order to match bottom hole pressure, injector well operational conditions should be changed therefore changing reservoir parameters will not affect bottom hole pressure of the injector well in matching.

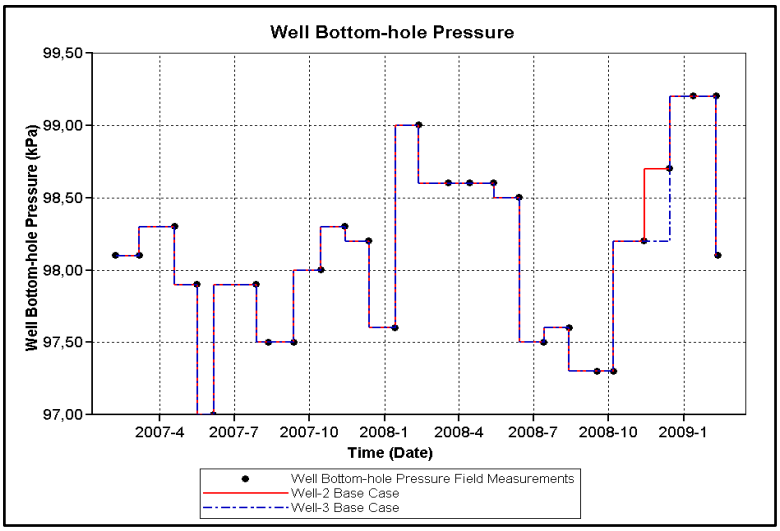


**Figure 47: Bottom-hole pressures according to producer wells, Well-2 and Well-3.**

Various factors control methane flow in coalbed as cleat permeability, cleat porosity, gas content, diffusion time etc. According to these results, key coalbed parameters were varied to match the field measurements.

## 5.2 CASE-1

For the first case, cleat permeability of the coal seam was changed. Permeability is the intrinsic property of porous media which relates to pressure drop and flow rate. The flow characteristics in coalbeds are diffusion from micropores matrix which is a slow process to macroporous structure and coal cleat system. The rate limiting parameter for the coal is the ability of the gas to flow through the macropores and cleat system (Sieddle & Arri, 1990). Therefore in Case-1 the cleat permeability in x and j direction was decreased to 0.1 to reduce computed methane rates and in z-direction cleat permeability is decreased to 0.01 as a rule of thumb for communicating layers $k_v=k_h/10$ (Paul, Simulating Coalbed Methane Reservoirs). The other parameters were kept

constant. Table 8 shows key parameters, used for calibration of the base model with history matching approach, used in Case-1.

**Table 8: Model parameters used in Case-1**

| Case-1 | | Direction | |
|---|---|---|---|
| | x | y | z |
| Cleat Permeability (md) | 0.1 | 0.1 | 0.01 |
| Cleat Porosity (%) | 2 | | |
| Water Saturation (%) | 0.3 | | |
| Fracture Spacing (m) | 0.5 | 0.25 | 0.1 |
| Diffusion Time (days) | 100 | | |
| Langmuir Pressure (kPa) | | 1034 | |
| Gas Content ($m^3$/ton) | | 6.24279 | |

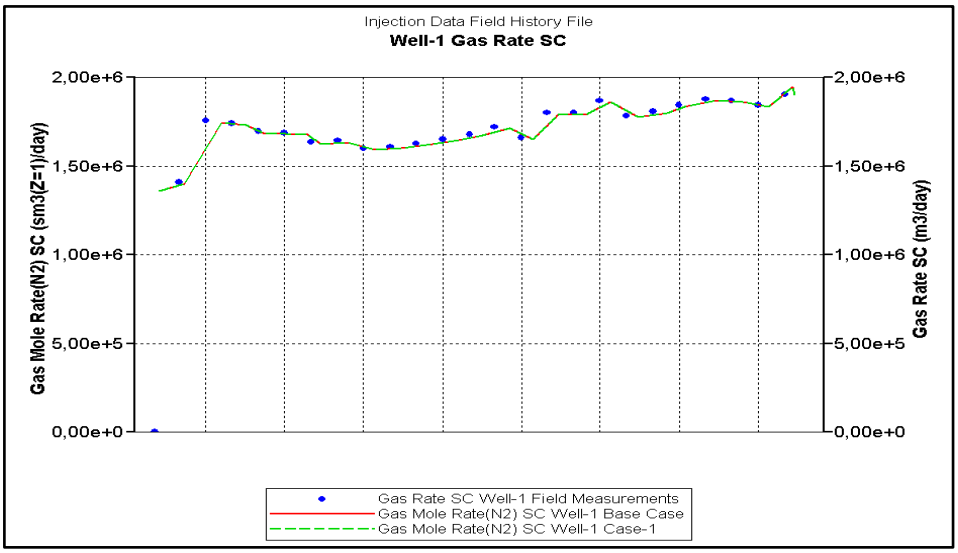


**Figure 48: Well-1 injection rates from Base Case and Case-1 results and field measurements**

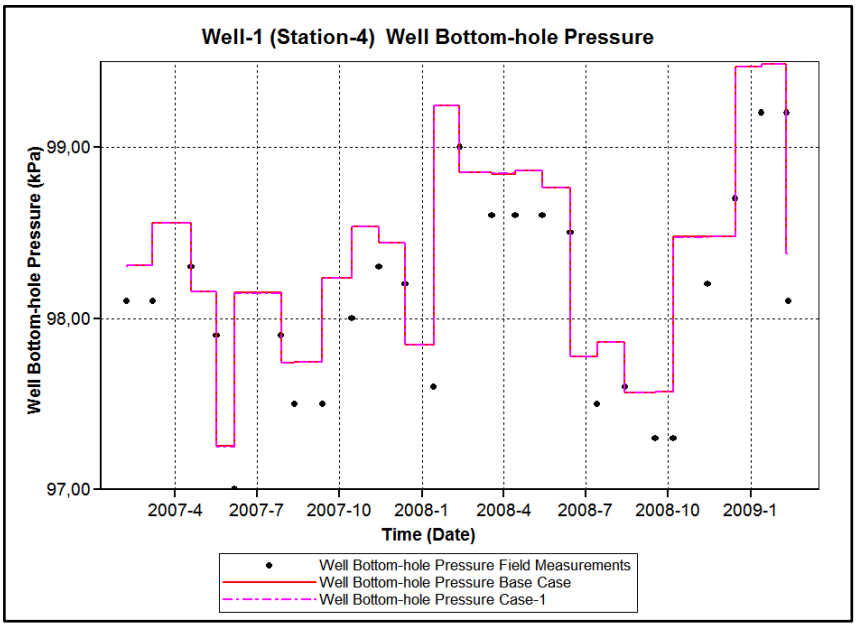


**Figure 49: Bottomhole pressures at Well-1 (Station-4) for Case-1**

Injection rates and bottomhole pressures computed in Case-1 is exactly same as with the Base Case which due to intentionally defined operational constraint to Well-1. Therefore for the rest of the study in order to see the effect of change in reservoir parameters on methane production rates, injector well run results does not repeated.

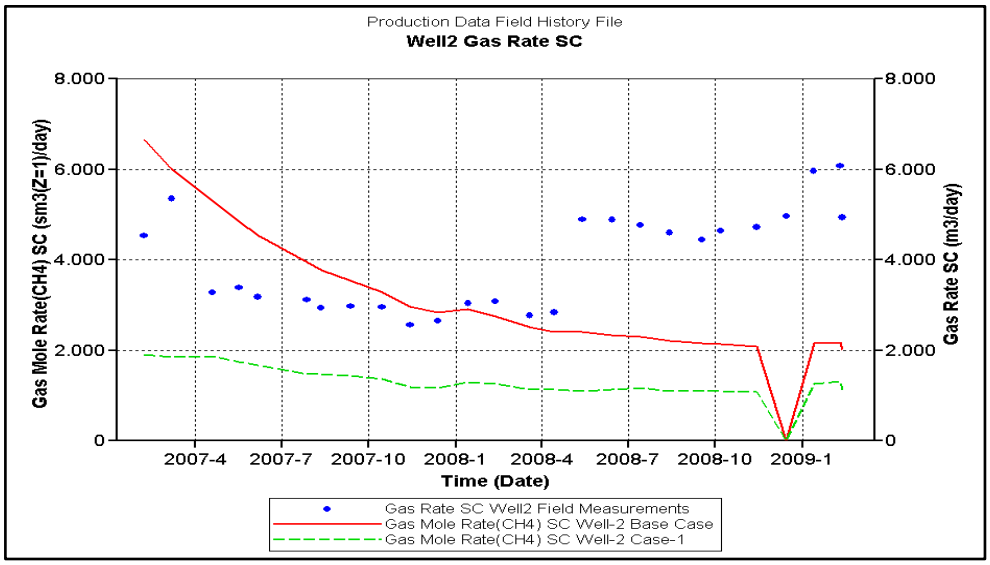


**Figure 50: Well-2 methane production rates from Base Case, Field Measurements and Case-1**

In Figure 50, the effect of decrease in permeability is seen clearly. In this case (Case-1) permeability values for x and y direction were used as 0.1 md and for z direction 0.01 md. From this figure, it can be concluded that these permeability values could be assumed as the lowest limit values in convergence trials to correct value for this model.

The rates were decreased to zero value at 15.12.2008. This could be due to a calculation error done by simulator or because of defined operational constraint simulator could not calculate the value and report as zero.

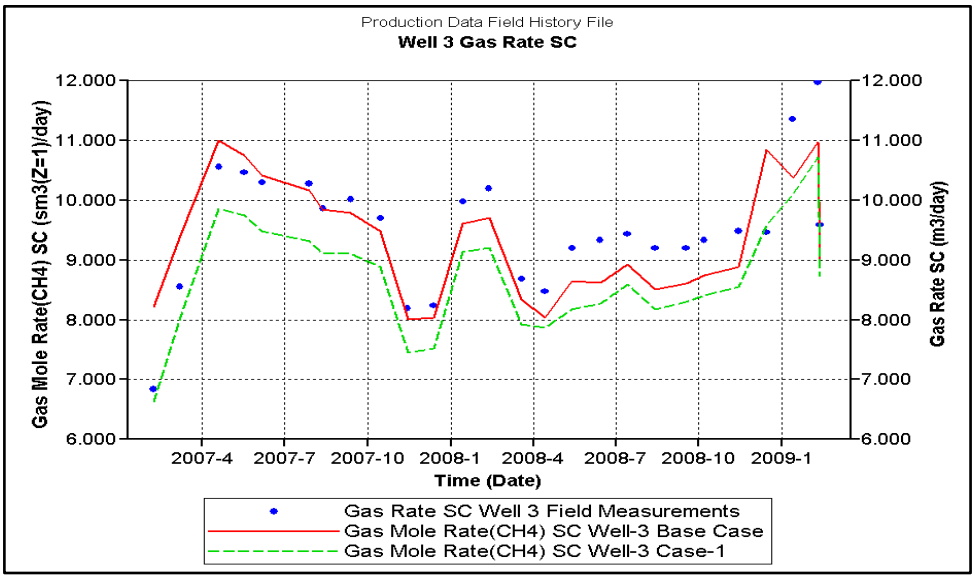


**Figure 51: Well-3 methane rates from Base Case, Field Measurements and Case-1.**

The effect of permeability change is seen for Well-3 as decrease in rates as expected.

Considering the location of the wells and the gas flow direction, Well-3 is closer than Well-2 to the injector well (Well-1), therefore in Well-2 velocity of gas flow through ventilation roads defined should be minimum and permeability would affect more significantly in this area than Well-3.

Another reason could be cleat orientation in well locations. Injected nitrogen flows through the ventilation road and during this flow at Well-3 location flow was orthogonal to x-direction. On the other hand at Well-2 location flow was orthogonal to y-direction.

The cleat structure suggests permeability in coalbeds should anisotropic, since the face cleats are generally better developed and the other set of fractures perpendicular to this well-developed fractures are butt cleats which are generally terminate at face cleats and not well-development as face cleats (Gash, Volz, Potter, & Corgan, 1993). Permeability should be the greatest parallel to face cleat. This effect could be seen according to the well locations.

## 5.3 CASE-2

According to results of Case-1, Case-2 was constructed to see the effect of permeability anisotropy. Therefore for x-direction, fracture permeability was assigned as 6 md and the other parameters were kept constant.

**Table 9: Case-2 model parameters**

| **Case-2** | | Direction | |
|---|---|---|---|
| | x | y | z |
| Cleat Permeability (md) | 6 | 4 | 1 |
| Cleat Porosity (%) | 2 | | |
| Water Saturation (%) | 0.3 | | |
| Fracture Spacing (m) | 0.5 | 0.25 | 0.1 |
| Diffusion Time (days) | 100 | | |
| Langmuir Pressure (kPa) | | 1034 | |
| Gas Content ($m^3$/ton) | | 6.24279 | |

Results are presented Figure 52 and Figure 53.

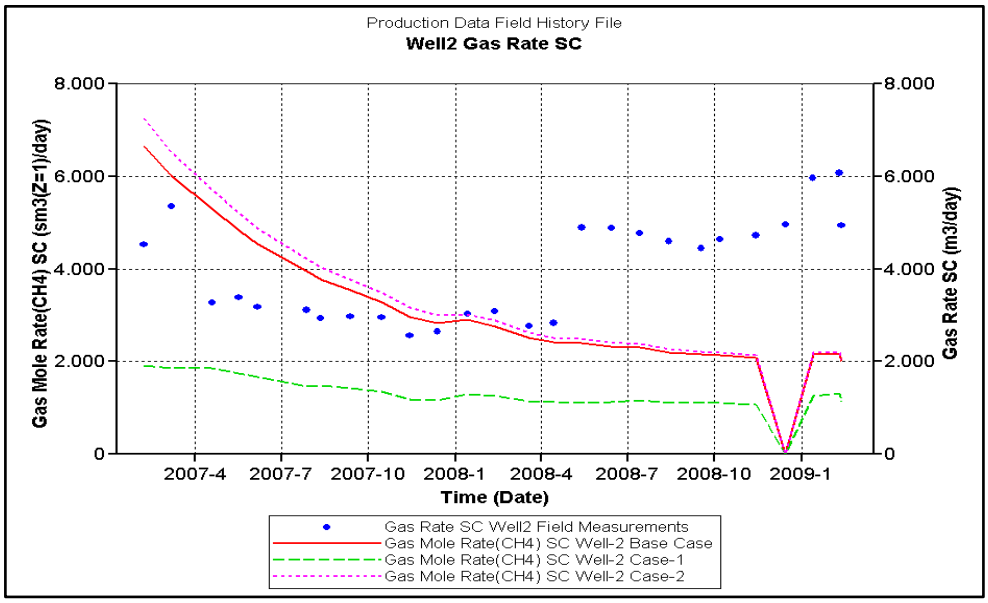


**Figure 52: Well-2 methane production rates.**

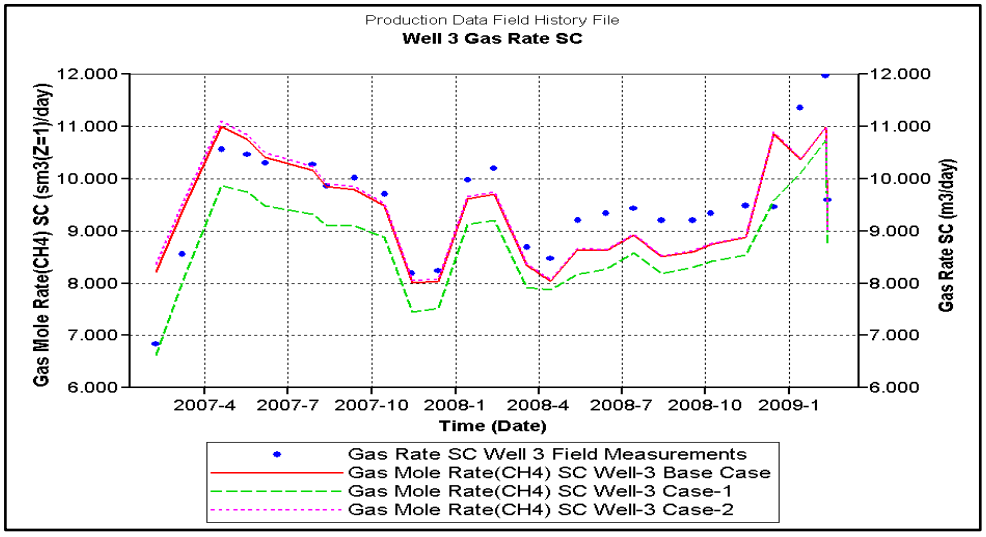


**Figure 53: Well-3 methane production rates.**

From Figure 52 and Figure 53 increase in methane rates due to increase in fracture permeability in x-direction. Although rates were not changed dramatically, 6 md

permeability values could be accepted as the highest limit value for permeability adjustment. It can be clearly seen that in Figure 53 permeability change did not affect methane rates much with respect to the Base Case rates.

## 5.4 CASE-3

Since permeability anisotropy and effects was tried to formed, in Case-3 fracture permeability values were defined as 3 md for x-direction and 1 md for y-direction. The other parameters were kept constant as values in Base Case.

**Table 10: Case-3 model parameters**

| Case-3 | | Direction | |
|---|---|---|---|
| | x | y | z |
| Cleat Permeability (md) | 3 | 1 | 1 |
| Cleat Porosity (%) | 2 | | |
| Water Saturation (%) | 0.3 | | |
| Fracture Spacing (m) | 0.5 | 0.25 | 0.1 |
| Diffusion Time (days) | 100 | | |
| Langmuir Pressure (kPa) | | 1034 | |
| Gas Content ($m^3$/ton) | | 6.24279 | |

Results for this trial could be seen in figures Figure 54 and Figure 55.

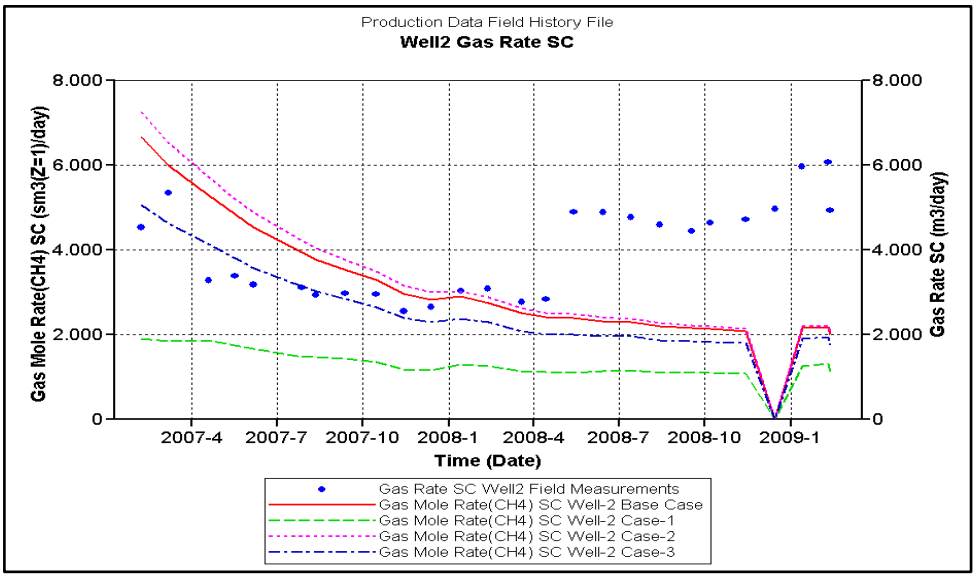


**Figure 54: Well-2 methane production rates for Base Case and Cases 1, 2 and 3.**

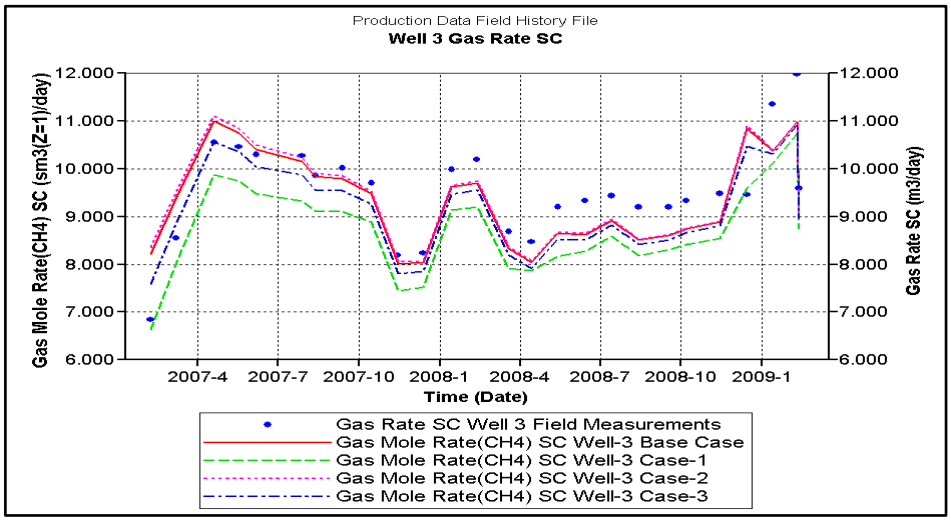


**Figure 55: Well-3 methane production rates for Base Case, Cases 1, 2 and 3.**

In Well-2 (Figure 54 ), Case-3 methane rates were closer for early times. On the other hand after 14.01.2008 field measurements showed increase in methane rates but

computed rates for Case-3 showed a uniform decline. Field behavior could not match in this trial also. At Well-3 (Figure 55) results of Case-3 run gave values as averaged values of Case-2 and Case-1 but computed rates are still too high to have a match regarding Well-3 field measurements.

## 5.5 CASE-4

After this point on, modifications for model parameters were done on the Case-3 model.

For Case-4 vertical fracture permeability and gas relative permeability for cleat system were redefined. Vertical fracture permeability was assigned as 0.15 which is approximately 1/10 of the geometric average of fracture permeabilities in x and y direction.

$$k_h = \sqrt{k_x k} \qquad \textbf{Equation 4}$$

$$k_v = k_h / 10 \qquad \textbf{Equation 5}$$

**Table 11: Model parameters for Case-4**

| Case-4 | | Direction | |
|---|---|---|---|
| | x | y | z |
| Cleat Permeability (md) | 3 | 1 | 0.15 |
| Cleat Porosity (%) | 2 | | |
| Water Saturation (%) | 0.3 | | |
| Fracture Spacing (m) | 0.5 | 0.25 | 0.1 |
| Diffusion Time (days) | 100 | | |
| Langmuir Pressure (kPa) | | 1034 | |
| Gas Content ($m^3$/ton) | | 6.24279 | |

Results for this run can be seen in Figure 56, and Figure 57.

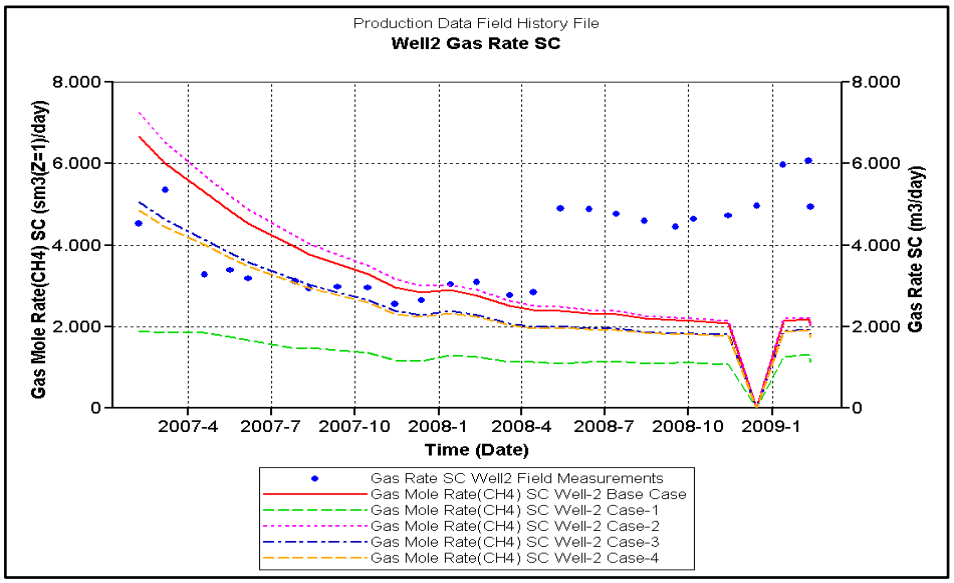


**Figure 56: Well-2 production history for Case-4**

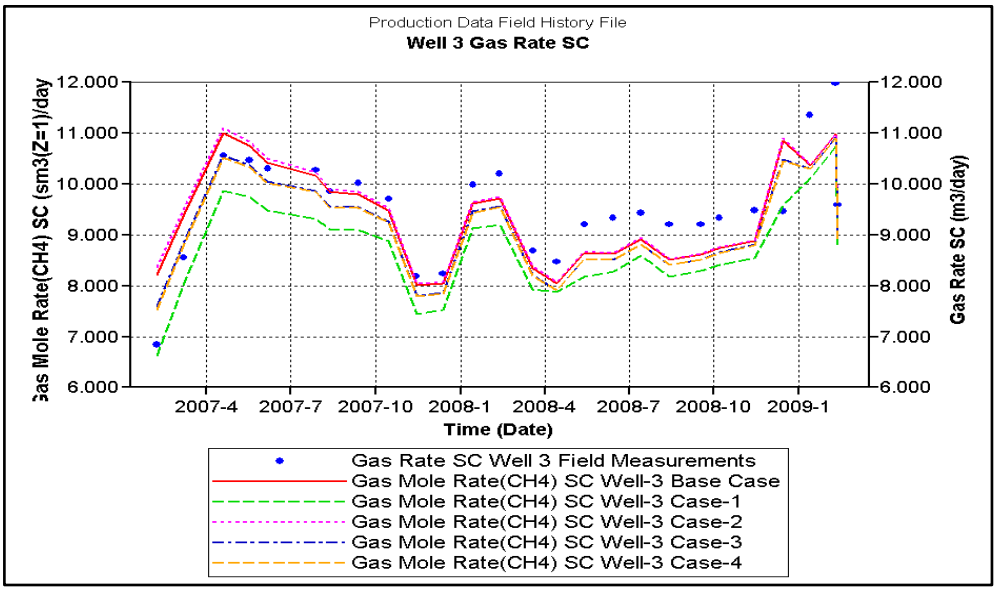


**Figure 57: Well-3 production history for Case-4**

From Figure 56 and Figure 57 it can be seen that vertical permeability was not a critical factor for production for our model. Vertical permeability manipulation did not affect perceptible neither the rates nor the general behavior of the production curves.

For next case, diffusion time of the coal matrix changed from 100 days to 300 days in order to converge to the early time rates and behavior.

**Table 12: Model parameters for Case-5**

| Case-5 | | Direction | |
|---|---|---|---|
| | x | y | z |
| Cleat Permeability (md) | 3 | 1 | 0.15 |
| Cleat Porosity (%) | 2 | | |
| Water Saturation (%) | 0.3 | | |
| Fracture Spacing (m) | 0.5 | 0.25 | 0.1 |
| Diffusion Time (days) | 300 | | |
| Langmuir Pressure (kPa) | | 1034 | |
| Gas Content ($m^3$/ton) | | 6.24279 | |

The following plots Figure 58 and Figure 59 were results of the Case-5.

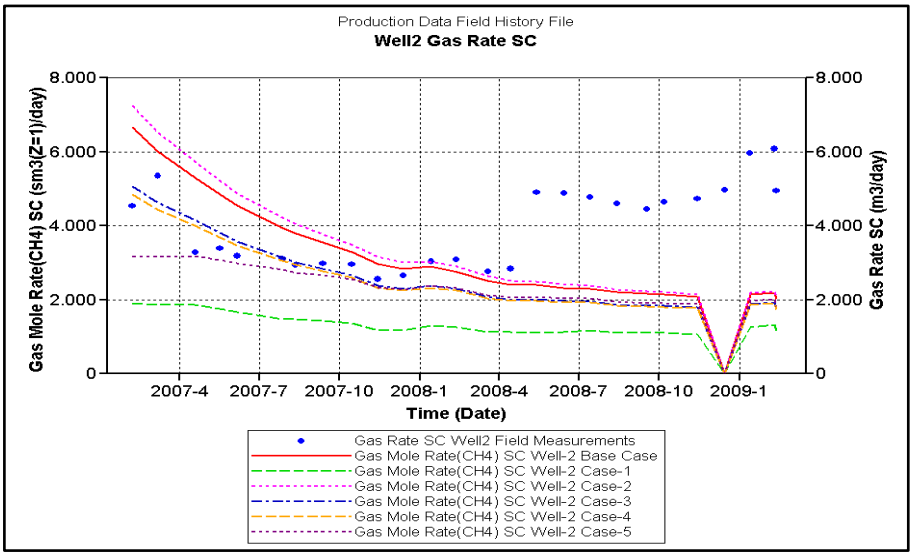


**Figure 58: Well-2, methane production rates for field measurements and Base Case, Cases-1, 2, 3, 4 and 5.**

In Figure 58, effect of change in diffusion time of matrix is seen. Diffusion time affects the rates of early times. The effect is significant at the curve of Case-5, at early times of production; rates were lower than the other cases.

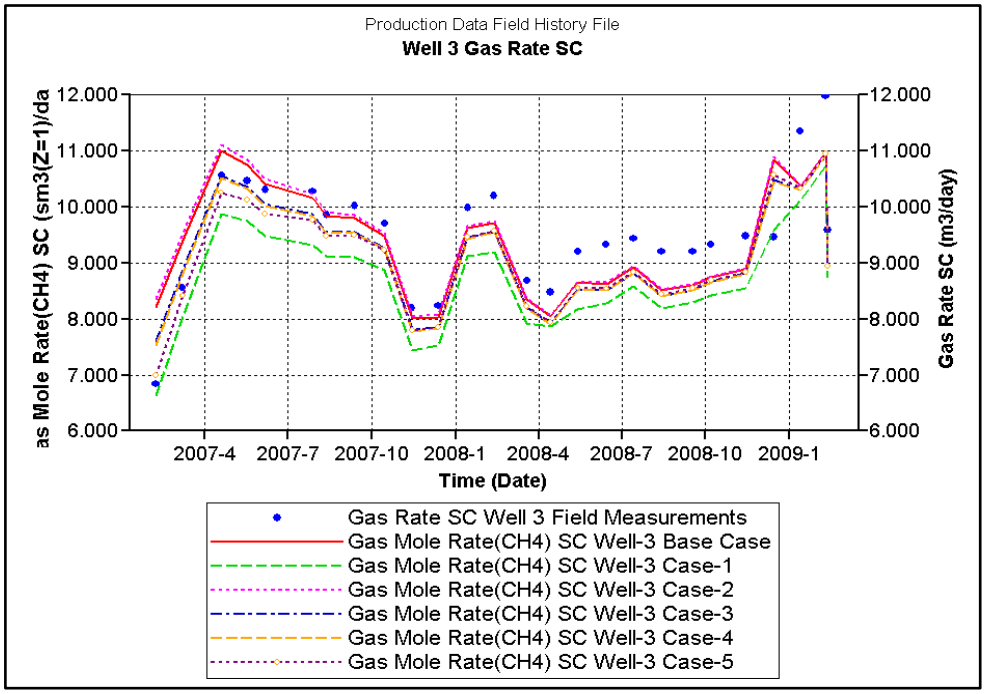


**Figure 59: Well-3, methane production rates for field measurements and Base Case, Cases-1, 2, 3, 4 and 5.**

Early production rates in this case (Case-5) are almost matched with the field measurements. However, other rates according to the later dates were not matched with the field measurements.

## 5.6 CASE-6

In this case, according to the results of the former results, cleat permeability for x and y directions were arranged as 4 and 6 md accordingly. Model parameters are present in Table 13.

**Table 13: Model parameters for Case-6**

| Case-6 | | | |
|---|---|---|---|
| | direction | | |
| | x | y | z |
| Cleat Permeability (md) | 4 | 6 | 1 |
| Cleat Porosity (%) | 2 | | |
| Water Saturation (%) | 0.3 | | |
| Fracture Spacing (m) | 0.5 | 0.25 | 0.1 |
| Diffusion Time (days) | 300 | | |
| Langmuir Pressure (kPa) | | 1034 | |
| Gas Content ($m^3$/ton) | | 6.24279 | |

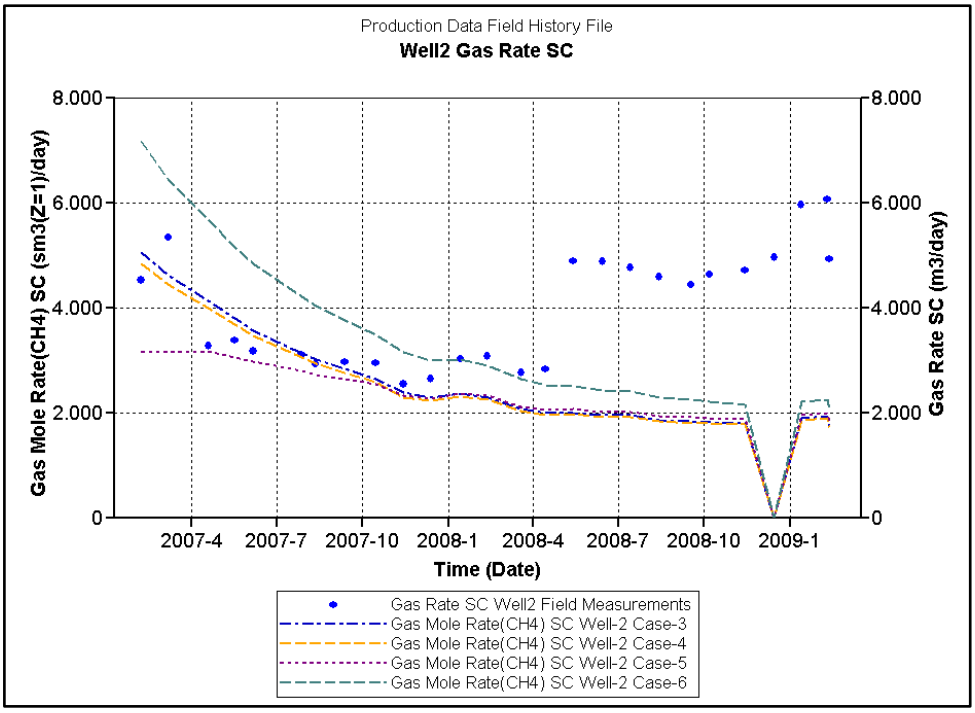


**Figure 60: Well-2 methane production rates for cases 3, 4, 5 and 6 with field measurements.**

For production well Well-2, methane production rates were not matched with the field measurements. The reason for this phenomenon could be stress dependent permeability of cleats. As stated by Gray (1987), coal matrix shrinks when the adsorbed gas in coal matrix desorbs and this increases the permeability by rising cleat aperture. Furthermore, as reported by Seidle and Huitt (1995) coal matrix swells and shrinks as gas is first adsorbed then desorbed and the amount of swelling depends on coal rank and sorbed gas composition.

Matrix shrinkage, swelling and net confining stress on the cleat surfaces are combined in Palmer and Mansoori (P&M) model to predict the absolute cleat permeability and porosity with respect to reservoir pressure during methane production. However, in our base model, we did not include this effect by implementing the Palmer and Mansoori

model this can be the reason for rates after 14.40.2008 did not matched with field measurements.

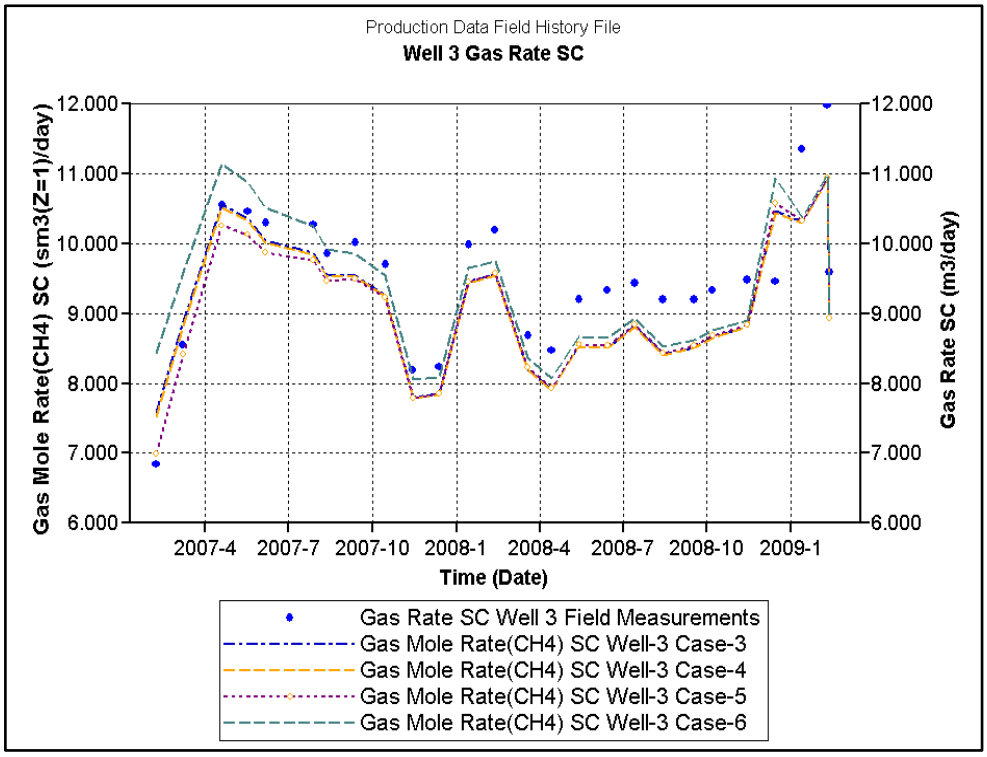


**Figure 61: Well-3 methane production rates for cases 3, 4, 5 and 6 with field measurements.**

Rate differentiation was seen in this figure (Figure 61) also. If the rates till 14.04.2008 were matched, later rates did not follow, so we could not place a curve match with field measurements for all times.

## 5.7 CASE-7

For this case (Case-7) cleat permeability values were changed as 5 md for x direction and 4 md for y direction. Also fracture spacings were changed in this model which directly affects the permeability of the seam, for x direction is redefined as 0.8 m and 0.4 m for y-direction. Diffusion time was increased to 400 days. Model parameters for Case-7 are in Table 14: Model parameters for Case-7.

**Table 14: Model parameters for Case-7**

| Case-7 | | | |
|---|---|---|---|
| | Direction | | |
| | x | y | z |
| Cleat permeability (md) | 5 | 4 | 1 |
| Cleat porosity (%) | 2 | | |
| Water saturation (%) | 0.3 | | |
| Fracture spacing (m) | 0.8 | 0.4 | 0.1 |
| Diffusion time (days) | 400 | | |
| Langmuir pressure (kPa) | | 1034 | |
| Gas content ($m^3$/ton) | | 6.24279 | |

Results for this case (Case-7) can be seen in Figure 62 and Figure 63.

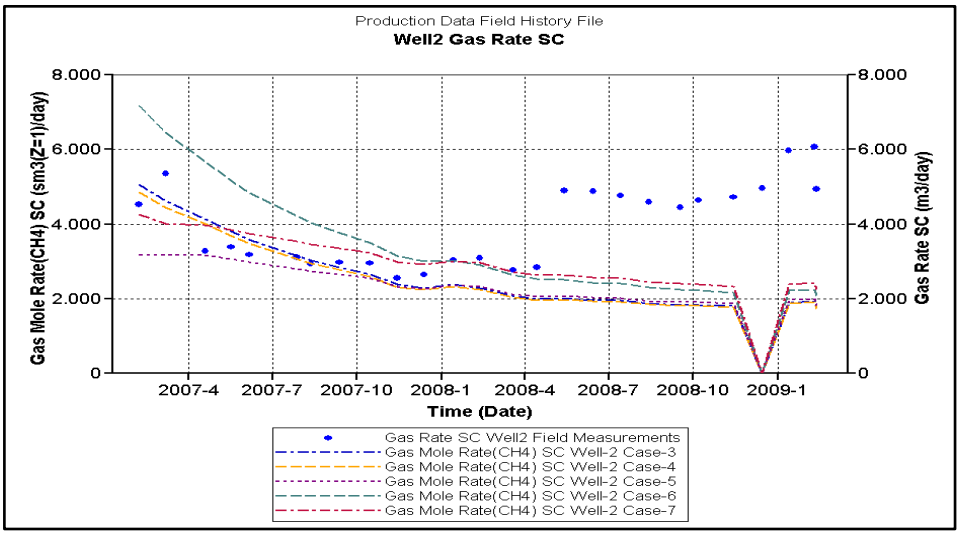


**Figure 62: Well-2 methane production rates.**

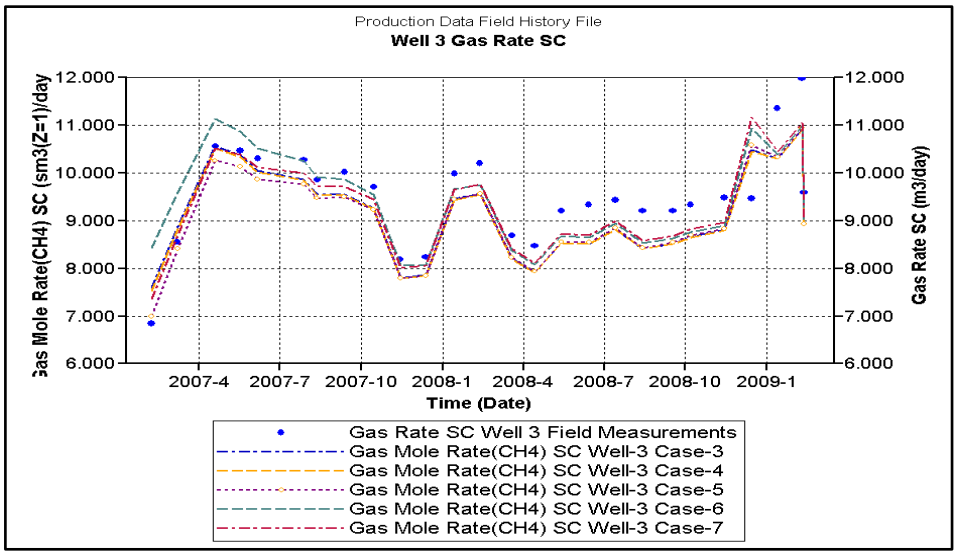


**Figure 63: Well-3 methane production rates.**

From these results, it is clearly seen that a better match established according to changes done, in Case-7. Although rates did not matched, general behavior of rates was gained from model built.

## 5.8 CASE-8

In Case-8, altered parameter was Langmuir pressure. Till this point, effect of permeability, porosity and diffusion time was experienced. After this point model parameters were kept constant as Case-7 except Langmuir pressure and Langmuir volume.

Recalling methane liberation from coal is defined by Langmuir isotherm depending on pressure of the coal seam and gas content of the seam, Langmuir isotherm parameters were changed in the model accordingly. Effect of Langmuir pressure and Langmuir volume on methane liberation and rates were discussed in Chapter-2 section "2.5.3 Methane Adsorption-Desorption Behavior". As seen in Figure 13 for different $P_L$ values, slope of the curves are different. For lower $P_L$ values, Langmuir isotherm curve has a higher slope indicating higher gas content. According to this behavior, in the model $P_L$ value was increased from 1034 kPa to 1500 kPa in Case-8. Model parameters are given in Table 9.

**Table 15: Case-8 model parameters**

| Case-8 | | Direction | |
|---|---|---|---|
| | x | y | z |
| Cleat Permeability (md) | 5 | 4 | 1 |
| Cleat Porosity (%) | 2 | | |
| Water Saturation (%) | 0.3 | | |
| Fracture Spacing (m) | 0.8 | 0.4 | 0.1 |
| Diffusion Time (days) | 400 | | |
| Langmuir Pressure (kPa) | | 1500 | |
| Gas Content ($m^3$/ton) | | 6.24279 | |

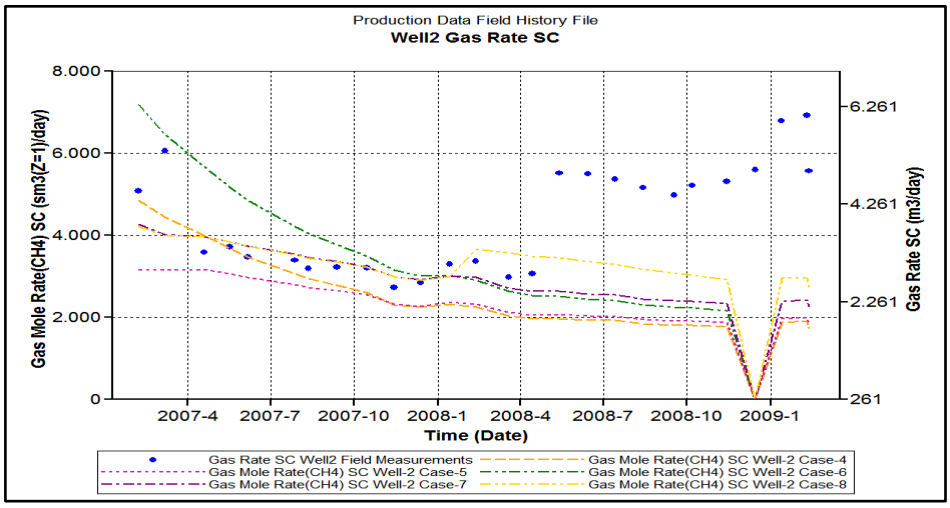


**Figure 64: Case-8 run results for Well-2 (Station 1)**

As seen in Figure 64, computed methane rates from Well-2 (Station-1) started to follow general behavior of the field. Increase in field rates during 13.12.2007-19.03.2008 was also observed from the model runs.

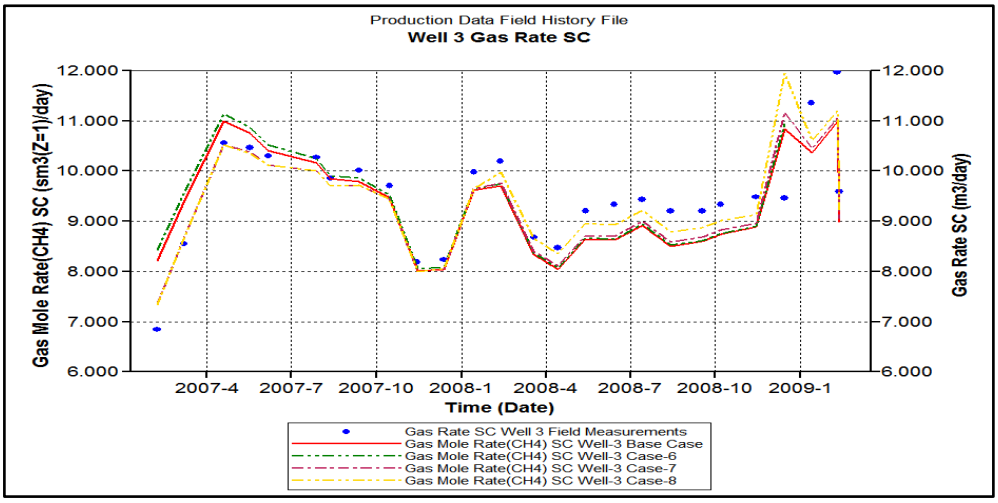


**Figure 65: Case-8 run results for Well-3 (Station-3)**

In this figure (Figure 65), till 12.02.2008, methane rates did not differ from Case-7's resultant rates; however, after 12.02.2008 rates increased significantly and followed the general behavior.

## 5.9 CASE-9

In this case, effect of gas content was observed. Gas content of the coal seam was decreased to 5 $m^3$/ton from 6.24 $m^3$/ton and the other parameters kept constant as in Case-7.

**Table 16: Case-9 Model parameters**

| Case-9 | | | |
|---|---|---|---|
| | Direction | | |
| | x | y | z |
| Cleat permeability (md) | 5 | 4 | 1 |
| Cleat porosity (%) | 2 | | |
| Water saturation (%) | 0.3 | | |
| Fracture spacing (m) | 0.8 | 0.4 | 0.1 |
| Diffusion time (days) | 400 | | |
| Langmuir pressure (kPa) | | 1034 | |
| Gas content ($m^3$/ton) | | 5 | |

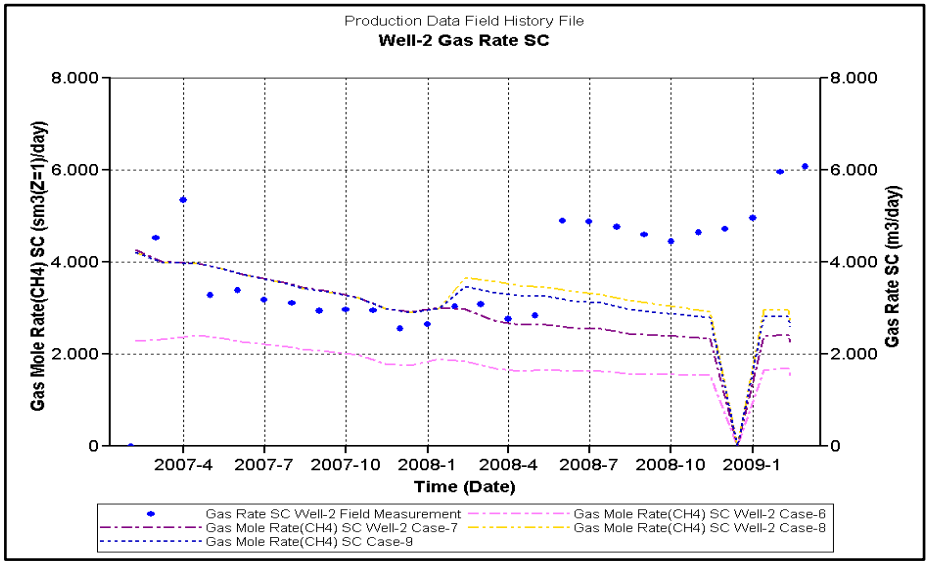


**Figure 66: Well-2 methane rates for Cases 6, 7, 8 and 9.**

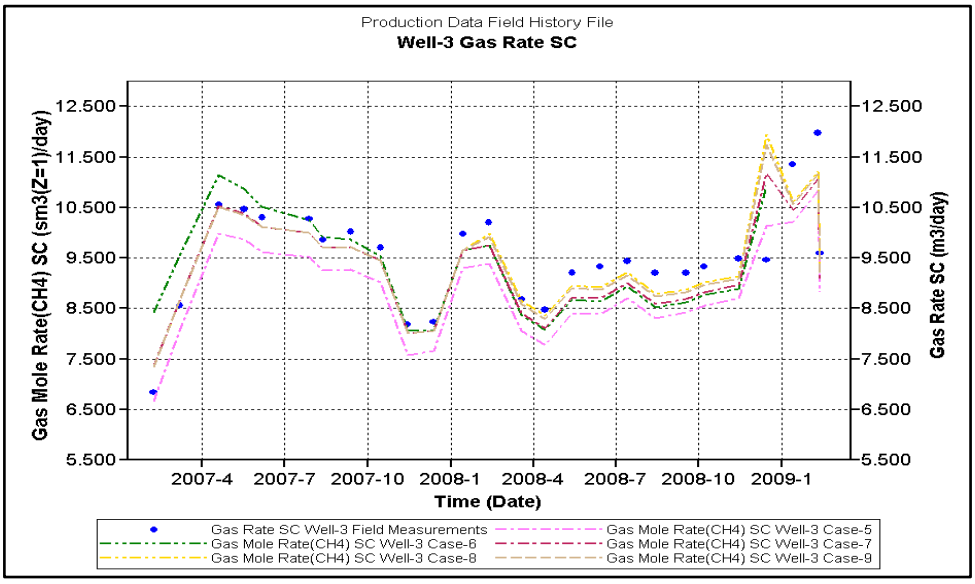


**Figure 67: Well-3 methane rates for Cases 6, 7, 8 and 9.**

According to the decrease in gas content, rates were decreased, but they still show the general trend of the field data.

## 5.10 CASE-10

After reminding the effect of Langmuir pressure and Langmuir volume at Case-8 and Case-9, following runs defined to match the rates.

**Table 17: Case-10 used model parameters**

| Case-10 | Direction | | |
|---|---|---|---|
| | x | y | z |
| Cleat permeability (md) | 5 | 4 | 1 |
| Cleat porosity (%) | 2 | | |
| Water saturation (%) | 0.3 | | |
| Fracture spacing (m) | 0.8 | 0.4 | 0.1 |
| Diffusion time (days) | 400 | | |
| Langmuir pressure (kPa) | | 2000 | |
| Gas content ($m^3$/ton) | | 6.24279 | |

In Case-10 Langmuir Pressure increased to 2000 kPa and results of this run can be seen in Figure 68 and Figure 69.

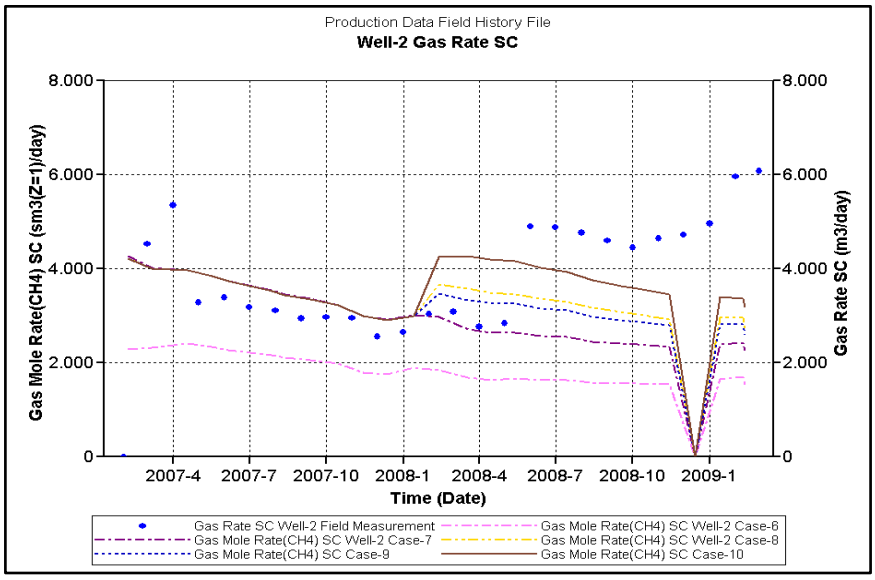


**Figure 68: Well-2 Methane rates for Cases 6, 7, 8, 9, 10.**

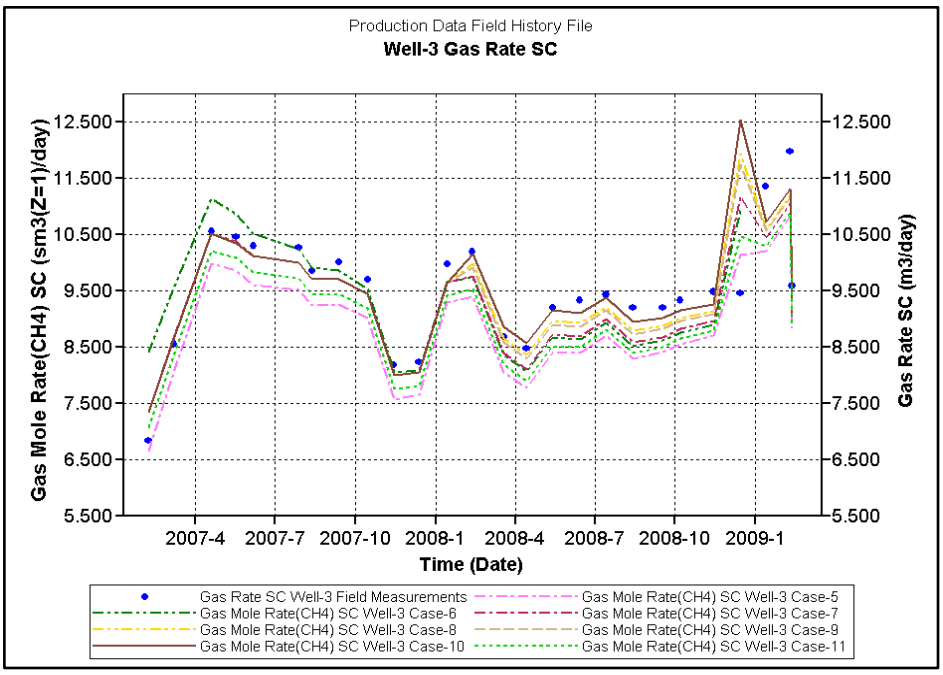


**Figure 69: Well-3 Methane rates for Cases 6, 7, 8, 9, 10.**

According to results of Case-10, increase in Langmuir pressure from 1500 kPa to 2000 kPa led increase in methane rates both in Well-2 and Well-3.

In Well-2 rates became closer than the other runs as showing the general trend of rates measured at field after 14.01.2008.

In Well-3 rates became closer than the other runs as in Well-2, however; at 15.12.2008 rates over computed and this over rates included in errors.

## 5.11 CASE-11

For Case-11, Langmuir pressure was defined as 2500 kPa gas content as 6 $m^3$/ton. Case model parameters are shown in Table 18.

**Table 18: Case-11 model parameters**

| Case-11 | Direction | | |
|---|---|---|---|
| | x | y | z |
| Cleat permeability (md) | 5 | 4 | 1 |
| Cleat porosity (%) | 2 | | |
| Water saturation (%) | 0.3 | | |
| Fracture spacing (m) | 0.8 | 0.4 | 0.1 |
| Diffusion time (days) | 400 | | |
| Langmuir pressure (kPa) | | 2500 | |
| Gas content ($m^3$/ton) | | 6 | |

Results for Case-11 are seen in Figure 70 and Figure 71 for Well-2 and Well-3 accordingly.

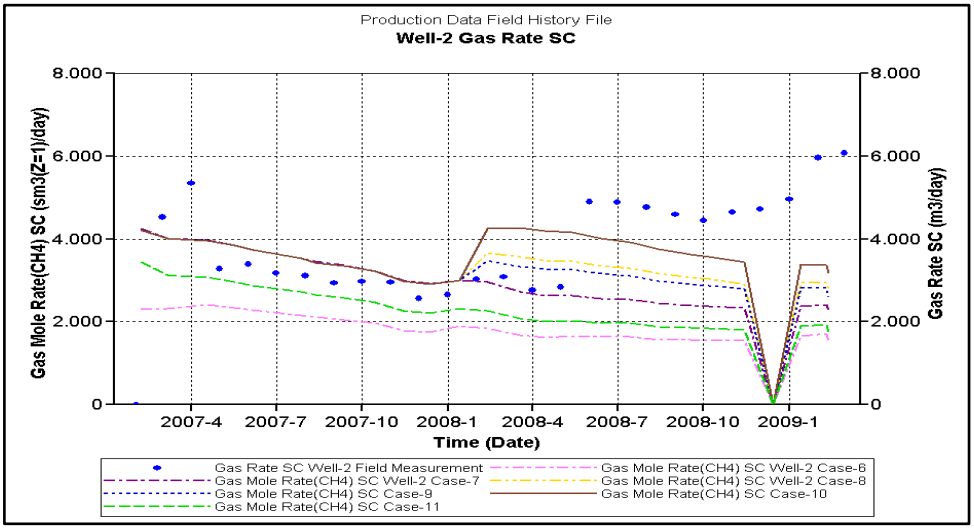


**Figure 70: Well-2 Methane rates for Cases 6, 7, 8, 9, 10 and 11.**

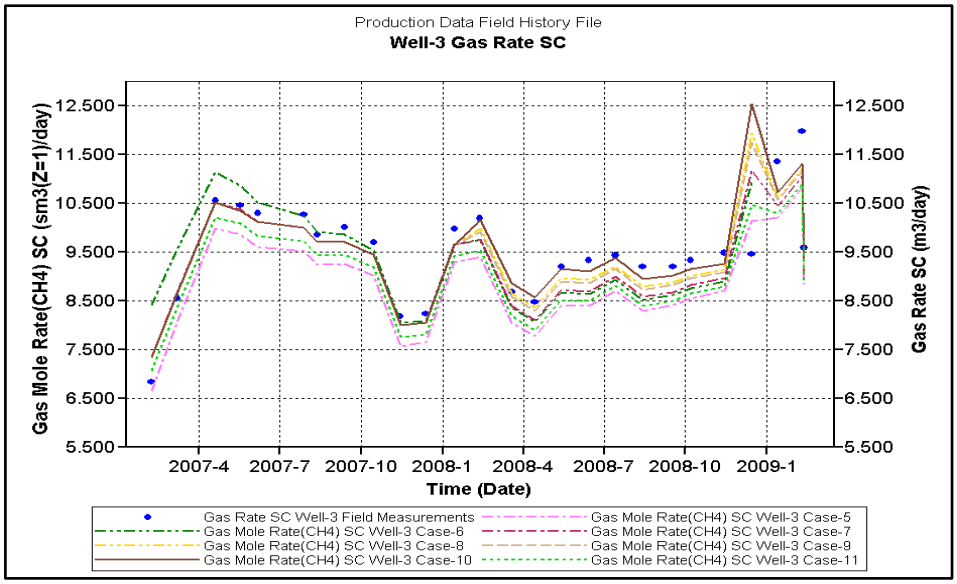


**Figure 71: Well-3 Methane rates for Cases 6, 7, 8, 9, 10 and 11.**

According to Figure 70 and Figure 71, methane rates were decreased according to the increased $P_L$.

## 5.12 CASE-12

In this case Langmuir pressure and Langmuir volume both changed. Langmuir pressure again defined as 2000 kPa and Langmuir volume defined as 5 $m^3$/ton.

**Table 19: Case-12 model parameters**

| Case-12 | Direction | | |
|---|---|---|---|
| | x | y | z |
| Cleat permeability (md) | 5 | 4 | 1 |
| Cleat porosity (%) | 2 | | |
| Water saturation (%) | 0.3 | | |
| Fracture spacing (m) | 0.8 | 0.4 | 0.1 |
| Diffusion time (days) | 400 | | |
| Langmuir pressure (kPa) | | 2500 | |
| Gas content ($m^3$/ton) | | 5 | |

Results of Case-12 can be seen at the following figures (Figure 72, Figure 73).

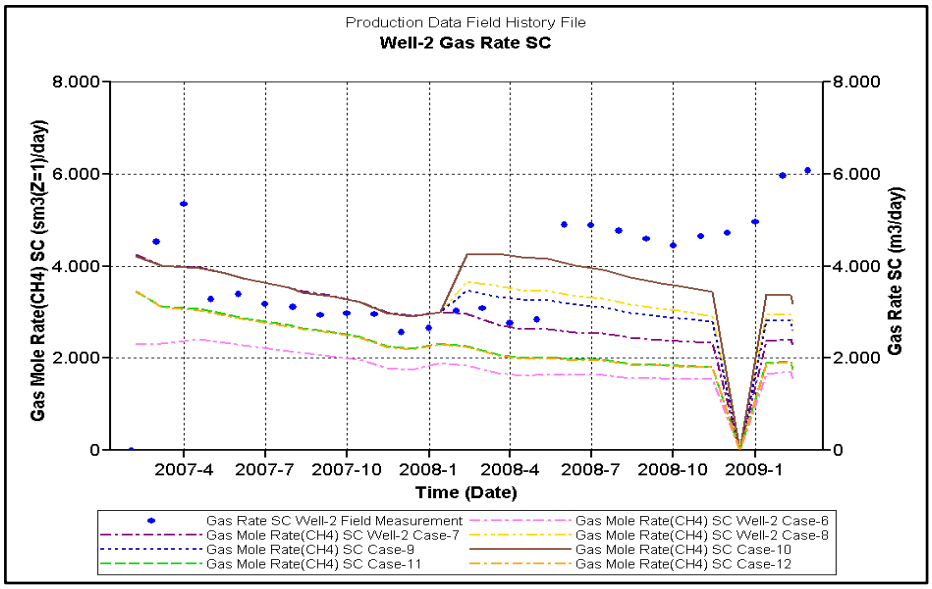


**Figure 72: Well-2 Methane rates for Cases 6, 7, 8, 9, 10, 11 and 12.**

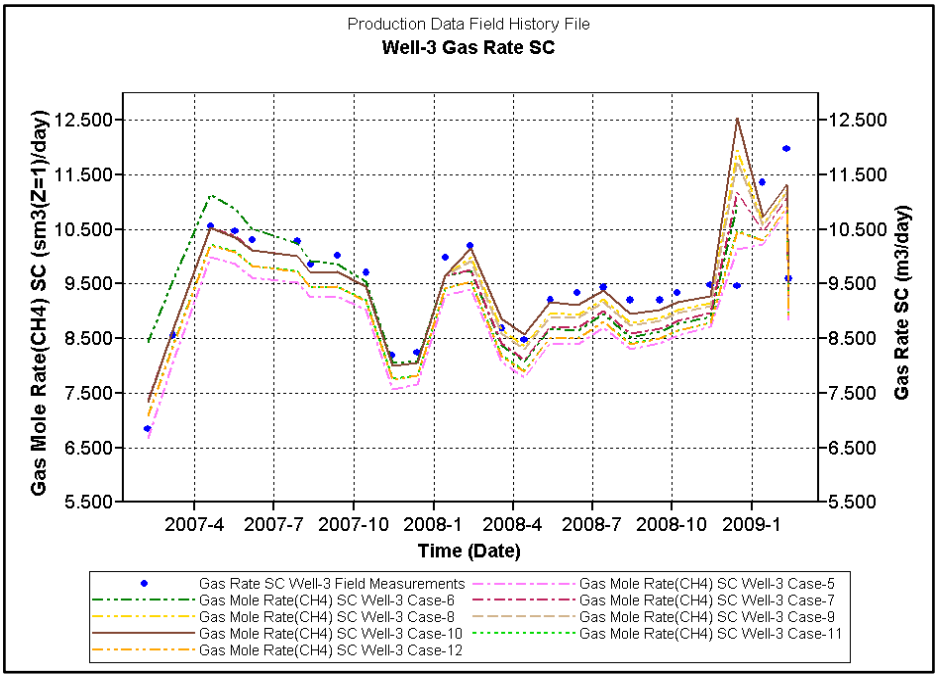


**Figure 73: Well-3 Methane rates for Cases 6, 7, 8, 9, 10, 11 and 12.**

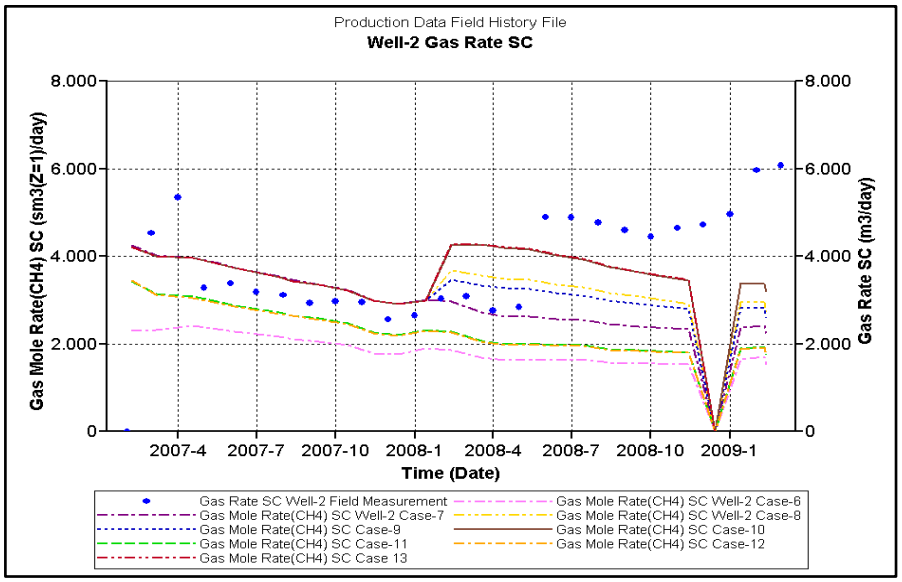


**Figure 74: Well-2 Methane rates for Cases 6, 7, 8, 9, 10, 11, 12 and 13.**

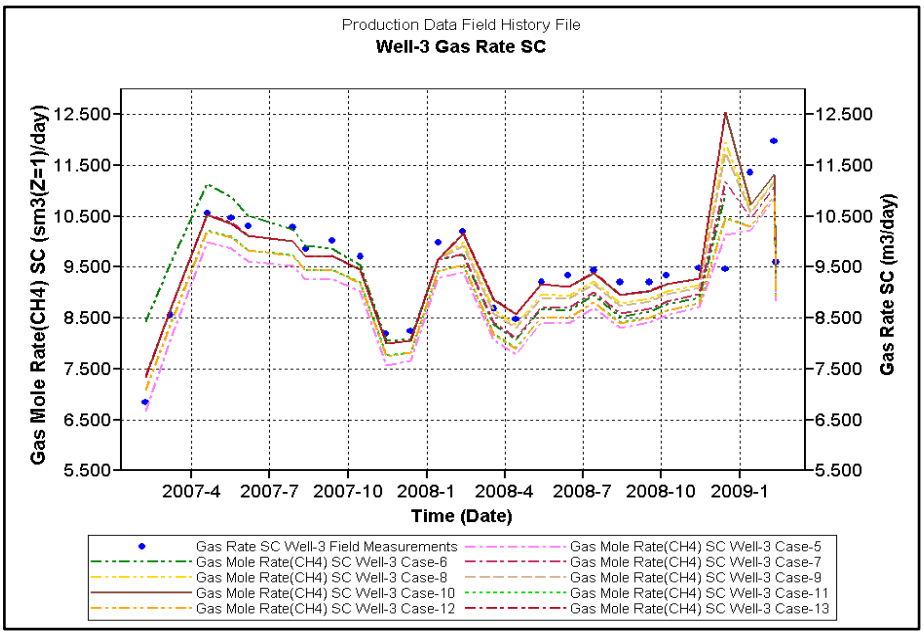


**Figure 75 Well-3 Methane rates for Cases 6, 7, 8, 9, 10, 11, 12 and 13**

As seen in Figure 74 and Figure 75, combinational effect of Langmuir pressure and Langmuir volume came closer to the field rates and almost gives the same rates with Case-10. For a better understanding over all case parameters are listed in Table 20, and changed parameters and new values for each case are seen in red.

**Table 20: Reservoir parameters used for each cases**

| | Base Case | | | Case-1 | | | Case-2 | | |
|---|---|---|---|---|---|---|---|---|---|
| | **x** | **y** | **z** | **x** | **y** | **z** | **x** | **y** | **z** |
| Cleat Permeability (md) | 4 | 4 | 1 | 0.1 | 0.1 | 0.01 | 6 | 4 | 1 |
| Cleat Porosity (%) | 2 | | | 2 | | | 2 | | |
| Water Saturation (%) | 0.3 | | | 0.3 | | | 0.3 | | |
| Fracture Spacing (m) | 0.5 | 0.25 | 0.1 | 0.5 | 0.25 | 0.1 | 0.5 | 0.25 | 0.1 |
| Diffusion Time (days) | 100 | | | 100 | | | 100 | | |
| Langmuir Pressure (kPa) | 1034 | | | 1034 | | | 1034 | | |
| Gas Content ($m^3$/ton) | 6.24279 | | | 6.24279 | | | 6.24279 | | |
| | **Case-3** | | | **Case-4** | | | **Case-5** | | |
| | **x** | **y** | **z** | **x** | **y** | **z** | **x** | **y** | **z** |
| Cleat Permeability (md) | 3 | 1 | 1 | 3 | 1 | 0.15 | 3 | 1 | 0.15 |
| Cleat Porosity (%) | 2 | | | 2 | | | 2 | | |
| Water Saturation (%) | 0.3 | | | 0.3 | | | 0.3 | | |
| Fracture Spacing (m) | 0.5 | 0.25 | 0.1 | 0.5 | 0.25 | 0.1 | 0.5 | 0.25 | 0.1 |
| Diffusion Time (days) | 100 | | | 100 | | | 300 | | |
| Langmuir Pressure (kPa) | 1034 | | | 1034 | | | 1034 | | |
| Gas Content ($m^3$/tonne) | 6.24279 | | | 6.24279 | | | 6.24279 | | |
| | **Case-6** | | | **Case-7** | | | **Case-8** | | |
| | **x** | **y** | **z** | **x** | **y** | **z** | **x** | **y** | **z** |
| Cleat Permeability (md) | 4 | 6 | 1 | 5 | 4 | 1 | 5 | 4 | 1 |
| Cleat Porosity (%) | 2 | | | 2 | | | 2 | | |
| Water Saturation (%) | 0.3 | | | 0.3 | | | 0.3 | | |
| Fracture Spacing (m) | 0.5 | 0.25 | 0.1 | 0.8 | 0.4 | 0.1 | 0.8 | 0.4 | 0.1 |
| Diffusion Time (days) | 300 | | | 400 | | | 400 | | |
| Langmuir Pressure (kPa) | 1034 | | | 1034 | | | 1500 | | |
| Gas Content ($m^3$/tonne) | 6.24279 | | | 6.24279 | | | 6.24279 | | |

| | Case-9 | | | Case-10 | | | Case-11 | | |
|---|---|---|---|---|---|---|---|---|---|
| | **x** | **y** | **z** | **x** | **y** | **z** | **x** | **y** | **z** |
| Cleat Permeability (md) | 5 | 4 | 1 | 5 | 4 | 1 | 5 | 4 | 1 |
| Cleat Porosity (%) | 2 | | | 2 | | | 2 | | |
| Water Saturation (%) | 0.3 | | | 0.3 | | | 0.3 | | |
| Fracture Spacing (m) | 0.8 | 0.4 | 0.1 | 0.8 | 0.4 | 0.1 | 0.8 | 0.4 | 0.1 |
| Diffusion Time (days) | 400 | | | 400 | | | 400 | | |
| Langmuir Pressure (kPa) | 1034 | | | 2000 | | | 2500 | | |
| Gas Content ($m^3$/tonne) | 5 | | | 6.24279 | | | 6 | | |
| | **Case-12** | | | **Case-13** | | | | | |
| | **x** | **y** | **z** | **x** | **y** | **z** | | | |
| Cleat Permeability (md) | 5 | 4 | 1 | 5 | 4 | 1 | | | |
| Cleat Porosity (%) | 2 | | | 2 | | | | | |
| Water Saturation (%) | 0.3 | | | 0.3 | | | | | |
| Fracture Spacing (m) | 0.8 | 0.4 | 0.1 | 0.8 | 0.4 | 0.1 | | | |
| Diffusion Time (days) | 400 | | | 400 | | | | | |
| Langmuir Pressure (kPa) | 2000 | | | 2500 | | | | | |
| Gas Content ($m^3$/tonne) | 5 | | | 7.5 | | | | | |

In order to see all of the case results and find the best fitted case to field data, Figure 76 and Figure 77 are presented below.

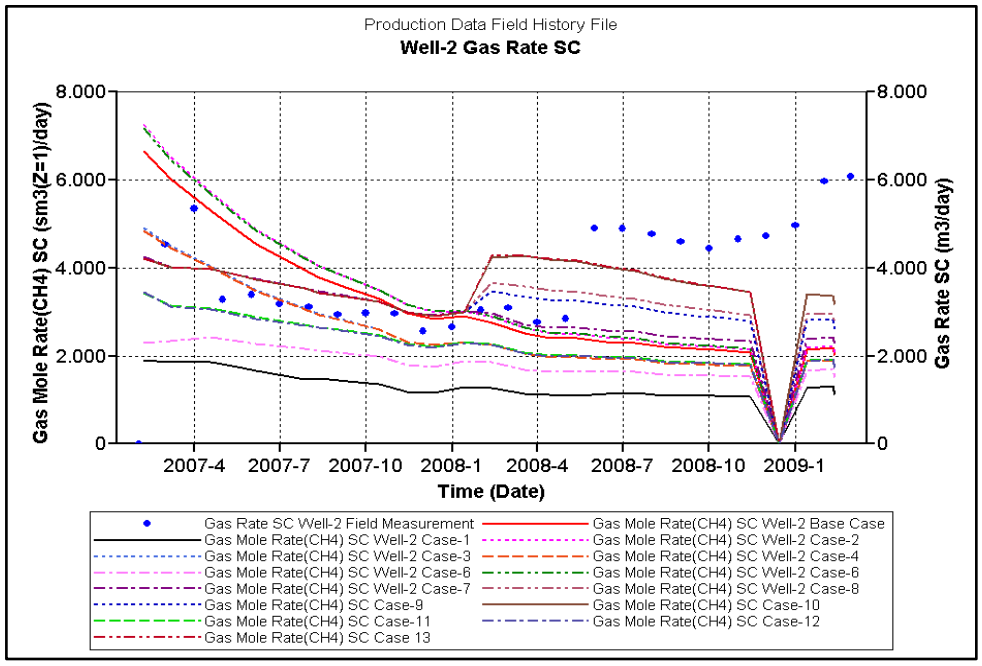


**Figure 76: Overall cases results for Well-2**

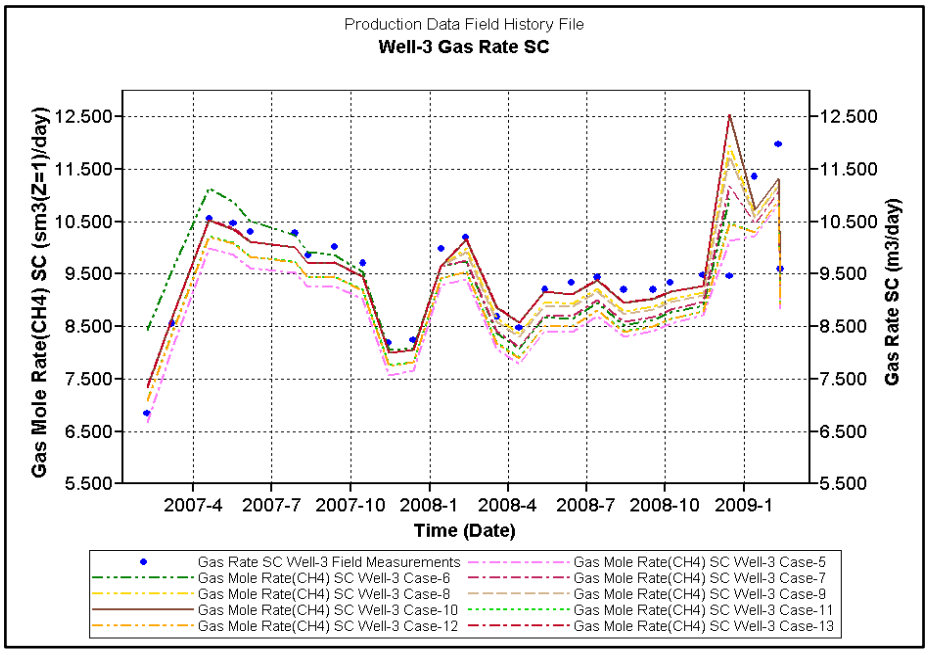


**Figure 77: Overall cases results for Well-3.**

Determining the best fitted case to the field measurements requires error calculation between case resultant rates and field measurements for each well.

In statistical modeling process, root mean squared error method is a commonly used method, representing the difference between the actual observations and the response predicted by the model. It is a quadratic scoring rule used to determine whether the model does not fit the data.

In this method, the difference between forecasted values and corresponding observed values are each squared and then averaged overall sample. Then square root of the average is taken. Since errors are squared before averaged, results of this method give relatively high weight to large errors.

$$RMSE(\theta_1, \theta_2) = \sqrt{MSE(\theta_1, \theta_2)} = \sqrt{E(\theta_1 - \theta_2)^2} = \sqrt{\frac{\sum_{i=1}^{n} (x_{1,i} - x_{2,i})^2}{n}}$$

**Equation 6**

According to Equation 6, fitting errors were computed for Well-2 and Well-3 for each case and as seen in Figure 78 and Figure 79.

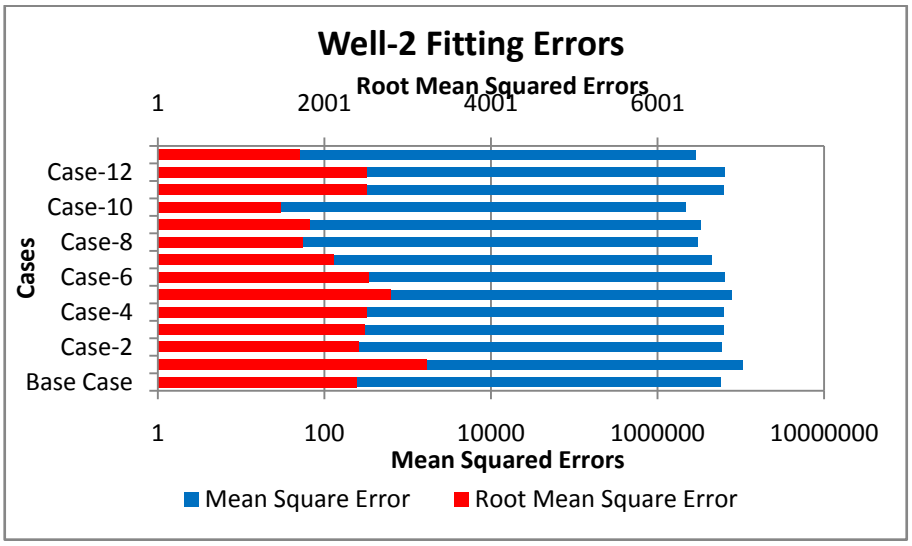


**Figure 78: Well-2 computed fitting errors.**

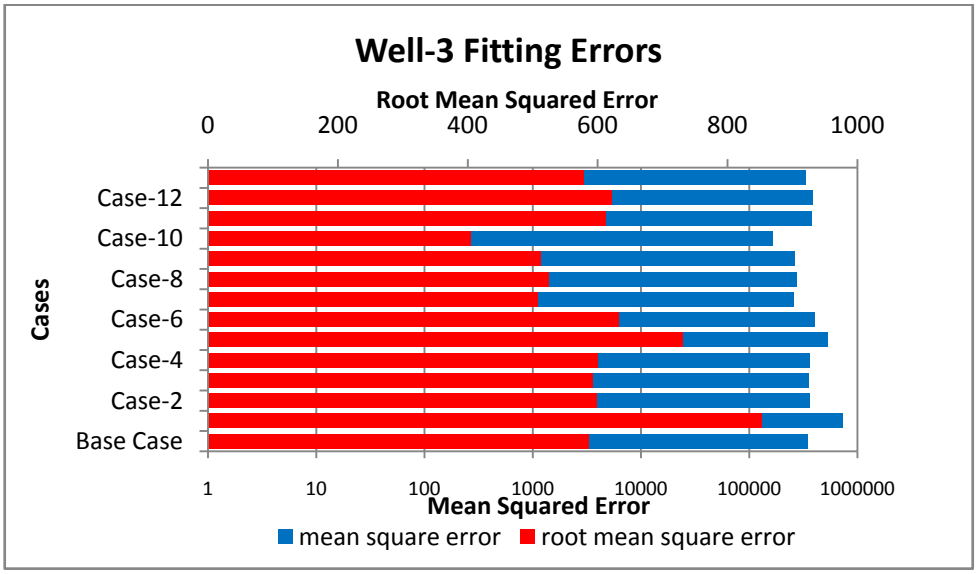


**Figure 79: Well-3 computed fitting errors.**

From Figure 78 and Figure 79, it is clear that the least error corresponds to the results of Case-10.

# CHAPTER 6

# CONCLUSIONS

In this study, methane emissions from longwall panels and their production potentials were investigated and studies worked on this issue was presented as well as the projects practiced or have been implementing in different countries were mentioned. In addition to these basic concepts according to coaled methane and coal mine methane were discussed and the importance of capturing and utilizing methane emissions not only for safety reasons but also the environmental point of view was expressed once more.

This study was the first study practiced for using ventilation air measurements as an input to a numerical simulation. A three dimensional coalbed methane reservoir model was constructed inclusive this study and a history match analysis technique was used to determine reservoir parameters of coal seam overlying Yeni Çeltek Coal Mine abandoned panels.

Through the light of this study;

- Cleat permeability and Langmuir pressure are being the most crucial parameters in the coal reservoir affected the rate of methane production.
- Depending on the error calculations, at Case-10, best results were obtained. According to the best match, characteristic properties of the coal seam overlies to the abandoned panels present in Table 21. Although it may be the best estimate, for more accurate results of reservoir properties of the coal seam, these values should confirmed with well test interpretation or field production data.

**Table 21: Resultant coal seam parameters**

| Case-10 | Direction | | |
|---|---|---|---|
| | x | y | z |
| Cleat permeability (md) | 5 | 4 | 1 |
| Cleat porosity (%) | 2 | | |
| Water saturation (%) | 0.3 | | |
| Fracture spacing (m) | 0.8 | 0.4 | 0.1 |
| Diffusion time (days) | 400 | | |
| Langmuir pressure (kPa) | | 2000 | |
| Gas content ($m^3$/ton) | | 6.24279 | |

- For a better understanding of the seam parameters, geomechanical changes due to the methane desorption, shrinkage and swelling feature, and their effects should be considered.

- Results of the model runs were not matched in Well-1 however the rates in this well could be increased regarding of a new panel activity or increase in mining activity in those days (after 2008-6), therefore mining activities report should be checked to be ensure.

- Characterization of the coal seam is a very important step to be taken before the degasification methods used to know the properties of the coal strata and limits according to these properties. Characterization studies results in saving money from expensive and time consuming operations.

- Integration of ventilation data measured in airways with the numerical reservoir

simulation and using history matching technique to determine reservoir and fluid flow parameters is a promising method in terms of time and economics.

# REFERENCES

Fekete Associates Inc. (2010). CBM Concepts. Retrieved November 02, 2010, from Fekete Reservoir Engineering Software & Services: http://www.fekete.com/software/cbm/media/webhelp/c-te-concepts.htm

Roffe , S. R., & Bauder, J. W. From Prehistory to the Pipeline . The Fingerprint of Coal Bed Methane.
Department of Land Resources and Environmental Sciences.

(2011, January 15). Retrieved from Geohistory: http://geohistory.valdosta.edu/basics/basic_coal.html

Advanced Resources International Inc. (November 1993). Characterization of Fruitland Coal Through Reservoir Simulation. GRI.

Ahmed, T., Centilmen, A., & Roux, B. (2006). A Generalized Material Balance Equation for Coalbed Methane Reservoirs. SPE Annual Technical Conference.

Ahmed, U., Johnston, D., & Colson, L. (1991). An Advanced and Integrated Approach to Coal Formation Evaluation.

Aminian, K., & Mohaghegh, S. (2007). Coalbed Methane Reservoir Engineering.

BP. (2007). Conjuring with Coal. (29-32).

Bryant, A. (2010). Coal. Retrieved 12 12, 2010, from geology.com: htpp://geology.com/rocks/coal.shtml

Coal-Seq Project Update: Field Studies of ECBM Recovery/CO2 Sequestration in Coal Seams. (n.d.).

Computer Modeling Group. (n.d.). CMG GEM Simulator manual.

Cote, M., Collings, R., Pilcher, R., & Talkington, C. (2004, April). Methane Emmissions From Abondoned Coal Mines in the United States: Emission Inventory Metodology and 1990-2002 Emissions Estimates. U.S Enviromental Protection Agency.

Courtesy of Ruby Canyon Engineering. (2010).

Einsele, G. (2000). Sedimantary Basins: Evolution, Facies, and Sediment Budget 2nd ed. Tuebingen: Springer.

Enever, J. R., & Hennig, A. (1997). The relationship between permeability and effective stress for Australian coals and its implications with respect to coalbed methane exploration and reservoir modelling. International coalbed methane symposium (pp. 13-22). Tuscaloosa: The university of Alabama.

Enever, J. R., & Hennig, A. (1997). The relationship between permeability and effective stress for Australian coals and its implications with respect to coalbed methane exploration and reservoir modelling,. International coalbed methane symposium.

Enviromental Protecting Agency. (February 2002). Coal Mine Methane-Reiew of the Mechanisms for Control of Emissions.

EPA. (n.d.). Retrieved from United States Enviromental Protection Agency: www.epa.gov/cmop/docs/cmm_recovery.pdf

EPA. ( 2009). Enviromental Protecting Agency Coal Mine Methane Recovery, a Primmer. EPA.

EPA. (June 2004 ). Evaluation of Impacts to Underground Sources . Chapter 3: Characteristics of CBM Production and Associated HF Practices.

EPA. (2004). Evaluation of Impacts to Underground Sources June 2004. Chapter 5: Summary of Coalbed Methane Descriptions. EPA.

EPA. (June 2004). Evaluation of Impacts to Underground Sources. Chapter-5 Summary of Coalbed Methane Descriptions. EPA.

EPRI. (1999). Enhanced Oil Recovery Scoping Study. Palo Alto: EPRI.

Ertekin, T. S. (1988). Production performance analysis of horizontal drainage wells for the degasification of coal seams. Journal of Petroleum Technology , 625-632.

Esterhuizen, G., & Karacan, C. ( 2005). Development of Numerical Models to Investigate Permeability Changes and Gas Emission around Longwall Mining Panel. Alaska Rocks 2005, The 40th U.S. Symposium on Rock Mechanics (USRMS): Rock Mechanics for Energy, Mineral and Infrastructure Development in the Northern Regions. Anchorage, Alaska, : American Rock Mechanics Association .

Evert Hoek, E. T. (1990). Underground excavations in rock. Taylor & Francis .

Fanchi, J. R. (1990, August). claculation of parachors for compositional simulation. SPE Reservoir Engineering , 433-436.

Fernland, & Henry. (2011, 01 25). Global Methane Initiative. Retrieved 01 25, 2011, from globalmethane: http://www.globalmethane.org/gmi/

Flores, R. (2008, November 5). Coalbed Methane: Gas of the Past, Present, and Future. Retrieved December 01, 2010, from SciTopics: http://www.scitopics.com/Coalbed_Methane_Gas_of_the_Past_Present_and_Future.html

Flores, R. M. (1998). Coalbed Methane: From Hazard to resource. International Journal of Coal Geology , Volume 35 (Issues 1-4), 3-26.

Franklin, P., Scheehle, E., Collings, R. C., & Pilcher, R. C. (October 2004). Proposed Methodology for Estimating Emission Inventories From abondoned Coal Mines. 2006 IPCC National Greenhouse Gas Inventories Guidelines Fourth Authors/Experts Meeting. Arusha, Tanzania.

Future Supply and Emerging Resources Coal Bed Natural Gas. (n.d.). Retrieved July 5, 2010, from http://www.netl.doe.gov/technologies/oil-gas/futuresupply/coalbedng/coalbed_ng.html

Gash, B., Volz, R. F., Potter, G., & Corgan, J. M. (1993). The Effects of Cleat Orientation and Confining Pressure on Cleat Porosity, Permeability and Relative Permeability in Coal. Proceedings of the 1993 International Coalbed Methane Symposium. Birmingham ,Alabama.

General Directorate of Turkish Coal Enterprises TKI , Turkish Statistical Institute. (2010, March 13). Turkish Coal Production & Consumption 2009. Retrieved December 01, 2010, from GlobalTrade.net: http://www.globaltrade.net/international-trade-import-exports/f/market-research/text/Turkey/Mining-and-Quarrying-Coal-and-Lignite-Turkish-Coal-Production---Consumption-2009.html

Geohistory.valdosta.edu. (2010). Retrieved 02 01, 2011, from Geohistory.valdosta.edu: goehistory.valdosta.edu./basics/basic_coal.html

Geology.com. (2010). Retrieved 02 01, 2011, from Geology.com: http://geology.com/rocks/coal.shtml

Gilman, A., & Beckie, R. (2000). Flow of coalbed methane to a gallery. Transport in porous media 41 , pp. 1-16.

Global Methane Initiatives. (2010). Retrieved 01 15, 2011, from Global Methane Initiatives: http://www.globalmethane.org/partners/index.aspx

Göktaş, B., & Ertekin, T. (1999). Development of a Local Grid-Refinement Technique for Accurate Representation of Cavity - Completed Wells in Reservoir Simulators. SPE Journal Vol.4 , Vol. 4 (No.3), 187-195.

Guo, X., Du, Z., & Li, S. (2003). Computer modeling and simulation of coalbed methane reservoir.

Güney, M. (1972). An assesment of the methane content and the firedamp emission from certain coal seam in Kozlu district, Zonguldak Coal Field.

Halliburton. (2007). Chapter 3 Sorption. In CBM Principles and Practices (pp. 143-185).

http://geohistory.valdosta.edu/basics/basic_coal.htm Retrieved from http://geohistory.valdosta.edu/basics/basic_coal.html

International Coal Bed Methane Conference. (2005). Bochum.

IPCC (Intergovermental Panel on Climate Change). (2001). Climate Change 2001: The Scientific Basis. Cambridge, UK.

Jones, A., Ahmed, U., Abou-Sayed, A. S., Mahyera, A., & Sakashita, B. (1982). Fractured vertical wells versus horizontal boreholes for methane drainage in advance of mining U.S. coals, Seam gas drainage with particular reference to the working seam., (pp. 172-201).

Karaca, C., Diamond, W., & Schatzel, S. (2007). Numerical analysis of the influence of in-seam horizontal methane drainage boreholes on longwall face emission rates. International Journal of Coal Geology , 72, 15-32.

Karacan, Ö. C. (2008). Evaluation of the relative importance coalbed reservoir parameters for prediction of methane inflow ratesduring mining of longwall development entries. 34 (9).

Karacan, Ö. C. (2008). Modeling and prediction of ventilation methane emissions of U.S. longwall mines using supervised artificial neural networks. International Journal of Coal Geology , 73 (3-4).

Karacan, Ö. C. (2009). Reconciling longwall gob gas reservoirs and venthole production performances using multiple-rate drawdown well test analysis.

Karacan, Ö. C., Diamond, W. P., Esterhuizen, G. S., & Schatzel, S. J. (May 18-19, 2005). Numerical Analysis of the Impact of Longwall Panel Width on Methane Emissions

and Performance of Gob Gas Ventholes. Tuscaloosa, AL: University of Alabama,.

Karacan, Ö. C., Felicia, R. A., Michael, C., & Sally, P. (2010). Coal mine methane: a review of capture and utilization technologies with benefits to mining safett and to greenhouse gas reduction.

Karayigit, A. I., Eris, E., & Cicioglu, E. (1996). Coal geology, chemical and petrographical characteristics, and implementations for coalbed methane development of subbituminous coal fram the Sorgun and Suluova basins, Turkey. Geological Publications, London, special Publications , v.109, pp. 325-338.

King, G. E. (1991). State of the art modeling for unconventional gas recovery. SPE Formation Evaluation , 63-72.

Koperna, G. J., & Reistenberg, D. (2009). Carbon Dioxide Enhanced Coalbed Methane and Storage: Is There Promise? San Diego, California: SPE.

Kuurskraa, V. A., & Stevens, S. H. (2009). Worldwide Gas Shales and Unconventional Gas: A Status Report. Copenhag.

Kyle, B. (2010, May 13). Wikipedia. Retrieved from Wikipedia, The Free Encyclopedia: http://en.wikipedia.org/wiki/Departure_function

Levine, J. R. (1996). Model study of the influence of matrix shrinkage on absolute permeability of coal bed reservoirs. Coalbed Methane and Coal Geology, Geological Society, London, Special Publications , 197-212.

Library and Archives Canada. Coal. Library and Archives Canada.

Lunarzewski, L. (1998). Gas emission prediction and recovery in underground coal mines. International Journal of Coal Geology , 117–145.

Major, T. (1996). Genesis and The Origin of Coal and Oil, 2nd Edition. Apologetics Press.

Mavor, M., Close, J., & McBane, R. (1994, December). Formation Evaluation of Exploration Coalbed-Methane Wells. SPE Formation Evaluation , 285-294.

Miller, B. G. (2005). In Coal Energy Systems (p. 1). Elsevier Academic Press.

Mohaghegh, S., & Aminian, K. (2007). Coalbed Methane Reservoir Engineering.

Morad, K., Mireault, R., & Dean, L. (October,2008). Coalbedmethane Fundamentals. Reservoir Engineering for Geologists , 23-26.

Nelson, C. R. (1999). Effects of Coalbed Reservoir Property Analysis Methods on Gas-In-Place Estimates. 1999 SPE Eastern Regional Meeting. West Virginia: SPE.

Oraee, K., & Goodarzi, A. (2010). Mathematical Modeling of Coal Seam Methane Drainage in Longwall Mining.

Paul, G. W. (n.d.). Simulating Coalbed Methane Reservoirs. Advanced Resources International, Inc.

Paul, G. W. Simulating Coalbed Methane Reservoirs.

Peng, S. S., & Chaing, H. S. (1984). SME Mining Handbook.

Presents, H. C. (n.d.). Retrieved Mayıs 15, 2010, from Heritage Community Foundation: http://www.abheritage.ca/abresources/index.html

Rank of Caol. (2010). Retrieved January 11, 2011, from Underground Coal: http://www.undergroundcoal.com.au/outburst/rank.html

Rank of Coal. (2010). Retrieved January 11, 2011, from Underground Coal: http://www.undergroundcoal.com.au/outburst/rank.html

Reeves, S. R. The Coal_Seq Project: Key Results from Field, Laboratory, and Modeling Studies.

Reeves, S., & Oudinot, A. (2005). The Tiffany Unit N2-ECBM Pilot – A Reservoir and

Economic.

Riese, W., Pellzmann, W. L., & Snyder, G. T. (2005). New insights on the hydrocarbon system of the Fruitland Formation coal beds, northern San Juan Basin, Colorado and New Mexico, USA. In T. G. America, Coal Systems Analysis Special Paper 378 (pp. 73-111). Colorado: The Geological Society of America, Inc.

S. Badr, U. O. Three-dimensional strain softening modeling of deep longwall coal mine layouts. Colorado School of Mines, Golden, Colorado, USA .

Saghafi, A. (2001). Coal Seam Gas Reservoir Characterization. Gas from Coal Symposium. Brisbane.

Saulsberry, J. S., & Schraufnagel, R. (1996). A guide to coalbed methane reservoir engineering. Chicago Ill : Gas Research Institue.

Schatzel, C. &. A typical long-wall face. NOISH, Pittsburg Research Laboratory.

Schatzel, S. J., Karacan, C. Ö., Krog, R. B., Esterhuizen, G. S., & Goodman, G. V. (2008). Guidelines for the Prediction and Control of Methane Emissions on Longwall. Pittsburg, PA: Department of Health nad Human Servises (NOISH).

Schobert, H. H. (1989). Chem I. Supplement: I. The Classification and Origin of Coal. Journal of Chemical Education , Volume 66 (03), 242-244.

Schobert, H. H. (1989). Chem I. Supplement: I. The Classification and Origin of Coal. Journal of Chemical Education , Volume 66 (03), 242-244.

Schobert, H. H. (1989). The Geochemistry of Coal. Journal of Chemical Education , Volume 66 (Number 3), 242-244.

Sieddle, & Arri. (1990).

Sinclair, J. (1960). Winning Coal. Londan: Pitman Press.

Speight, J. G. (2005). Hand Book of Coal Analysis. John Wiley nad Sons, Inc.

Speight, J. G. (2005). Handbook of Coal Analysis. John,Wiley &Sons, Inc.

Speight, J. (2005). Hand Book Of Coal Analysis.

Speight, J. (2005). Hand Book Of Coal Analysis.

Stefanko, R. (1983). Coal Mining Technology Theory and Practice. New York: Society of Mining Engineers .

Suarez-Ruiz, I., & Crelling, J. C. (2008). Applied Coal Petrology. In The Role of Petrolgy in Coal Utilization (p. 55). Elsevier.

Suarez-Ruiz, I., & Crelling, J. C. (2008). Applied Coal Petrology. In I. Suarez-Ruiz, & J. C. Crelling, The Role of Petrology in Coal Utilization (p. 55). Elsevier.

Suarez-Ruiz, I., & Crelling, J. C. (2008). Applied Coal Petrology The Role of Petrolgy in Coal Utilization. 55.

Taşel, E., Ozan, T., Unver, E., & Bildik, M. (2001). New Anchorage Capacity Testing System and Pull-Out Applications in Yeniçeltek Coal Mine. 17th International Mining Congress and Exhibition of Turitey- IMCET2001,.

Thakur, P. C. (n.d.). Optimized degasification and ventilation for gassy coal mines.

The Coal Resource: A Comprehensive Overview of Coal.

U.Ahmed, D. J. (1991, October 6-9). An Advanced and Integrated Approach to Coal Formation Evaluation.

U.S. Enviromental Protection Agency. (April 2004). Methane Emission From Abondoned Coal Mines In The United States: Emission Inventory Methodology and 1990-2002 Emissions Estimates.

Uner, M., Kose, N., Gokten, S., & Okan, P. (2008). Financial and economic factors affecting the lignite prices in Turkey: An analysis of Soma and Can lignites. Resources Policy (33), pp. 230-239.

United Nations. (2010).

Unver, B., & Yasitli, N. E. (2005). 3-D numerical modeling of stresses around a longwall panel with top coal caving. The Journal of The South African Institute of Mining and Metallurgy , 105 (MAY/JUNE ).

Unver, B., & Yasitli, N. E. (2006). modeling of strata mavement with a special referance to caving mechanism in thick coal seam. International Journal of Coal Geology (66).

US Enviromental Protecting Agency. (2003).

US EPA. (2003).

US EPA. ( 2009). Coal Mine Methane Recovery, a Primmer.

Vaziri, H., Wang, X., Palmer, I. D., Khodaverdian, M., & McLennan, J. (1997). Back Analysis of Coalbed Strength Properties from Field Measurements of Wellbore Cavitation and Methane Production. 34 (6).

Westport Technology Center, Intertek. (n.d.). Retrieved 5 13, 2010, from www.westport1.com

World Coal Institude. (n.d.). Retrieved from http://www.worldcoal.org/coal/coal-seam-methane/coal-mine-methane/

World Energy Council. (2010). 2010 Survey of Energy Resources. World Energy Council.

Yeni Çeltek Coal Enterprise. (n.d.).

Yeni Çeltek Coal Enterprise. (n.d.). Mine Plan.

Yeni Çeltek Coal Enterprises . (n.d.).

Zuber, M. D., & Boyer, C. M. (2010). Integrated ReservoirCharacterization for Optimization of Unconventional Gas Production.

Zuber, M. D., Sawyer, W., Schraufnagel, R. A., & Kuuskraa, V. A. (1987). The use of

simulation and history matching to determine critical coalbed methane reservoir parameters. Proceedings of the SPE/DOE Low Permeability Reservoirs Symposium, (pp. 307-316). Denver, Colorado.

# APPENDIX

```
RESULTS SIMULATOR GEM

RESULTS SECTION INOUT

*INUNIT *SI

*INTERRUPT *INTERACTIVE

*RANGECHECK *ON

*XDR *ON

*MAXERROR  20

*SUMMARY

*WPRN *WELL  *TIME

*WPRN *GRID  *TIME

*WPRN *ITER  *BRIEF

*WSRF *WELL *TIME

*WSRF *GRID *TIME

*DIARY *CHANGES

*OUTPRN *WELL *PSPLIT

*OUTPRN *GRID PRES

*OUTPRN *RES *ALL

*OUTSRF *WELL  *PSPLIT

*OUTSRF *GRID KRG PRES SG SW Y 'CH4' Y 'N2' Z 'CH4' Z 'N2'

*OUTSRF *RES *NONE
```

```
*DIM *MDALP 11851272 **$ ModelBuilder passed through this Keyword
RESULTS XOFFSET 0.
RESULTS YOFFSET 0.
RESULTS ROTATION 0
RESULTS AXES-DIRECTIONS 1. -1. 1.
GRID VARI 204 260 2
KDIR DOWN
DI CON 3.
DJ CON 3.
DK KVAR
        2. 3.
DTOP
        53040*0
DUALPOR
SHAPE GK
**$ RESULTS PROP NULL MATRIX  Units: Dimensionless
**$ RESULTS PROP Minimum Value: 1  Maximum Value: 1
**$ 0 = NULL block, 1 = Active block
NULL MATRIX CON 1.0
**$ RESULTS PROP NULL FRACTURE  Units: Dimensionless
**$ RESULTS PROP Minimum Value: 1  Maximum Value: 1
**$ 0 = NULL block, 1 = Active block
NULL FRACTURE CON 1.0
**$ RESULTS PROP PINCHOUTARRAY  Units: Dimensionless
**$ RESULTS PROP Minimum Value: 1  Maximum Value: 1
```

```
**$ 0 = PINCHED block, 1 = Active block
PINCHOUTARRAY CON 1.
RESULTS SECTION GRID
RESULTS SECTION NETPAY
**$ RESULTS PROP NETPAY MATRIX  Units: m
**$ RESULTS PROP Minimum Value: 2  Maximum Value: 3
NETPAY MATRIX KVAR
        2.0  3.0
**$ RESULTS PROP NETPAY FRACTURE  Units: m
**$ RESULTS PROP Minimum Value: 2  Maximum Value: 3
NETPAY FRACTURE KVAR
        2.0 3.0
RESULTS SECTION NETGROSS
RESULTS SECTION POR
**$ RESULTS PROP POR MATRIX  Units: Dimensionless
**$ RESULTS PROP Minimum Value: 0.0005  Maximum Value: 0.999
POR MATRIX CON 0.0005
MOD     1:51 126:126 2:2 = 0.1
        51:51 83:125 2:2 = 0.1
        52:113 83:83 2:2 = 0.1
        114:143 83:83 2:2 = 0.1
        143:143 84:148 2:2 = 0.1
        143:143 149:207 2:2 = 0.1
        143:143 208:230 2:2 = 0.1
        69:142 230:230 2:2 = 0.1
```

69:69 231:260 2:2 = 0.1

**$ RESULTS PROP POR FRACTURE  Units: Dimensionless

**$ RESULTS PROP Minimum Value: 0.01  Maximum Value: 0.999

POR FRACTURE CON 0.02

MOD  1:51 126:126 2:2 = 0.999

51:51 83:125 2:2 = 0.999

52:113 83:83 2:2 = 0.999

114:143 83:83 2:2 = 0.999

143:143 84:148 2:2 = 0.999

143:143 149:207 2:2 = 0.999

143:143 208:230 2:2 = 0.999

69:142 230:230 2:2 = 0.999

69:69 231:260 2:2 = 0.999

RESULTS SECTION PERMS

**$ RESULTS PROP PERMI MATRIX  Units: md

**$ RESULTS PROP Minimum Value: 0.0001  Maximum Value: 1E+009

PERMI MATRIX CON 0.0001

MOD  1:51 126:126 2:2 = 10

51:51 83:125 2:2 = 10

52:113 83:83 2:2 = 10

114:143 83:83 2:2 = 10

143:143 84:148 2:2 = 10

143:143 149:207 2:2 = 10

143:143 208:230 2:2 = 10

69:142 230:230 2:2 = 10

69:69 231:260 2:2 = 10

**$ RESULTS PROP PERMI FRACTURE  Units: md

**$ RESULTS PROP Minimum Value: 1  Maximum Value: 1E+009

PERMI FRACTURE CON 4.

MOD  1:51 126:126 2:2 = 1000000000

51:51 83:125 2:2 = 1000000000

52:113 83:83 2:2 = 1000000000

114:143 83:83 2:2 = 1000000000

143:143 84:148 2:2 = 1000000000

143:143 149:207 2:2 = 1000000000

143:143 208:230 2:2 = 1000000000

69:142 230:230 2:2 = 1000000000

69:69 231:260 2:2 = 1000000000

**$ RESULTS PROP PERMJ MATRIX  Units: md

**$ RESULTS PROP Minimum Value: 0.0001  Maximum Value: 1E+009

PERMJ MATRIX CON 0.0001

MOD  1:51 126:126 2:2 = 10

51:51 83:125 2:2 = 10

52:113 83:83 2:2 = 10

114:143 83:83 2:2 = 10

143:143 84:148 2:2 = 10

143:143 149:207 2:2 = 10

143:143 208:230 2:2 = 10

69:142 230:230 2:2 = 10

69:69 231:260 2:2 = 10

**$ RESULTS PROP PERMJ FRACTURE  Units: md

**$ RESULTS PROP Minimum Value: 1  Maximum Value: 1E+009

PERMJ FRACTURE CON 4.

MOD  1:51 126:126 2:2 = 1000000000

51:51 83:125 2:2 = 1000000000

52:113 83:83 2:2 = 1000000000

114:143 83:83 2:2 = 1000000000

143:143 84:148 2:2 = 1000000000

143:143 149:207 2:2 = 1000000000

143:143 208:230 2:2 = 1000000000

69:142 230:230 2:2 = 1000000000

69:69 231:260 2:2 = 1000000000

**$ RESULTS PROP PERMK MATRIX  Units: md

**$ RESULTS PROP Minimum Value: 0.0001  Maximum Value: 1E+009

PERMK MATRIX CON 0.0001

MOD  1:51 126:126 2:2 = 10

51:51 83:125 2:2 = 10

52:113 83:83 2:2 = 10

114:143 83:83 2:2 = 10

143:143 84:148 2:2 = 10

143:143 149:207 2:2 = 10

143:143 208:230 2:2 = 10

69:142 230:230 2:2 = 10

69:69 231:260 2:2 = 10

**$ RESULTS PROP PERMK FRACTURE  Units: md

**$ RESULTS PROP Minimum Value: 1 Maximum Value: 1E+009

PERMK FRACTURE CON 1.0

MOD 1:51 126:126 2:2 = 1000000000

51:51 83:125 2:2 = 1000000000

52:113 83:83 2:2 = 1000000000

114:143 83:83 2:2 = 1000000000

143:143 84:148 2:2 = 1000000000

143:143 149:207 2:2 = 1000000000

143:143 208:230 2:2 = 1000000000

69:142 230:230 2:2 = 1000000000

69:69 231:260 2:2 = 1000000000

RESULTS SECTION TRANS

**$ RESULTS PROP TRANSI MATRIX Units: Dimensionless

**$ RESULTS PROP Minimum Value: 1 Maximum Value: 1000

TRANSI MATRIX CON 1.0

MOD 1:51 126:126 2:2 = 1000

51:51 83:125 2:2 = 1000

52:113 83:83 2:2 = 1000

114:143 83:83 2:2 = 1000

143:143 84:148 2:2 = 1000

143:143 149:207 2:2 = 1000

143:143 208:230 2:2 = 1000

69:142 230:230 2:2 = 1000

69:69 231:260 2:2 = 1000

**$ RESULTS PROP TRANSI FRACTURE Units: Dimensionless

**$ RESULTS PROP Minimum Value: 1  Maximum Value: 1000

TRANSI FRACTURE CON 1.

MOD  1:51 126:126 2:2 = 1000

51:51 83:125 2:2 = 1000

52:113 83:83 2:2 = 1000

114:143 83:83 2:2 = 1000

143:143 84:148 2:2 = 1000

143:143 149:207 2:2 = 1000

143:143 208:230 2:2 = 1000

69:142 230:230 2:2 = 1000

69:69 231:260 2:2 = 1000

**$ RESULTS PROP TRANSJ MATRIX  Units: Dimensionless

**$ RESULTS PROP Minimum Value: 1  Maximum Value: 1000

TRANSJ MATRIX CON 1.0

MOD  1:51 126:126 2:2 = 1000

51:51 83:125 2:2 = 1000

52:113 83:83 2:2 = 1000

114:143 83:83 2:2 = 1000

143:143 84:148 2:2 = 1000

143:143 149:207 2:2 = 1000

143:143 208:230 2:2 = 1000

69:142 230:230 2:2 = 1000

69:69 231:260 2:2 = 1000

**$ RESULTS PROP TRANSJ FRACTURE  Units: Dimensionless

**$ RESULTS PROP Minimum Value: 1  Maximum Value: 1000

TRANSJ FRACTURE CON 1.0

MOD 1:51 126:126 2:2 = 1000

51:51 83:125 2:2 = 1000

52:113 83:83 2:2 = 1000

114:143 83:83 2:2 = 1000

143:143 84:148 2:2 = 1000

143:143 149:207 2:2 = 1000

143:143 208:230 2:2 = 1000

69:142 230:230 2:2 = 1000

69:69 231:260 2:2 = 1000

**$ RESULTS PROP TRANSK MATRIX Units: Dimensionless

**$ RESULTS PROP Minimum Value: 1 Maximum Value: 1000

TRANSK MATRIX CON 1.

MOD 1:51 126:126 2:2 = 1000

51:51 83:125 2:2 = 1000

52:113 83:83 2:2 = 1000

114:143 83:83 2:2 = 1000

143:143 84:148 2:2 = 1000

143:143 149:207 2:2 = 1000

143:143 208:230 2:2 = 1000

69:142 230:230 2:2 = 1000

69:69 231:260 2:2 = 1000

**$ RESULTS PROP TRANSK FRACTURE Units: Dimensionless

**$ RESULTS PROP Minimum Value: 1 Maximum Value: 1000

TRANSK FRACTURE CON 1.

MOD 1:51 126:126 2:2 = 1000

51:51 83:125 2:2 = 1000

52:113 83:83 2:2 = 1000

114:143 83:83 2:2 = 1000

143:143 84:148 2:2 = 1000

143:143 149:207 2:2 = 1000

143:143 208:230 2:2 = 1000

69:142 230:230 2:2 = 1000

69:69 231:260 2:2 = 1000

**$ RESULTS PROP TRANLI MATRIX Units: Dimensionless

**$ RESULTS PROP Minimum Value: 1 Maximum Value: 1000

TRANLI MATRIX CON 1.

MOD 1:51 126:126 2:2 = 1000

51:51 83:125 2:2 = 1000

52:113 83:83 2:2 = 1000

114:143 83:83 2:2 = 1000

143:143 84:148 2:2 = 1000

143:143 149:207 2:2 = 1000

143:143 208:230 2:2 = 1000

69:142 230:230 2:2 = 1000

69:69 231:260 2:2 = 1000

**$ RESULTS PROP TRANLI FRACTURE Units: Dimensionless

**$ RESULTS PROP Minimum Value: 1 Maximum Value: 1000

TRANLI FRACTURE CON 1.

MOD 1:51 126:126 2:2 = 1000

51:51 83:125 2:2 = 1000

52:113 83:83 2:2 = 1000

114:143 83:83 2:2 = 1000

143:143 84:148 2:2 = 1000

143:143 149:207 2:2 = 1000

143:143 208:230 2:2 = 1000

69:142 230:230 2:2 = 1000

69:69 231:260 2:2 = 1000

**$ RESULTS PROP TRANLJ MATRIX  Units: Dimensionless

**$ RESULTS PROP Minimum Value: 1  Maximum Value: 1000

TRANLJ MATRIX CON 1.

MOD  1:51 126:126 2:2 = 1000

51:51 83:125 2:2 = 1000

52:113 83:83 2:2 = 1000

114:143 83:83 2:2 = 1000

143:143 84:148 2:2 = 1000

143:143 149:207 2:2 = 1000

143:143 208:230 2:2 = 1000

69:142 230:230 2:2 = 1000

69:69 231:260 2:2 = 1000

**$ RESULTS PROP TRANLJ FRACTURE  Units: Dimensionless

**$ RESULTS PROP Minimum Value: 1  Maximum Value: 1000

TRANLJ FRACTURE CON 1.

MOD  1:51 126:126 2:2 = 1000

51:51 83:125 2:2 = 1000

52:113 83:83 2:2 = 1000

114:143 83:83 2:2 = 1000

143:143 84:148 2:2 = 1000

143:143 149:207 2:2 = 1000

143:143 208:230 2:2 = 1000

69:142 230:230 2:2 = 1000

69:69 231:260 2:2 = 1000

**$ RESULTS PROP TRANLK MATRIX  Units: Dimensionless

**$ RESULTS PROP Minimum Value: 1  Maximum Value: 1000

TRANLK MATRIX CON 1.

MOD 1:51 126:126 2:2 = 1000

51:51 83:125 2:2 = 1000

52:113 83:83 2:2 = 1000

114:143 83:83 2:2 = 1000

143:143 84:148 2:2 = 1000

143:143 149:207 2:2 = 1000

143:143 208:230 2:2 = 1000

69:142 230:230 2:2 = 1000

69:69 231:260 2:2 = 1000

**$ RESULTS PROP TRANLK FRACTURE  Units: Dimensionless

**$ RESULTS PROP Minimum Value: 1  Maximum Value: 1000

TRANLK FRACTURE CON 1.

MOD 1:51 126:126 2:2 = 1000

51:51 83:125 2:2 = 1000

52:113 83:83 2:2 = 1000

114:143 83:83 2:2 = 1000

143:143 84:148 2:2 = 1000

143:143 149:207 2:2 = 1000

143:143 208:230 2:2 = 1000

69:142 230:230 2:2 = 1000

69:69 231:260 2:2 = 1000

RESULTS SECTION FRACS

**$ RESULTS PROP DIFRAC  Units: m

**$ RESULTS PROP Minimum Value: 0.1  Maximum Value: 0.5

DIFRAC CON 0.5

MOD 1:51 126:126 2:2 = 0.1

51:51 83:125 2:2 = 0.1

52:113 83:83 2:2 = 0.1

114:143 83:83 2:2 = 0.1

143:143 84:148 2:2 = 0.1

143:143 149:207 2:2 = 0.1

143:143 208:230 2:2 = 0.1

69:142 230:230 2:2 = 0.1

69:69 231:260 2:2 = 0.1

**$ RESULTS PROP DJFRAC  Units: m

**$ RESULTS PROP Minimum Value: 0.1  Maximum Value: 0.25

DJFRAC CON 0.25

MOD 1:51 126:126 2:2 = 0.1

51:51 83:125 2:2 = 0.1

52:113 83:83 2:2 = 0.1

114:143 83:83 2:2 = 0.1

143:143 84:148 2:2 = 0.1

143:143 149:207 2:2 = 0.1

143:143 208:230 2:2 = 0.1

69:142 230:230 2:2 = 0.1

69:69 231:260 2:2 = 0.1

**$ RESULTS PROP DKFRAC  Units: m

**$ RESULTS PROP Minimum Value: 0.1  Maximum Value: 0.1

DKFRAC CON 0.1

MOD 1:51 126:126 2:2 = 0.1

51:51 83:125 2:2 = 0.1

52:113 83:83 2:2 = 0.1

114:143 83:83 2:2 = 0.1

143:143 84:148 2:2 = 0.1

143:143 149:207 2:2 = 0.1

143:143 208:230 2:2 = 0.1

69:142 230:230 2:2 = 0.1

69:69 231:260 2:2 = 0.1

RESULTS SECTION GRIDNONARRAYS

CPOR  MATRIX  5.E-06

PRPOR MATRIX  100.0

CPOR  FRACTURE 0.0005

PRPOR FRACTURE 100.0

RESULTS SECTION VOLMOD

RESULTS SECTION SECTORLEASE

```
RESULTS SECTION ROCKCOMPACTION
RESULTS SECTION GRIDOTHER
RESULTS SECTION MODEL
*MODEL        *PR
*NC           2  2
*COMPNAME     'CH4'       'N2'
*HCFLAG       1           0
*TRES         30.
*PCRIT         45.400000   33.500000
*TCRIT         190.60000   126.20000
*AC            0.008000    0.040000
*VCRIT          0.099000    0.089500
*MW            16.04300    28.01300
*PCHOR          77.00000    41.00000
*SG            0.300000    0.809000
*TB           -161.45000  -195.75000
*BIN
    0.031
*DENW         1000.8
*REFPW        101.325
RESULTS SECTION MODELARRAYS
RESULTS SECTION ROCKFLUID
*ROCKFLUID
*RPT 1  *DRAINAGE
*SWT
```

0.200000  0.000000  0.000006  0.000000

0.450000  0.024065  0.000000  0.000000

0.600000  0.0493088  0.000000  0.000000

0.750000  0.0882927  0.000000  0.000000

0.900000  0.127650  0.000000  0.000000

0.950000  0.154878  0.000000  0.000000

0.999900  0.200000  0.000000  0.000000

*SGT

0.005000  0.000000  0.000006  0.000000

0.010000  0.0460829  0.000000  0.000000

0.050000  0.103687  0.000000  0.000000

0.250000  0.236175  0.000000  0.000000

0.300000  0.259217  0.000000  0.000000

0.400000  0.309908  0.000000  0.000000

0.520000  0.366359  0.000000  0.000000

0.600000  0.403226  0.000000  0.000000

0.800000  0.500000  0.000000  0.000000

*RPT 2  *DRAINAGE

*SWT

0.200000  0.000000  0.000006  0.000000

0.450000  0.004065  0.000000  0.000000

0.600000  0.00967086  0.000000  0.000000

0.750000  0.0195056  0.000000  0.000000

0.900000  0.0417978  0.000000  0.000000

0.950000  0.054878  0.000000  0.000000

0.999900  0.0711382  0.000000  0.000000

*SGT

0.005000  0.000000  0.000006  0.000000

0.010000  0.0562602  0.000000  0.000000

0.050000  0.172811  0.000000  0.000000

0.250000  0.470046  0.000000  0.000000

0.300000  0.532258  0.000000  0.000000

0.400000  0.619816  0.000000  0.000000

0.520000  0.735023  0.000000  0.000000

0.600000  0.817972  0.000000  0.000000

0.800000  1.000000  0.000000  0.000000

*RPT 3  *DRAINAGE

*SWT

0.200000  0.000000  0.000006  0.000000

0.450000  0.024065  0.000000  0.000000

0.600000  0.0493088  0.000000  0.000000

0.750000  0.0882927  0.000000  0.000000

0.900000  0.127650  0.000000  0.000000

0.950000  0.154878  0.000000  0.000000

0.999900  0.200000  0.000000  0.000000

*SGT

0.005000  0.000000  0.000006  0.000000

0.010000  0.0460829  0.000000  0.000000

0.050000  0.103687  0.000000  0.000000

0.250000  0.236175  0.000000  0.000000

0.300000  0.259217  0.000000  0.000000

0.400000  0.309908  0.000000  0.000000

0.520000  0.366359  0.000000  0.000000

0.600000  0.403226  0.000000  0.000000

0.800000  0.500000  0.000000  0.000000

*RPT 4  *DRAINAGE

*SWT

0.200000  0.000000  0.000006  0.000000

0.450000  0.00458956  0.000000  0.000000

0.600000  0.011310  0.000000  0.000000

0.750000  0.0213087  0.000000  0.000000

0.900000  0.041470  0.000000  0.000000

0.950000  0.054878  0.000000  0.000000

0.999900  0.0711382  0.000000  0.000000

*SGT

0.005000  0.000000  0.000006  0.000000

0.010000  0.900000  0.000000  0.000000

0.050000  1.000000  0.000000  0.000000

0.250000  1.000000  0.000000  0.000000

0.300000  1.000000  0.000000  0.000000

0.400000  1.000000  0.000000  0.000000

0.520000  1.000000  0.000000  0.000000

0.600000  1.000000  0.000000  0.000000

0.800000  1.000000  0.000000  0.000000

*KROIL *STONE2 *SWSG

RESULTS SECTION ROCKARRAYS

**$ RESULTS PROP RTYPE MATRIX  Units: Dimensionless

**$ RESULTS PROP Minimum Value: 1  Maximum Value: 3

RTYPE MATRIX CON 1.

MOD 1:51 126:126 2:2 = 3

51:51 83:125 2:2 = 3

52:113 83:83 2:2 = 3

114:143 83:83 2:2 = 3

143:143 84:148 2:2 = 3

143:143 149:207 2:2 = 3

143:143 208:230 2:2 = 3

69:142 230:230 2:2 = 3

69:69 231:260 2:2 = 3

**$ RESULTS PROP RTYPE FRACTURE  Units: Dimensionless

**$ RESULTS PROP Minimum Value: 2  Maximum Value: 4

RTYPE FRACTURE CON 2.

MOD 1:51 126:126 2:2 = 4

51:51 83:125 2:2 = 4

52:113 83:83 2:2 = 4

114:143 83:83 2:2 = 4

143:143 84:148 2:2 = 4

143:143 149:207 2:2 = 4

143:143 208:230 2:2 = 4

69:142 230:230 2:2 = 4

69:69 231:260 2:2 = 4

**$ RESULTS PROP ADGMAXC 'CH4' MATRIX  Units: gmole/kg

**$ RESULTS PROP Minimum Value: 0.263539  Maximum Value: 0.263539

ADGMAXC 'CH4' MATRIX CON 0.263539

**$ RESULTS PROP ADGMAXC 'CH4' FRACTURE  Units: gmole/kg

**$ RESULTS PROP Minimum Value: 0  Maximum Value: 0

ADGMAXC 'CH4' FRACTURE CON 0

**$ RESULTS PROP ADGCSTC 'CH4' MATRIX  Units: 1/kPa

**$ RESULTS PROP Minimum Value: 0.000967118  Maximum Value: 0.000967118

ADGCSTC 'CH4' MATRIX CON 0.000967118

**$ RESULTS PROP ADGCSTC 'CH4' FRACTURE  Units: 1/kPa

**$ RESULTS PROP Minimum Value: 0  Maximum Value: 0

ADGCSTC 'CH4' FRACTURE CON 0

**$ RESULTS PROP ROCKDEN MATRIX  Units: kg/m3

**$ RESULTS PROP Minimum Value: 1435  Maximum Value: 1435

ROCKDEN MATRIX CON 1435.

**$ RESULTS PROP ROCKDEN FRACTURE  Units: kg/m3

**$ RESULTS PROP Minimum Value: 1435  Maximum Value: 1435

ROCKDEN FRACTURE CON 1435.

**$ RESULTS PROP COAL-DIF-TIME 'CH4' MATRIX  Units: day

**$ RESULTS PROP Minimum Value: 100  Maximum Value: 100

COAL-DIF-TIME 'CH4' MATRIX CON 100.

MOD 1:51 126:126 2:2 = 0

    51:51 83:125 2:2 = 0

    52:113 83:83 2:2 = 0

    114:143 83:83 2:2 = 0

```
        143:143 84:148 2:2 = 0
        143:143 149:207 2:2 = 0
        143:143 208:230 2:2 = 0
        69:142 230:230 2:2 = 0
        69:69 231:260 2:2 = 0
RESULTS SECTION INIT
*INITIAL
*USER_INPUT
*NREGIONS 1
*SEPARATOR
  101.325     15.5556
RESULTS SECTION INITARRAYS
RESULTS SPEC 'Water Saturation' FRACTURE
RESULTS SPEC SPECNOTCALCVAL -99999
RESULTS SPEC REGION 'All Layers (Whole Grid)'
RESULTS SPEC REGIONTYPE 'REGION_WHOLEGRID'
RESULTS SPEC LAYERNUMB 0
RESULTS SPEC PORTYPE 2
RESULTS SPEC CON 0.2
RESULTS SPEC STOP
RESULTS SPEC 'Pressure' MATRIX
RESULTS SPEC SPECNOTCALCVAL -99999
RESULTS SPEC REGION 'All Layers (Whole Grid)'
RESULTS SPEC REGIONTYPE 'REGION_WHOLEGRID'
RESULTS SPEC LAYERNUMB 0
```

RESULTS SPEC PORTYPE 1

RESULTS SPEC CON 517

RESULTS SPEC STOP

RESULTS SPEC 'Pressure' FRACTURE

RESULTS SPEC SPECNOTCALCVAL -99999

RESULTS SPEC REGION 'All Layers (Whole Grid)'

RESULTS SPEC REGIONTYPE 'REGION_WHOLEGRID'

RESULTS SPEC LAYERNUMB 0

RESULTS SPEC PORTYPE 2

RESULTS SPEC CON 517

RESULTS SPEC STOP

RESULTS SPEC 'Water Saturation' MATRIX

RESULTS SPEC SPECNOTCALCVAL -99999

RESULTS SPEC REGION 'All Layers (Whole Grid)'

RESULTS SPEC REGIONTYPE 'REGION_WHOLEGRID'

RESULTS SPEC LAYERNUMB 0

RESULTS SPEC PORTYPE 1

RESULTS SPEC CON 0.05

RESULTS SPEC STOP

RESULTS SPEC 'Grid Thickness'

RESULTS SPEC SPECNOTCALCVAL -99999

RESULTS SPEC REGION 'Layer 1 - Whole layer'

RESULTS SPEC REGIONTYPE 'REGION_LAYER'

RESULTS SPEC LAYERNUMB 1

RESULTS SPEC PORTYPE 1

RESULTS SPEC CON 2

RESULTS SPEC REGION 'Layer 2 - Whole layer'

RESULTS SPEC REGIONTYPE 'REGION_LAYER'

RESULTS SPEC LAYERNUMB 2

RESULTS SPEC PORTYPE 1

RESULTS SPEC CON 3

RESULTS SPEC STOP

RESULTS SPEC 'Global Composition$C' 'N2' FRACTURE

RESULTS SPEC SPECNOTCALCVAL -99999

RESULTS SPEC REGION 'All Layers (Whole Grid)'

RESULTS SPEC REGIONTYPE 'REGION_WHOLEGRID'

RESULTS SPEC LAYERNUMB 0

RESULTS SPEC PORTYPE 2

RESULTS SPEC CON 0

RESULTS SPEC STOP

RESULTS SPEC 'Global Composition$C' 'N2' MATRIX

RESULTS SPEC SPECNOTCALCVAL -99999

RESULTS SPEC REGION 'All Layers (Whole Grid)'

RESULTS SPEC REGIONTYPE 'REGION_WHOLEGRID'

RESULTS SPEC LAYERNUMB 0

RESULTS SPEC PORTYPE 1

RESULTS SPEC CON 0

RESULTS SPEC STOP

RESULTS SPEC 'Global Composition$C' 'CH4' FRACTURE

RESULTS SPEC SPECNOTCALCVAL -99999

```
RESULTS SPEC REGION 'All Layers (Whole Grid)'
RESULTS SPEC REGIONTYPE 'REGION_WHOLEGRID'
RESULTS SPEC LAYERNUMB 0
RESULTS SPEC PORTYPE 2
RESULTS SPEC CON 1
RESULTS SPEC STOP
RESULTS SPEC 'Global Composition$C' 'CH4' MATRIX
RESULTS SPEC SPECNOTCALCVAL -99999
RESULTS SPEC REGION 'All Layers (Whole Grid)'
RESULTS SPEC REGIONTYPE 'REGION_WHOLEGRID'
RESULTS SPEC LAYERNUMB 0
RESULTS SPEC PORTYPE 1
RESULTS SPEC CON 1
RESULTS SPEC STOP
**$ RESULTS PROP SW MATRIX  Units: Dimensionless
**$ RESULTS PROP Minimum Value: 0.05  Maximum Value: 0.05
SW MATRIX CON 0.05
**$ RESULTS PROP SW FRACTURE  Units: Dimensionless
**$ RESULTS PROP Minimum Value: 0.01  Maximum Value: 0.2
SW FRACTURE CON 0.2
MOD 1:51 126:126 2:2 = 0.01
        51:51 83:125 2:2 = 0.01
        52:113 83:83 2:2 = 0.01
        114:143 83:83 2:2 = 0.01
        143:143 84:148 2:2 = 0.01
```

143:143 149:207 2:2 = 0.01

143:143 208:230 2:2 = 0.01

69:142 230:230 2:2 = 0.01

69:69 231:260 2:2 = 0.01

**$ RESULTS PROP PRES MATRIX  Units: kPa

**$ RESULTS PROP Minimum Value: 517  Maximum Value: 517

PRES MATRIX CON 517.

MOD 1:51 126:126 2:2 = 98

51:51 83:125 2:2 = 98

52:113 83:83 2:2 = 98

114:143 83:83 2:2 = 98

143:143 84:148 2:2 = 98

143:143 149:207 2:2 = 98

143:143 208:230 2:2 = 98

69:142 230:230 2:2 = 98

69:69 231:260 2:2 = 98

**$ RESULTS PROP PRES FRACTURE  Units: kPa

**$ RESULTS PROP Minimum Value: 517  Maximum Value: 517

PRES FRACTURE CON 517.

MOD 1:51 126:126 2:2 = 98

51:51 83:125 2:2 = 98

52:113 83:83 2:2 = 98

114:143 83:83 2:2 = 98

143:143 84:148 2:2 = 98

143:143 149:207 2:2 = 98

143:143 208:230 2:2 = 98

69:142 230:230 2:2 = 98

69:69 231:260 2:2 = 98

**$ RESULTS PROP ZGLOBALC 'CH4' MATRIX  Units: Dimensionless

**$ RESULTS PROP Minimum Value: 0  Maximum Value: 1

ZGLOBALC 'CH4' MATRIX CON 1.

MOD 1:51 126:126 2:2 = 0

51:51 83:125 2:2 = 0

52:113 83:83 2:2 = 0

114:143 83:83 2:2 = 0

143:143 84:148 2:2 = 0

143:143 149:207 2:2 = 0

143:143 208:230 2:2 = 0

69:142 230:230 2:2 = 0

69:69 231:260 2:2 = 0

**$ RESULTS PROP ZGLOBALC 'CH4' FRACTURE  Units: Dimensionless

**$ RESULTS PROP Minimum Value: 0  Maximum Value: 1

ZGLOBALC 'CH4' FRACTURE CON 1.

MOD 1:51 126:126 2:2 = 0

51:51 83:125 2:2 = 0

52:113 83:83 2:2 = 0

114:143 83:83 2:2 = 0

143:143 84:148 2:2 = 0

143:143 149:207 2:2 = 0

143:143 208:230 2:2 = 0

69:142 230:230 2:2 = 0

69:69 231:260 2:2 = 0

**$ RESULTS PROP ZGLOBALC 'N2' MATRIX  Units: Dimensionless

**$ RESULTS PROP Minimum Value: 0  Maximum Value: 1

ZGLOBALC 'N2' MATRIX CON 0

MOD 1:51 126:126 2:2 = 1

51:51 83:125 2:2 = 1

52:113 83:83 2:2 = 1

114:143 83:83 2:2 = 1

143:143 84:148 2:2 = 1

143:143 149:207 2:2 = 1

143:143 208:230 2:2 = 1

69:142 230:230 2:2 = 1

69:69 231:260 2:2 = 1

**$ RESULTS PROP ZGLOBALC 'N2' FRACTURE  Units: Dimensionless

**$ RESULTS PROP Minimum Value: 0  Maximum Value: 1

ZGLOBALC 'N2' FRACTURE CON 0

MOD 1:51 126:126 2:2 = 1

51:51 83:125 2:2 = 1

52:113 83:83 2:2 = 1

114:143 83:83 2:2 = 1

143:143 84:148 2:2 = 1

143:143 149:207 2:2 = 1

143:143 208:230 2:2 = 1

69:142 230:230 2:2 = 1

69:69 231:260 2:2 = 1

RESULTS SECTION NUMERICAL

*NUMERICAL

*DTMAX 365.

*DTMIN 0.0000001

*NEWTONCYC 30

*NORTH 30

*PIVOT *ON

*ITERMAX 100

*AIM *OFF

*NORM *PRESS 100.

*NORM *GMOLAR 0.15

*NORM *SATUR 0.15

*MAXCHANGE *PRESS 500

*MAXCHANGE *GMOLAR 1.

*MAXCHANGE *SATUR 1.

*MAXCPU 3.E+05

*MODILU *ON

*CONVERGE *PRESS 10.

*CONVERGE *MAXRES *LOOSE

*TWOPTFLUX *IRREGULAR

RESULTS SECTION NUMARRAYS

RESULTS SECTION GBKEYWORDS

RUN

DATE 2007 01 08

```
DATE 2007 01 10
DTWELL 1.
**$ RESULTS PROP AIMSET MATRIX  Units: Dimensionless
**$ RESULTS PROP Minimum Value: 1  Maximum Value: 1
AIMSET MATRIX CON 1.
**$ RESULTS PROP AIMSET FRACTURE  Units: Dimensionless
**$ RESULTS PROP Minimum Value: 1  Maximum Value: 1
AIMSET FRACTURE CON 1.
WELL  1 'Well-1'
INJECTOR 'Well-1'
INCOMP SOLVENT  0.005 0.995
OPERATE MAX BHP  98.1 CONT
OPERATE MAX STG  1.36512E+06 CONT
GEOMETRY K 0.5 0.37 1. 0.
PERF GEO  QUAD 'Well-1'
        69 260 2 1. OPEN FLOW-FROM 'SURFACE'
WELL  2 'Well-2'
PRODUCER 'Well-2'
OPERATE MIN BHP  98.1 CONT
GEOMETRY K 0.5 0.37 1. 0.
PERF GEO  QUAD 'Well-2'
        1 126 2 1. OPEN FLOW-TO 'SURFACE'
WELL  3 'Well-3'
PRODUCER 'Well-3'
OPERATE MIN BHP  98.1 CONT
```

```
GEOMETRY K 0.5 0.37 1. 0.
PERF GEO   'Well-3'
        143 212 2 1. OPEN FLOW-TO 'SURFACE'
DATE 2007 02 06
INJECTOR 'Well-1'
INCOMP SOLVENT  0.006 0.994
OPERATE MAX BHP  98.1 CONT
OPERATE MAX STG  1.40832E+06 CONT
GEOMETRY K 0.5 0.37 1. 0.
PERF GEO  QUAD 'Well-1'
        69 260 2 1. OPEN FLOW-FROM 'SURFACE'
PRODUCER 'Well-2'
OPERATE MIN BHP  98.1 CONT
GEOMETRY K 0.5 0.37 1. 0.
PERF GEO  QUAD 'Well-2'
        1 126 2 1. OPEN FLOW-TO 'SURFACE'
PRODUCER 'Well-3'
OPERATE MIN BHP  98.1 CONT
GEOMETRY K 0.5 0.37 1. 0.
PERF GEO   'Well-3'
        143 212 2 1. OPEN FLOW-TO 'SURFACE'
DATE 2007 03 07
INJECTOR 'Well-1'
INCOMP SOLVENT  0.006 0.994
OPERATE MAX BHP  98.3 CONT
```

```
OPERATE MAX STG  1.7568E+06 CONT
GEOMETRY K 0.5 0.37 1. 0.
PERF GEO  QUAD 'Well-1'
        69 260 2 1. OPEN FLOW-FROM 'SURFACE'
PRODUCER 'Well-2'
OPERATE MIN BHP  98.3 CONT
GEOMETRY K 0.5 0.37 1. 0.
PERF GEO  QUAD 'Well-2'
        1 126 2 1. OPEN FLOW-TO 'SURFACE'
PRODUCER 'Well-3'
OPERATE MIN BHP  98.3 CONT
GEOMETRY K 0.5 0.37 1. 0.
PERF GEO   'Well-3'
        143 212 2 1. OPEN FLOW-TO 'SURFACE'
DATE 2007 04 19
INJECTOR 'Well-1'
INCOMP SOLVENT  0.006 0.994
OPERATE MAX BHP  97.9 CONT
OPERATE MAX STG  1.73952E+06 CONT
GEOMETRY K 0.5 0.37 1. 0.
PERF GEO  QUAD 'Well-1'
        69 260 2 1. OPEN FLOW-FROM 'SURFACE'
PRODUCER 'Well-2'
OPERATE MIN BHP  97.9 CONT
GEOMETRY K 0.5 0.37 1. 0.
```

```
PERF GEO  QUAD 'Well-2'
        1 126 2 1. OPEN FLOW-TO 'SURFACE'
PRODUCER 'Well-3'
OPERATE MIN BHP  97.9 CONT
GEOMETRY K 0.5 0.37 1. 0.
PERF GEO   'Well-3'
        143 212 2 1. OPEN FLOW-TO 'SURFACE'
DATE 2007 05 17
INJECTOR 'Well-1'
INCOMP SOLVENT  0.006 0.994
OPERATE MAX BHP  97. CONT
OPERATE MAX STG  1.69488E+06 CONT
GEOMETRY K 0.5 0.37 1. 0.
PERF GEO  QUAD 'Well-1'
        69 260 2 1. OPEN FLOW-FROM 'SURFACE'
PRODUCER 'Well-2'
OPERATE MIN BHP  97. CONT
GEOMETRY K 0.5 0.37 1. 0.
PERF GEO  QUAD 'Well-2'
        1 126 2 1. OPEN FLOW-TO 'SURFACE'
PRODUCER 'Well-3'
OPERATE MIN BHP  97. CONT
GEOMETRY K 0.5 0.37 1. 0.
PERF GEO   'Well-3'
        143 212 2 1. OPEN FLOW-TO 'SURFACE'
```

```
DATE 2007 06 06
INJECTOR 'Well-1'
INCOMP SOLVENT  0.006 0.994
OPERATE MAX BHP  97.9 CONT
OPERATE MAX STG  1.68624E+06 CONT
GEOMETRY K 0.5 0.37 1. 0.
PERF GEO  QUAD 'Well-1'
        69 260 2 1. OPEN FLOW-FROM 'SURFACE'
PRODUCER 'Well-2'
OPERATE MIN BHP  97.9 CONT
GEOMETRY K 0.5 0.37 1. 0.
PERF GEO  QUAD 'Well-2'
        1 126 2 1. OPEN FLOW-TO 'SURFACE'
PRODUCER 'Well-3'
OPERATE MIN BHP  97.9 CONT
GEOMETRY K 0.5 0.37 1. 0.
PERF GEO   'Well-3'
        143 212 2 1. OPEN FLOW-TO 'SURFACE'
DATE 2007 07 28
INJECTOR 'Well-1'
INCOMP SOLVENT  0.006 0.994
OPERATE MAX BHP  97.5 CONT
OPERATE MAX STG  1.6344E+06 CONT
GEOMETRY K 0.5 0.37 1. 0.
PERF GEO  QUAD 'Well-1'
```

```
        69 260 2 1. OPEN FLOW-FROM 'SURFACE'
PRODUCER 'Well-2'
OPERATE MIN BHP  97.5 CONT
GEOMETRY K 0.5 0.37 1. 0.
PERF GEO  QUAD 'Well-2'
        1 126 2 1. OPEN FLOW-TO 'SURFACE'
PRODUCER 'Well-3'
OPERATE MIN BHP  97.5 CONT
GEOMETRY K 0.5 0.37 1. 0.
PERF GEO   'Well-3'
        143 212 2 1. OPEN FLOW-TO 'SURFACE'
DATE 2007 08 12
INJECTOR 'Well-1'
INCOMP SOLVENT  0.006 0.994
OPERATE MAX BHP  97.5 CONT
OPERATE MAX STG  1.64304E+06 CONT
GEOMETRY K 0.5 0.37 1. 0.
PERF GEO  QUAD 'Well-1'
        69 260 2 1. OPEN FLOW-FROM 'SURFACE'
PRODUCER 'Well-2'
OPERATE MIN BHP  97.5 CONT
GEOMETRY K 0.5 0.37 1. 0.
PERF GEO  QUAD 'Well-2'
        1 126 2 1. OPEN FLOW-TO 'SURFACE'
PRODUCER 'Well-3'
```

```
OPERATE MIN BHP  97.5 CONT
GEOMETRY K 0.5 0.37 1. 0.
PERF GEO   'Well-3'
        143 212 2 1. OPEN FLOW-TO 'SURFACE'
DATE 2007 09 12
INJECTOR 'Well-1'
INCOMP SOLVENT  0.006 0.994
OPERATE MAX BHP  98. CONT
OPERATE MAX STG  1.59984E+06 CONT
GEOMETRY K 0.5 0.37 1. 0.
PERF GEO  QUAD 'Well-1'
        69 260 2 1. OPEN FLOW-FROM 'SURFACE'
PRODUCER 'Well-2'
OPERATE MIN BHP  98. CONT
GEOMETRY K 0.5 0.37 1. 0.
PERF GEO  QUAD 'Well-2'
        1 126 2 1. OPEN FLOW-TO 'SURFACE'
PRODUCER 'Well-3'
OPERATE MIN BHP  98. CONT
GEOMETRY K 0.5 0.37 1. 0.
PERF GEO   'Well-3'
        143 212 2 1. OPEN FLOW-TO 'SURFACE'
DATE 2007 10 15
INJECTOR 'Well-1'
INCOMP SOLVENT  0.005 0.995
```

```
OPERATE MAX BHP  98.3 CONT
OPERATE MAX STG  1.60848E+06 CONT
GEOMETRY K 0.5 0.37 1. 0.
PERF GEO  QUAD 'Well-1'
        69 260 2 1. OPEN FLOW-FROM 'SURFACE'
PRODUCER 'Well-2'
OPERATE MIN BHP  98.3 CONT
GEOMETRY K 0.5 0.37 1. 0.
PERF GEO  QUAD 'Well-2'
        1 126 2 1. OPEN FLOW-TO 'SURFACE'
PRODUCER 'Well-3'
OPERATE MIN BHP  98.3 CONT
GEOMETRY K 0.5 0.37 1. 0.
PERF GEO   'Well-3'
        143 212 2 1. OPEN FLOW-TO 'SURFACE'
DATE 2007 11 14
INJECTOR 'Well-1'
INCOMP SOLVENT  0.005 0.995
OPERATE MAX BHP  98.2 CONT
OPERATE MAX STG  1.62576E+06 CONT
GEOMETRY K 0.5 0.37 1. 0.
PERF GEO  QUAD 'Well-1'
        69 260 2 1. OPEN FLOW-FROM 'SURFACE'
PRODUCER 'Well-2'
OPERATE MIN BHP  98.2 CONT
```

```
GEOMETRY K 0.5 0.37 1. 0.
PERF GEO  QUAD 'Well-2'
        1 126 2 1. OPEN FLOW-TO 'SURFACE'
PRODUCER 'Well-3'
OPERATE MIN BHP  98.2 CONT
GEOMETRY K 0.5 0.37 1. 0.
PERF GEO   'Well-3'
        143 212 2 1. OPEN FLOW-TO 'SURFACE'
DATE 2007 12 13
INJECTOR 'Well-1'
INCOMP SOLVENT  0.006 0.994
OPERATE MAX BHP  97.6 CONT
OPERATE MAX STG  1.65268E+06 CONT
GEOMETRY K 0.5 0.37 1. 0.
PERF GEO  QUAD 'Well-1'
        69 260 2 1. OPEN FLOW-FROM 'SURFACE'
PRODUCER 'Well-2'
OPERATE MIN BHP  97.6 CONT
GEOMETRY K 0.5 0.37 1. 0.
PERF GEO  QUAD 'Well-2'
        1 126 2 1. OPEN FLOW-TO 'SURFACE'
PRODUCER 'Well-3'
OPERATE MIN BHP  97.6 CONT
GEOMETRY K 0.5 0.37 1. 0.
PERF GEO   'Well-3'
```

```
        143 212 2 1. OPEN FLOW-TO 'SURFACE'
DATE 2008 01 14
INJECTOR 'Well-1'
INCOMP SOLVENT  0.006 0.994
OPERATE MAX BHP  99. CONT
OPERATE MAX STG  1.6776E+06 CONT
GEOMETRY K 0.5 0.37 1. 0.
PERF GEO  QUAD 'Well-1'
        69 260 2 1. OPEN FLOW-FROM 'SURFACE'
PRODUCER 'Well-2'
OPERATE MIN BHP  99. CONT
GEOMETRY K 0.5 0.37 1. 0.
PERF GEO  QUAD 'Well-2'
        1 126 2 1. OPEN FLOW-TO 'SURFACE'
PRODUCER 'Well-3'
OPERATE MIN BHP  99. CONT
GEOMETRY K 0.5 0.37 1. 0.
PERF GEO   'Well-3'
        143 212 2 1. OPEN FLOW-TO 'SURFACE'
DATE 2008 02 12
INJECTOR 'Well-1'
INCOMP SOLVENT  0.005 0.995
OPERATE MAX BHP  98.6 CONT
OPERATE MAX STG  1.7208E+06 CONT
GEOMETRY K 0.5 0.37 1. 0.
```

```
PERF GEO  QUAD 'Well-1'
        69 260 2 1. OPEN FLOW-FROM 'SURFACE'
PRODUCER 'Well-2'
OPERATE MIN BHP  98.6 CONT
GEOMETRY K 0.5 0.37 1. 0.
PERF GEO  QUAD 'Well-2'
        1 126 2 1. OPEN FLOW-TO 'SURFACE'
PRODUCER 'Well-3'
OPERATE MIN BHP  98.6 CONT
GEOMETRY K 0.5 0.37 1. 0.
PERF GEO   'Well-3'
        143 212 2 1. OPEN FLOW-TO 'SURFACE'
DATE 2008 03 19
INJECTOR 'Well-1'
INCOMP SOLVENT  0.005 0.995
OPERATE MAX BHP  98.6 CONT
OPERATE MAX STG  1.66032E+06 CONT
GEOMETRY K 0.5 0.37 1. 0.
PERF GEO  QUAD 'Well-1'
        69 260 2 1. OPEN FLOW-FROM 'SURFACE'
PRODUCER 'Well-2'
OPERATE MIN BHP  98.6 CONT
GEOMETRY K 0.5 0.37 1. 0.
PERF GEO  QUAD 'Well-2'
        1 126 2 1. OPEN FLOW-TO 'SURFACE'
```

```
PRODUCER 'Well-3'
OPERATE MIN BHP  98.6 CONT
GEOMETRY K 0.5 0.37 1. 0.
PERF GEO   'Well-3'
        143 212 2 1. OPEN FLOW-TO 'SURFACE'
DATE 2008 04 14
INJECTOR 'Well-1'
INCOMP SOLVENT  0.005 0.995
OPERATE MAX BHP  98.6 CONT
OPERATE MAX STG  1.8E+06 CONT
GEOMETRY K 0.5 0.37 1. 0.
PERF GEO  QUAD 'Well-1'
        69 260 2 1. OPEN FLOW-FROM 'SURFACE'
PRODUCER 'Well-2'
OPERATE MIN BHP  98.6 CONT
GEOMETRY K 0.5 0.37 1. 0.
PERF GEO  QUAD 'Well-2'
        1 126 2 1. OPEN FLOW-TO 'SURFACE'
PRODUCER 'Well-3'
OPERATE MIN BHP  98.6 CONT
GEOMETRY K 0.5 0.37 1. 0.
PERF GEO   'Well-3'
        143 212 2 1. OPEN FLOW-TO 'SURFACE'
DATE 2008 05 14
INJECTOR 'Well-1'
```

```
INCOMP SOLVENT  0.005 0.995
OPERATE MAX BHP  98.5 CONT
OPERATE MAX STG  1.8E+06 CONT
GEOMETRY K 0.5 0.37 1. 0.
PERF GEO  QUAD 'Well-1'
        69 260 2 1. OPEN FLOW-FROM 'SURFACE'
PRODUCER 'Well-2'
OPERATE MIN BHP  98.5 CONT
GEOMETRY K 0.5 0.37 1. 0.
PERF GEO  QUAD 'Well-2'
        1 126 2 1. OPEN FLOW-TO 'SURFACE'
PRODUCER 'Well-3'
OPERATE MIN BHP  98.5 CONT
GEOMETRY K 0.5 0.37 1. 0.
PERF GEO   'Well-3'
        143 212 2 1. OPEN FLOW-TO 'SURFACE'
DATE 2008 06 14
INJECTOR 'Well-1'
INCOMP SOLVENT  0.005 0.995
OPERATE MAX BHP  97.9 CONT
OPERATE MAX STG  1.86912E+06 CONT
GEOMETRY K 0.5 0.37 1. 0.
PERF GEO  QUAD 'Well-1'
        69 260 2 1. OPEN FLOW-FROM 'SURFACE'
PRODUCER 'Well-2'
```

```
OPERATE MIN BHP  97.5 CONT
GEOMETRY K 0.5 0.37 1. 0.
PERF GEO  QUAD 'Well-2'
        1 126 2 1. OPEN FLOW-TO 'SURFACE'
PRODUCER 'Well-3'
OPERATE MIN BHP  97.5 CONT
GEOMETRY K 0.5 0.37 1. 0.
PERF GEO   'Well-3'
        143 212 2 1. OPEN FLOW-TO 'SURFACE'
DATE 2008 07 14
INJECTOR 'Well-1'
INCOMP SOLVENT  0.005 0.995
OPERATE MAX BHP  97.6 CONT
OPERATE MAX STG  1.78272E+06 CONT
GEOMETRY K 0.5 0.37 1. 0.
PERF GEO  QUAD 'Well-1'
        69 260 2 1. OPEN FLOW-FROM 'SURFACE'
PRODUCER 'Well-2'
OPERATE MIN BHP  97.6 CONT
GEOMETRY K 0.5 0.37 1. 0.
PERF GEO  QUAD 'Well-2'
        1 126 2 1. OPEN FLOW-TO 'SURFACE'
PRODUCER 'Well-3'
OPERATE MIN BHP  97.6 CONT
GEOMETRY K 0.5 0.37 1. 0.
```

```
PERF GEO   'Well-3'
        143 212 2 1. OPEN FLOW-TO 'SURFACE'
DATE 2008 08 14
INJECTOR 'Well-1'
INCOMP SOLVENT  0.005 0.995
OPERATE MAX BHP  97.3 CONT
OPERATE MAX STG  1.80864E+06 CONT
GEOMETRY K 0.5 0.37 1. 0.
PERF GEO  QUAD 'Well-1'
        69 260 2 1. OPEN FLOW-FROM 'SURFACE'
PRODUCER 'Well-2'
OPERATE MIN BHP  97.3 CONT
GEOMETRY K 0.5 0.37 1. 0.
PERF GEO  QUAD 'Well-2'
        1 126 2 1. OPEN FLOW-TO 'SURFACE'
PRODUCER 'Well-3'
OPERATE MIN BHP  97.3 CONT
GEOMETRY K 0.5 0.37 1. 0.
PERF GEO   'Well-3'
        143 212 2 1. OPEN FLOW-TO 'SURFACE'
DATE 2008 09 17
INJECTOR 'Well-1'
INCOMP SOLVENT  0.005 0.995
OPERATE MAX BHP  97.3 CONT
OPERATE MAX STG  1.8432E+06 CONT
```

```
GEOMETRY K 0.5 0.37 1. 0.
PERF GEO  QUAD 'Well-1'
        69 260 2 1. OPEN FLOW-FROM 'SURFACE'
PRODUCER 'Well-2'
OPERATE MIN BHP  97.3 CONT
GEOMETRY K 0.5 0.37 1. 0.
PERF GEO  QUAD 'Well-2'
        1 126 2 1. OPEN FLOW-TO 'SURFACE'
PRODUCER 'Well-3'
OPERATE MIN BHP  97.3 CONT
GEOMETRY K 0.5 0.37 1. 0.
PERF GEO   'Well-3'
        143 212 2 1. OPEN FLOW-TO 'SURFACE'
DATE 2008 10 07
INJECTOR 'Well-1'
INCOMP SOLVENT  0.005 0.995
OPERATE MAX BHP  98.2 CONT
OPERATE MAX STG  1.87776E+06 CONT
GEOMETRY K 0.5 0.37 1. 0.
PERF GEO  QUAD 'Well-1'
        69 260 2 1. OPEN FLOW-FROM 'SURFACE'
PRODUCER 'Well-2'
OPERATE MIN BHP  98.2 CONT
GEOMETRY K 0.5 0.37 1. 0.
PERF GEO  QUAD 'Well-2'
```

```
        1 126 2 1. OPEN FLOW-TO 'SURFACE'
PRODUCER 'Well-3'
OPERATE MIN BHP  98.2 CONT
GEOMETRY K 0.5 0.37 1. 0.
PERF GEO   'Well-3'
        143 212 2 1. OPEN FLOW-TO 'SURFACE'
DATE 2008 11 14
INJECTOR 'Well-1'
INCOMP SOLVENT  0.005 0.995
OPERATE MAX BHP  98.7 CONT
OPERATE MAX STG  1.86912E+06 CONT
GEOMETRY K 0.5 0.37 1. 0.
PERF GEO  QUAD 'Well-1'
        69 260 2 1. OPEN FLOW-FROM 'SURFACE'
PRODUCER 'Well-2'
OPERATE MIN BHP  98.7 CONT
GEOMETRY K 0.5 0.37 1. 0.
PERF GEO  QUAD 'Well-2'
        1 126 2 1. OPEN FLOW-TO 'SURFACE'
PRODUCER 'Well-3'
OPERATE MIN BHP  98.2 CONT
GEOMETRY K 0.5 0.37 1. 0.
PERF GEO   'Well-3'
        143 212 2 1. OPEN FLOW-TO 'SURFACE'
DATE 2008 12 15
```

```
INJECTOR 'Well-1'
INCOMP SOLVENT  0.006 0.994
OPERATE MAX BHP  99.2 CONT
OPERATE MAX STG  1.8432E+06 CONT
GEOMETRY K 0.5 0.37 1. 0.
PERF GEO  QUAD 'Well-1'
        69 260 2 1. OPEN FLOW-FROM 'SURFACE'
PRODUCER 'Well-2'
OPERATE MIN BHP  99.2 CONT
GEOMETRY K 0.5 0.37 1. 0.
PERF GEO  QUAD 'Well-2'
        1 126 2 1. OPEN FLOW-TO 'SURFACE'
PRODUCER 'Well-3'
OPERATE MIN BHP  99.2 CONT
GEOMETRY K 0.5 0.37 1. 0.
PERF GEO   'Well-3'
        143 212 2 1. OPEN FLOW-TO 'SURFACE'
DATE 2009 01 13
INJECTOR 'Well-1'
INCOMP SOLVENT  0.006 0.994
OPERATE MAX BHP  99.2 CONT
OPERATE MAX STG  1.95696E+06 CONT
GEOMETRY K 0.5 0.37 1. 0.
PERF GEO  QUAD 'Well-1'
        69 260 2 1. OPEN FLOW-FROM 'SURFACE'
```

```
PRODUCER 'Well-2'
OPERATE MIN BHP  99.2 CONT
GEOMETRY K 0.5 0.37 1. 0.
PERF GEO  QUAD 'Well-2'
        1 126 2 1. OPEN FLOW-TO 'SURFACE'
PRODUCER 'Well-3'
OPERATE MIN BHP  99.2 CONT
GEOMETRY K 0.5 0.37 1. 0.
PERF GEO   'Well-3'
        143 212 2 1. OPEN FLOW-TO 'SURFACE'
DATE 2009 02 10
INJECTOR 'Well-1'
INCOMP SOLVENT  0.005 0.995
OPERATE MAX BHP  98.1 CONT
OPERATE MAX STG  1.90368E+06 CONT
GEOMETRY K 0.5 0.37 1. 0.
PERF GEO  QUAD 'Well-1'
        69 260 2 1. OPEN FLOW-FROM 'SURFACE'
PRODUCER 'Well-2'
OPERATE MIN BHP  98.1 CONT
GEOMETRY K 0.5 0.37 1. 0.
PERF GEO  QUAD 'Well-2'
        1 126 2 1. OPEN FLOW-TO 'SURFACE'
PRODUCER 'Well-3'
OPERATE MIN BHP  98.1 CONT
```

```
GEOMETRY K 0.5 0.37 1. 0.
PERF GEO   'Well-3'
         143 212 2 1. OPEN FLOW-TO 'SURFACE'
DATE 2009 02 12
STOP
************ TERMINATE SIMULATION ************
RESULTS SECTION WELLDATA
RESULTS SECTION PERFS
```